

การเปรียบเทียบสมรรถนะระหว่างการใช้ฟอรัมมิงค์วีย์ไอเน็ตและการสลายตัวของมีเทน
สำหรับระบบเซลล์เชื้อเพลิงชนิดออกไซด์แข็งที่มีการดักจับคาร์บอน



นางสาว นริศรา ไตรภพ

ศูนย์วิทยทรัพยากร
จุฬาลงกรณ์มหาวิทยาลัย

วิทยานิพนธ์นี้เป็นส่วนหนึ่งของการศึกษาตามหลักสูตรปริญญาวิศวกรรมศาสตรมหาบัณฑิต

สาขาวิชาวิศวกรรมเคมี ภาควิชาวิศวกรรมเคมี

คณะวิศวกรรมศาสตร์ จุฬาลงกรณ์มหาวิทยาลัย

ปีการศึกษา 2553

ลิขสิทธิ์ของจุฬาลงกรณ์มหาวิทยาลัย

PERFORMANCE COMPARISON BETWEEN METHANE STEAM REFORMING
AND DECOMPOSITION FOR SOLID OXIDE FUEL CELL SYSTEM
WITH CARBON CAPTURE



Miss Narisra Triphob

ศูนย์วิทยทรัพยากร
จุฬาลงกรณ์มหาวิทยาลัย

A Thesis Submitted in Partial Fulfillment of the Requirements
for the Degree of Master of Engineering Program in Chemical Engineering

Department of Chemical Engineering

Faculty of Engineering

Chulalongkorn University

Academic Year 2010

Copyright of Chulalongkorn University

Thesis Title PERFORMANCE COMPARISON BETWEEN METHANE
STEAM REFORMING AND DECOMPOSITION FOR
SOLID OXIDE FUEL CELL SYSTEM WITH CARBON
CAPTURE


By Miss Narisra Triphob

Field of Study Chemical Engineering

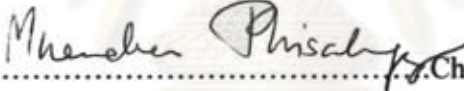
Thesis Advisor Professor Suttichai Assabumrungrat, Ph.D.

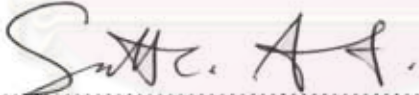
Thesis Co-advisor Associate Professor Tawatchai Charinpanitkul, Ph.D.

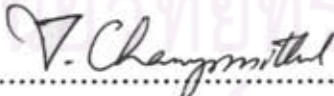
Accepted by the Faculty of Engineering, Chulalongkorn University in Partial
Fulfillment of the Requirements for the Master's Degree

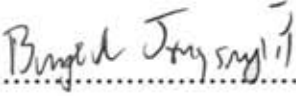

.....Dean of the Faculty of Engineering
(Associate Professor Boonsom Lerdhirunwong, Dr.Ing.)

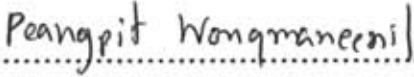
THESIS COMMITTEE


.....Chairman
(Associate Professor Muenduen Phisalaphong, Ph.D.)


.....Thesis Advisor
(Professor Suttichai Assabumrungrat, Ph.D.)


.....Thesis Co-advisor
(Associate Professor Tawatchai Charinpanitkul, D.Eng.)


.....Examiner
(Associate Professor Bunjerd Jongsomjit, Ph.D.)


.....External Examiner
(Peangpit Wongmaneevil, D.Eng.)

นริศรา ไตรภพ: การเปรียบเทียบสมรรถนะระหว่างการรีฟอร์มมิงด้วยไอน้ำและการสลายตัวของมีเทน สำหรับระบบเซลล์เชื้อเพลิงชนิดออกไซด์แข็งที่มีการดักจับคาร์บอน (PERFORMANCE COMPARISON BETWEEN METHANE STEAM REFORMING AND DECOMPOSITION FOR SOLID OXIDE FUEL CELL SYSTEM WITH CARBON CAPTURE) อ.ที่ปรึกษาวิทยานิพนธ์หลัก: ศ.ดร. สุทธิชัย อัสสะบำรุงรัตน์, อ.ที่ปรึกษาวิทยานิพนธ์ร่วม: รศ.ดร. ชวัลชัย ชรินพณิชกุล, 118 หน้า.

วิทยานิพนธ์นี้เสนอการผลิตเชื้อเพลิงไฮโดรเจนทางเลือกจากปฏิกิริยาการสลายตัวของมีเทน สำหรับนำมาใช้ทดแทนปฏิกิริยาการรีฟอร์มมิงมีเทนด้วยไอน้ำที่นิยมใช้ในระบบเซลล์เชื้อเพลิงชนิดออกไซด์แข็งทั่วไป โดยที่ปฏิกิริยาทั้งสองในระบบเซลล์เชื้อเพลิงนั้น จะถูกนำมาเปรียบเทียบทั้งในเชิงประสิทธิภาพและเศรษฐศาสตร์ เพื่อแสดงให้เห็นถึงคุณประโยชน์ของการนำปฏิกิริยาการสลายตัวของมีเทนมาใช้เป็นหน่วยผลิตเชื้อเพลิงไฮโดรเจนของระบบเซลล์เชื้อเพลิง สำหรับการวิเคราะห์ประสิทธิภาพของระบบเซลล์เชื้อเพลิงนั้นจะพิจารณาภายใต้สภาวะที่ระบบสามารถดำเนินการได้ด้วยตัวระบบเอง ไม่ต้องการพลังงานภายนอกมารองรับ ทั้งนี้พบว่าระบบเซลล์เชื้อเพลิงของปฏิกิริยาการสลายตัวของมีเทนจะให้ประสิทธิภาพรวมทางไฟฟ้าทั้งระบบน้อยกว่าในระบบเซลล์เชื้อเพลิงของปฏิกิริยาการรีฟอร์มมิงมีเทนด้วยไอน้ำ เนื่องจากคาร์บอนผลิตภัณฑ์ที่อยู่ในรูปของแข็ง ไม่ได้ถูกป้อนเข้าเซลล์เชื้อเพลิงเพื่อเผาและผลิตพลังงานออกมา แต่อย่างไรก็ตามระบบเซลล์เชื้อเพลิงของปฏิกิริยาการสลายตัวของมีเทนจะให้ค่าความหนาแน่นของไฟฟ้าที่สูงกว่าเนื่องจากปฏิกิริยาการสลายตัวนั้นจะให้เชื้อเพลิงไฮโดรเจนที่มีความบริสุทธิ์สูง จึงส่งผลให้ประสิทธิภาพทางไฟฟ้าของตัวเซลล์เชื้อเพลิงมีค่าที่สูงกว่า และให้ระบบมีขนาดเล็กและไม่ซับซ้อนเมื่อต้องคำนึงถึงการติดตั้งหน่วยดักจับและกักเก็บคาร์บอนเพิ่มเติม ที่มีความจำเป็นในระบบเซลล์เชื้อเพลิงของปฏิกิริยาการรีฟอร์มมิงมีเทนด้วยไอน้ำคือการลดมลพิษของก๊าซคาร์บอนไดออกไซด์ และสำหรับการวิเคราะห์ในเชิงเศรษฐศาสตร์นั้นพบว่า ระบบเซลล์เชื้อเพลิงชนิดออกไซด์แข็งที่ใช้ปฏิกิริยาการสลายตัวของมีเทนมีความคุ้มค่าในการลงทุนทางเศรษฐศาสตร์มากกว่าระบบที่ใช้ปฏิกิริยาการรีฟอร์มมิงมีเทนด้วยไอน้ำ เมื่อพิจารณาถึงคาร์บอนผลิตภัณฑ์ที่อยู่ในรูปของแข็งที่มีมูลค่า ถึงแม้ว่าจะวิเคราะห์ด้วยราคาของคาร์บอนแบล็กที่มีราคาค่าก็ตาม ท้ายที่สุดนี้ได้นแนะนำว่า ความสำเร็จของการนำระบบเซลล์เชื้อเพลิงชนิดออกไซด์แข็งที่นำเสนอขึ้นนี้ ไปใช้ให้เกิดประโยชน์ได้ ขึ้นกับการพัฒนาเทคโนโลยีของการผลิตร่วมของผลิตภัณฑ์ก๊าซไฮโดรเจน(เพื่อป้อนเข้าสู่เซลล์เชื้อเพลิง)และคาร์บอนที่มีมูลค่าตามที่ได้กล่าวมา เพื่อให้ได้ประสิทธิภาพรวมทางไฟฟ้าของระบบที่สูงขึ้น ระบบเซลล์เชื้อเพลิงของปฏิกิริยาการสลายตัวของมีเทนนี้ ควรจะมีการนำคาร์บอนที่ได้เป็นผลิตภัณฑ์ไปใช้ในการผลิตพลังงานไฟฟ้าเพิ่มเติมโดยผ่านระบบเซลล์เชื้อเพลิงชนิดป้อนคาร์บอนโดยตรง

ภาควิชา วิศวกรรมเคมี
สาขาวิชา วิศวกรรมเคมี
ปีการศึกษา 2553

ลายมือชื่อนิสิต Narisra Triphob (นริศรา ไตรภพ)
ลายมือชื่อ อ. ที่ปรึกษาวิทยานิพนธ์หลัก
ลายมือชื่อ อ. ที่ปรึกษาวิทยานิพนธ์ร่วม

5270345621: MAJOR CHEMICAL ENGINEERING

KEYWORDS: SOLID OXIDE FUEL CELL (SOFC)/ SIMULATION/ HYDROGEN PRODUCTION/ METHANE DECOMPOSITION/ CARBON CAPTURE AND STORAGE (CCS)/ THERMALLY SELF-SUFFICIENT OPERATION

NARISRA TRIPHOB: PERFORMANCE COMPARISON BETWEEN METHANE STEAM REFORMING AND DECOMPOSITION FOR SOLID OXIDE FUEL CELL SYSTEM WITH CARBON CAPTURE.
 ADVISOR: PROF. SUTTICHAJ ASSABUMRUNGRAT, Ph.D.,
 CO-ADVISOR: ASSOC. PROF. TAWATCHAI CHARINPANITKUL,
 D.Eng., 118 pp.

This thesis proposes the alternative hydrogen production of methane decomposition (MD) as a fuel processor to replace methane steam reforming (MSR) in the conventional solid oxide fuel cell (SOFC) system. In this work, comparison between the MD integrated with SOFC (MD-SOFC) and the MSR integrated with SOFC (MSR-SOFC) was performed in terms of SOFC performances and economic to demonstrate a benefit of using MD as a fuel processor. The performance analysis of SOFC system is evaluated based on thermally self-sufficient condition where no external energy is required for the system. Although the MD-SOFC system offers lower overall electrical efficiency than that of the MSR-SOFC as solid carbon is generated without being further combusted to generate energy; however, the MD-SOFC stack can be operated at higher power density due to high purity of hydrogen supplied to the fuel cell, resulting in higher stack cell electrical efficiency and smaller size of the system when compared to the MSR-SOFC. Moreover, the MD-SOFC system is less complicated and lower energy requirement than that of the MSR-SOFC as the CCS facility is not necessary to be included to reduce CO₂ emission. Economic analysis demonstrated that the SOFC system with MD is more competitive than the conventional system with MSR when considering the valuable by-products of solid carbon even with the low valued carbon black. Finally, it is recommended that the success of this proposed SOFC system with MD relies on the technology development on cogeneration of hydrogen and valuable carbon products. In order to achieve the higher overall electrical efficiency, the carbon product may be utilized to generate additional electrical power using direct carbon fuel cell (DCFC).

Department.....Chemical Engineering..... Student's Signature.....Narisra Triphob.....
 Field of Study.....Chemical Engineering..... Advisor's Signature.....Sutti. A.A......
 Academic Year.....2010..... Co-advisor's Signature.....V. Charinpanitkul.....

ACKNOWLEDGEMENTS

The author would like to show high sincere gratitude and appreciation to her thesis advisor, Professor Suttichai Assabumrungrat for his attentiveness, great guidance in both research study and life attitude throughout the author's research study otherwise it may be completed in a short time. Without the will power and good advice from her thesis co-advisor, Associate Professor Tawatchai Charinpanitkul, this work would never have been achieved. In addition, the author wishes to thank Assistant Professor Worapon Kiatkittipong and Dr. Suwimol Wongsakulphasatch of Department of Chemical Engineering, Faculty of Engineering and Industrial Technology, Silpakorn University, Nakhon Pathom, for their collaboration in further published material. The author would also be grateful to Associate Professor Muenduen Phisalaphong, as the chairman, Associate Professor Bunjerd Jongsomjit and Dr. Peangpit Wongmaneevil as the members of the thesis committee. The master degree scholarship and the thesis financial support from Chulalongkorn University, Thailand Research Fund (TRF) throughout the foundation of Sivavong Changkasiri are gratefully acknowledged.

Moreover, the author wishes to thank to the members of Center of Excellence on Catalysis and Catalysis Engineering, Department of Chemical Engineering, Faculty of Engineering and Chulalongkorn University for their assistance.

Finally, the author would like to respect and express great gratitude to her parents who always work hard, renounce and give the life direction. The author cannot completely achieve a success in overall education without the support from her warm family. All of the admiration and the most success of this work are devoted to her beloved parents.

CONTENTS

	page
ABSTRACT (THAI).....	iv
ABSTRACT (ENGLISH).....	v
ACKNOWLEDGEMENTS.....	vi
CONTENTS.....	vii
LIST OF TABLES.....	xi
LIST OF FIGURES.....	xii
NOMENCLATURES.....	xv
CHAPTERS	
I INTRODUCTION.....	1
1.1 Introduction.....	1
1.2 Objective.....	5
1.3 Scope of work.....	5
1.4 Thesis organization.....	6
II THEORY.....	7
2.1 Fuel cell.....	7
2.1.1 Basic principles of fuel cell.....	8
2.1.2 Major components of fuel cell.....	8
2.1.2.1 Electrodes.....	8
2.1.2.2 Electrolyte.....	9
2.1.2.3 Interconnector.....	9
2.1.3 Types of fuel cell.....	10
2.2 Solid oxide fuel cell (SOFC).....	12
2.2.1 Principle of solid oxide fuel cell (SOFC).....	13
2.2.2 Fuel gas for SOFC.....	14
2.2.3 Basic requirement of SOFC cell component.....	15
2.2.3.1 Specific component requirement of SOFC.....	15
2.2.3.2 Materials for SOFC cell components.....	15
2.2.4 SOFC operating characteristics.....	16
2.2.4.1 Open circuit voltage (OCV) or theoretical voltage.....	16
2.2.4.2 Actual cell potential.....	17

CHAPTERS	page
2.2.5 SOFC advantages and some drawbacks.....	18
2.2.5.1 SOFC advantages.....	18
2.2.5.2 Some drawbacks of SOFC.....	19
2.3 SOFC system for sustainable energy.....	20
2.3.1 Fuel processing unit.....	21
2.3.1.1Methane steam reforming (Conventional fuel processor).....	22
2.3.1.2Methane decomposition (Proposed reaction in fuel processor).....	24
2.3.2 SOFC unit.....	25
2.3.3 Power conditioner.....	25
2.3.4 Thermal energy recovery unit.....	25
2.3.5 CCS unit.....	26
III LITERATURE REVIEWS.....	28
3.1 Methane reforming reaction for H ₂ production.....	28
3.1.1 Methane steam reforming.....	29
3.1.2 Methane Partial oxidation.....	32
3.1.3 Autothermal reforming of methane.....	33
3.2 Further techniques integrated with MSR processor.....	34
3.3 Methane decomposition.....	37
3.4 SOFC system.....	41
3.5 Carbon capture and storage technologies (CCS)	46
3.5.1 CO ₂ capture or separation technology.....	47
3.5.2 CO ₂ compression to the liquid phase and transportation.....	49
3.5.3 CO ₂ Storage.....	50
IV SIMULATION.....	51
4.1 SOFC systems overview description.....	51
4.2 Fuel processors.....	54
4.3 SOFC STACK MODEL.....	55
4.3.1 Electrochemical model.....	57

CHAPTERS	page
4.3.1.1 Open circuit voltage.....	57
4.3.1.2 Actual cell potential.....	57
4.3.1.3 Overpotentials.....	57
4.3.2 SOFC calculation procedure.....	61
4.4 Supplementary equipments.....	65
4.4.1 Heat exchanger.....	65
4.4.2 Afterburner.....	66
4.5 Carbon capture and storage unit.....	66
4.5.1 CO ₂ separation from the exhaust gas.....	67
4.5.2 CO ₂ compression and transportation.....	68
4.5.3 CO ₂ Storage.....	69
4.5.4 SOFC efficiency with the further CCS application.....	69
4.6 Thermally self-sufficient operation ($Q_{\text{net}} = 0$).....	69
4.7 Economic analysis.....	70
V RESULTS AND DISCUSSION.....	73
5.1 Reaction characteristics of fuel processors.....	73
5.1.1 General Characteristics of fuel processing reaction.....	73
5.1.2 Appropriate operating condition of fuel processor.....	80
5.2 Performance analysis of solid oxide fuel cell (SOFC) system.....	83
5.2.1 Investigation of thermally self-sufficient condition ($Q_{\text{net}} = 0$)	84
5.2.1 SOFC performance analysis with the different fuel processors	
under thermally self-sufficient condition ($Q_{\text{net}} = 0$).....	87
5.3 Economic analysis.....	92
VI CONCLUSIONS AND RECOMMENDATIONS.....	97
6.1 Conclusions.....	97
6.2 Recommendations.....	99
REFERENCES.....	100
APPENDICES.....	113
APPENDIX A DETERMINING HEAT CAPACITY AND THE	
ENTHALPY CHANGE OF RELATED	
COMPOSITION.....	114

CHAPTERS	page
APPENDIX B DETERMINING GIBBS ENERGY OF FORMATION AND EQUILIBRIUM CONSTANT OF RELATED COMPOSITION.....	115
APPENDIX C LIST OF PUBLICATIONS.....	117
VITAE.....	118



ศูนย์วิทยทรัพยากร
จุฬาลงกรณ์มหาวิทยาลัย

LIST OF TABLES

	page
Table 2.1 Summary of characteristics and basic requirement of fuel cell types.....	11
Table 3.1 Comparison of three reforming reactions.....	29
Table 3.2 Summary of catalysts generally used for CH ₄ decomposition and their suitable operation temperature and carbon product characteristics.....	39
Table 4.1 Summary of model parameters.....	61
Table 4.2 Costing models and parameters used in the economic analysis....	72
Table 5.1 The performance and economic analysis of interesting SOFC systems.....	96
Table A1 Heat capacities of selected component (C_p).....	114
Table B1 Gibbs energy of formation of selected component (ΔG_f).....	116



 ศูนย์วิจัยทรัพยากร
 จุฬาลงกรณ์มหาวิทยาลัย

LIST OF FIGURES

	page
Figure 2.1 Schematic diagram of general fuel cell operation.....	7
Figure 2.2 Typical SOFC configuration (a) tubular cell (b) planar flat-plat...	12
Figure 2.3 Basic principle of SOFC operation (a) SOFC-H ⁺ (b) SOFC-O ²⁻ ...	13
Figure 2.4 Ideal and actual fuel cell voltage on various current density (V-I diagram)	17
Figure 2.5 SOFC systems for sustainable energy.....	20
Figure 2.6 Products of methane decomposition reaction.....	24
Figure 2.7 Carbon capture and storage facility (CCS).....	26
Figure 2.8 Advantage of CCS.....	27
Figure 3.1 Function of catalyst besides from catalyzed reaction.....	31
Figure 3.2 Different operating conditions for fuel reforming.....	33
Figure 3.3 Complex configuration of development of MSR.....	35
Figure 3.4 The two growth modes of filamentous carbon.....	40
Figure 3.5 Schematics of fluidized bed reactor with further mode in the study of a) Ahmed <i>et al.</i> (2009) b) Muradov <i>et al.</i> (2010).....	41
Figure 3.6 PEMFC experiment's result with the MD fuel processor.....	45
Figure 3.7 CCS The power plant with CCS technology.....	46
Figure 4.1 The conventional SOFC system configuration (with MSR in fuel processor).	52
Figure 4.2 The conventional SOFC system configuration integrated with CCS facility.....	53
Figure 4.3 The proposed SOFC system configuration (with MD in fuel processor).	53
Figure 4.4 Schematic diagrams of fuel processors: a) MSR b) MD.....	54
Figure 4.5 The flowchart of the calculation procedure in the program.....	62
Figure 4.6 The SOFC stack area separation for the electrochemical calculation.....	63
Figure 4.7 Three important steps in the CCS facility.....	66

Figure 5.1 Methane equilibrium conversions between conventional methane steam reforming (solid line with marker point) and decomposition (dash line) at the atmospheric pressure and varying temperature.....	74
Figure 5.2 Hydrogen to methane (H_2/CH_4) mole ratio between conventional methane steam reforming (solid line with marker points) and decomposition (dash line) at the atmospheric pressure and varying temperature.....	75
Figure 5.3 Hydrogen concentrations between conventional methane steam reforming (solid line with marker points) and decomposition (dash line) at the atmospheric pressure and varying temperature...	76
Figure 5.4 Total energy requirements of conventional methane steam reforming at the atmospheric pressure, varying temperature and steam to carbon ratio.....	77
Figure 5.5 Energy requirements of conventional methane steam reforming at the atmospheric pressure, varying high temperature and steam to carbon ratio.....	79
Figure 5.6 Energy requirements of methane decomposition at the atmospheric pressure, varying high temperature.....	79
Figure 5.7 Product distribution of conventional methane steam reforming ($H_2O:CH_4=2.5$) (solid line) and of decomposition (dash line) at atmospheric pressure and varying temperature (basis on 1 mole of pure methane for both processes)	82
Figure 5.8 Energy requirements between methane conventional steam reforming (solid line) and decomposition (dash line) at the atmospheric pressure and varying temperature.....	83
Figure 5.9 The thermally self-sufficient operation of SOFC integrated with conventional methane steam reforming fuel processor.....	84
Figure 5.10 The thermally self-sufficient operation of SOFC integrated with methane decomposition fuel processor.....	85

Figure 5.11 Q_{net} at different fuel utilization and operating voltage at 1073 K in conventional SOFC system with MSR, basis on 1 mole of pure methane ($\text{H}_2\text{O}:\text{CH}_4=2.5$)	86
Figure 5.12 Q_{net} at different fuel utilization and operating voltage at 1073 K. in proposed SOFC system with MD, basis on 1 mole of pure methane	86
Figure 5.13 Power density and fuel utilization at various operating voltages for different SOFC systems at the thermally self-sufficient operation ($Q_{\text{net}} = 0$).....	86
Figure 5.14 Voltage information at various fuel utilizations for different SOFC systems at the thermally self-sufficient operation ($Q_{\text{net}} = 0$).....	88
Figure 5.15 Thermal energy at various operating voltages for different SOFC systems at the thermally self-sufficient operation ($Q_{\text{net}} = 0$).....	89
Figure 5.16 The thermally self-sufficient operation of SOFC integrated with conventional methane steam reforming fuel processor and CCS facility.....	90
Figure 5.17 Electrical efficiency for different SOFC systems at the thermally self-sufficient operation ($Q_{\text{net}} = 0$).....	91
Figure 5.18 Q_{stack} and fuel utilization for different SOFC systems at the thermally self-sufficient operation ($Q_{\text{net}} = 0$).....	92
Figure 5.19 Power density and stack area for different SOFC systems at the energy self-sufficient operation ($Q_{\text{net}} = 0$).....	93

NOMENCLATURES

$A_{\text{single cell}}$	active area of SOFC single cell (m^2)
A_{total}	total active area of SOFC (m^2)
A_f	active area of f -th fuel utilization region (m^2)
C_p	heat capacity ($\text{J mol}^{-1} \text{K}^{-1}$)
C_{cell}	capital cost of SOFC single cell (\$)
$C_{\text{compressor}}$	capital cost of compressor (\$)
C_{stack}	capital cost of SOFC stack (\$)
$D_{i,K}$	Knudsen diffusivity of component I ($\text{cm}^2 \text{s}^{-1}$)
D_{A-B}	ordinary diffusivity of gas A versus gas B ($\text{cm}^2 \text{s}^{-1}$)
$D_{m(\text{eff})}$	effective diffusion coefficient of electrode m ($\text{cm}^2 \text{s}^{-1}$)
$D_{i,K(\text{eff})}$	effective Knudsen diffusivity of component I ($\text{cm}^2 \text{s}^{-1}$)
$D_{A-B(\text{eff})}$	effective ordinary diffusivity of gas A versus gas B ($\text{cm}^2 \text{s}^{-1}$)
E_a	actual electrical power consumption
E	theoretical open-circuit voltage of the cell (V)
E^0	theoretical open-circuit voltage of the cell at standard pressure (V)
E_{act}	activation energy (kJ mol^{-1})
F	Faraday constant (9.6495×10^4) (C mol^{-1})
G	Gibb's free energy (kJ mol^{-1})
ΔG_f	Gibbs energy of formation (kJ mol^{-1})
$\Delta G_{\text{reaction}}$	Gibbs energy for a reaction (kJ mol^{-1})
ΔH°	heat of reaction (kJ mol^{-1})
HP	power consumption in compressor (HP)
i	current density (A cm^{-2})
$i_{o,m}$	exchange current density of electrode m (A cm^{-2})
K_j	equilibrium constant of reactions j (various units)
l_m	thickness of electrode m (μm)
l_a	thickness of anode electrode (μm)
l_c	thickness of cathode electrode (μm)
L	thickness of electrolyte (μm)
n_i	mole of component i (mol)

N_{cell}	number of SOFC single cell (-)
N_{stack}	number of SOFC stack (-)
P	pressure (Pa)
p_{ave}	average power density (W cm^{-2})
p_i	partial pressure of component i (Pa)
p_i^1	inlet pressure of component i (Pa)
Q_{net}	difference between thermal energy demand and generation in SOFC system (kW)
Q_{stack}	thermal energy supplied from fuel cell stack (kW)
$Q_{\text{afterburner}}$	thermal energy supplied from after burner unit (kW)
R	gas constant ($8.3145 \text{ J mol}^{-1}\text{K}^{-1}$)
S/C	steam to carbon ratio
T	temperature (K)
U_f	fuel utilization (-)
V	cell voltage (V)
W	electricity requirement (kW)
W_{ccs}	electricity work consumed in carbon capture and storage unit (kW)
z	number of electron participating in the electrochemical reaction (-)

GREEK LETTERS

σ_{AB}	collision diameter (\AA)
Ω_D	collision integral (dimensionless)
ε_{AB}	Lennard-Jones energy interaction parameter scaled with respect to the Boltzman constant (dimensionless)
α	charge transfer coefficient (dimensionless)
ξ	electrode tortuosity (dimensionless)
δ_{O_2}	coefficient used in concentration overpotential (dimensionless)
η_{loss}	total loss (V)
η_{act}	activation loss (V)
η_{conc}	concentration loss (V)

η_{ohm}	ohmic loss (V)
η_{is}	isentropic efficiency
η_{m}	mechanism efficiency
γ	pre-exponential factor for electrode exchange current density (A m^{-2})

SUBSCRIPTS

a	anode
c	cathode
P _{ef}	power equivalent factor
ref	reference condition
MD	Methane decomposition
MSR	Methane steam reforming
WGS	water gas shift reaction
RWGS	reverse water gas shift reaction
CCS	Carbon capture and storage
SOFC	Solid oxide fuel cell
TER	Thermal to electrical ratio

ศูนย์วิทยทรัพยากร
จุฬาลงกรณ์มหาวิทยาลัย

CHAPTER I

INTRODUCTION

1.1 Introduction

Over the past decades, the continuous growth of the human's energy requirement has caused a number of problems such as shortage of natural resources, environmental problems and climate changes. With the traditional energy production technologies, combustion of fossil fuels has emitted a large amount of green house gases to the environment. Especially, CO₂ as a greenhouse gas has been considered as a main contributor for the global warming problem (Simbeck, 2004; Suelves *et al.*, 2005; Naser and Timothy, 2007; Edwards *et al.*, 2008 and Ahmed *et al.*, 2009). Moreover, it is produced around 21.3 billion tons per year (http://en.wikipedia.org/wiki/Fossil_fuel) resulting in the raising of the world temperature around 1.7 to 4.9 °C since 1990 (Boudghene Stambouli and traversa, 2002). Therefore, many researchers have focused on the development of alternative energy with high efficiency as well as environmental friendly power generation technologies.

Fuel cell is one of the promising clean technologies which directly transforms the chemical energy of a fuel into high efficiency electrical energy and reduces greenhouse gas emission (Karl and Gunter, 1995; Poirer and Sapundzhiev, 1997; Martin and Ralph, 2003). Especially in solid oxide fuel cell (SOFC) type, a variety of fuels (e.g. gasoline, diesel, alcohol, natural gas, coal, hydrocarbon and petroleum based substances) (Assabumrungrat *et al.*, 2005; Hernandez-Pachecco *et al.*, 2005; Hussain *et al.*, 2006; Naser and Timothy, 2007; Sangtongkitcharoen *et al.*, 2008; Patcharavorachot *et al.*, 2010 and Arponwichanop *et al.*, 2010) can be used in this SOFC systems due to its high operating temperatures (873-1273 K) (Boudghene Stambouli and Traversa, 2002; Douvartzides *et al.*, 2008 and Piroonlerkgul *et al.*, 2008; 2009). Furthermore, it has offered several advantages; for examples, chemical durability in SOFC stack, easy operation and high quality by-product thermal energy.

Typically, a SOFC system consists of 3 main parts; i.e., 1) a fuel processor for hydrogen production, 2) a SOFC unit which subsequently generates electricity from hydrogen and recovers useful thermal energy from spent fuel and 3) an afterburner where residual fuel is completely combusted in order to supply thermal energy coupled with SOFC to other energy consumption units.

Generally, the fuel processor plays an important role in order to produce and carry the H₂ fuel to the electrical generation step of SOFC stack. In the consideration of appropriate primary feed at fuel processor, methane is an attractive and convenient fuel for the SOFC system due to its availability, highest hydrogen to carbon ratio in the overall hydrocarbon substances and low cost (Ermakova *et al.*, 2000; Vivanpatarakij *et al.*, 2007 and Serrano *et al.*, 2010). There are several reaction routes for generating hydrogen from methane such as methane steam reforming (MSR), partial oxidation, autothermal reforming, and methane decomposition (Edward and Maitra, 1995; Suelves *et al.*, 2005; Bonura *et al.*, 2006; Vivanpatarakij *et al.*, 2007; Li *et al.*, 2008 and Wang *et al.*, 2009). Methane steam reforming (MSR) (Eq. 1.1) is probably the most well-established technology nowadays and widely used as the fuel processor in the conventional SOFC system. It offers the highest hydrogen production but with some disadvantages such as high reaction energy consumption, having carbon oxides and steam as impurities in the reformed gas and taking place of side reaction at changing temperature.



A number of researches have focused on the methane-fuelled SOFC systems by proposing several ways to improve the efficiency and performance of the systems. Due to the impurities in the reformed gas from the conventional SOFC system, membrane reactor technology (the combination of membrane and steam reforming reactor) (Powell and Qiao, 2006; Damen *et al.*, 2006) is a promising pre-carbon capture technology in power generation. Especially a palladium type membrane which is highly selective to hydrogen has been widely examined (Basile *et al.*, 2003; Galucci *et al.*, 2004; Fernandes and Soares Jr, 2006; Patel and Sunol, 2007). It was proposed to be employed as a fuel processor as it can offer high purity of hydrogen

and increase the methane conversion. Vivanpatarakij *et al.* (2009) presented the upgrading of SOFC system with the applications of various operation modes in membrane reactor considering the combined compressor and vacuum pump. However, this system is hardly provided in the real operation due to high cost of membrane material and high operating pressure (Sangtongkitcharoen *et al.*, 2008 and Piroonlerkgul *et al.*, 2009).

The addition of CaO-CO₂ acceptor and water-gas shift reactor are also proposed to provide the higher purity of hydrogen, since it is constructed after the fuel processor (Abanades, 2002; Choudary and Goodman, 2002; Barelli *et al.*, 2008; Grasa *et al.*, 2008; Vivanpatarakij *et al.*, 2009; Piroonlerkgul *et al.*, 2010). The removal of CO₂ from fuel prior to be fed in SOFC can improve SOFC performance (Iordanidisa *et al.*, 2006; Dalle Nogare *et al.*, 2007; Vivanpatarakij *et al.*, 2009 and Piroonlerkgul *et al.*, 2010). Although this technique can supply the high purity of hydrogen, little amount of CO₂ is also produced in the afterburner, consequently, the conventional SOFC system should be equipped with a carbon capture and storage (CCS) facility after the afterburner. CCS has a role in the reduction of global warming problem, because it prevents the CO₂ emitted to the atmosphere. This CCS generally has three main steps consisting of CO₂ separation, CO₂ compression to the liquid form for easy transport and storage of concentrated liquid CO₂ under the ocean or underground (geological formation) at depth of more than 800 meters (Damen *et al.*, 2006; 2007, Abu-khader, 2006 and Kurt *et al.*, 2009). However, this system may not be appropriate in the present time due to high capital cost with complex system and high energy demand (Poirer and Sapundzhiev., 1997; Piroonlerkgul *et al.*, 2008; 2009).



Methane decomposition (MD) (Eq. 1.2) is an interesting alternative reaction for hydrogen production as it requires lower energy consumption than conventional MSR. The gas product contains CO_x-free hydrogen due to absence of oxidant substances (steam, oxygen). Although the hydrogen generated from MD is less than that from MSR. It has performed more advantages for the SOFC. When using pure hydrogen generated by MD as a fuel, the performance of this SOFC is improved

better than the conventional SOFC (Eguchi *et al.*, 2002; Baron *et al.*, 2004; Suwanwarangkul *et al.*, 2006; Damen *et al.*, 2006; Bonura *et al.*, 2006; Yusuke *et al.*, 2009 and Piroonlerkgul *et al.*, 2009). Considering its by-products, MD produces a separated phase by-product as it only captures the carbon in to the valuable solid form. Therefore, no carbon oxides are presented to the SOFC, resulting in a long operation life time of the catalyst and SOFC stack (Takenaka *et al.*, 2001; Villacampa *et al.*, 2003; Coutelieris *et al.*, 2003 and Sangtongkitcharoen *et al.*, 2005). Furthermore, this solid carbon can be used as a commodity product in the various fields (e.g. adsorption material, membrane, catalyst, electrical devices and fuel cell) or sequestered (or stored) for future use (Muradov, 2001; Meyer, 2009 and Muradov *et al.*, 2010).

Regarding the global warming, MD is considered as an alternative fuel processor for MSR. Carbon in methane is first captured at the fuel processor in the form of solid carbon. Therefore, CCS facility is not necessary to capture CO₂ in the SOFC system with MD. The system would become less complicated and require lower cost and energy consumption. However, MD is not widely proposed to be the alternative fuel processor in SOFC system (Eguchi *et al.*, 2002; Baron *et al.*, 2004; Bonura *et al.*, 2006 and Yusuke *et al.*, 2009). The comparison of MD and MSR in terms of performance and economic analysis should be of interest in order to decide whether MD or conventional MSR is appropriate for a SOFC system.

Therefore, this study is aimed to evaluate and compare the performance between the two fuel processors; MSR and MD, particularly when carbon capture and storage is demanded for CO₂ capture in MSR. The SOFC systems are considered to operate at a thermally self-sufficient condition ($Q_{net} = 0$) (Sangtongkitcharoen *et al.*, 2005; Palazzi *et al.*, 2007; Vivanpatarakij *et al.*, 2009 and Piroonlerkgul *et al.*, 2008; 2009) at which no external energy is needed and the highest possible electrical power generation is achieved. Furthermore, the economic analysis is carried out to determine the appropriate fuel processor for the SOFC at the optimal operating condition (operating voltage and fuel utilization) based on the same net electrical power of 1MW. Better performances of the SOFC system and reduction of environmental problems are expected when the SOFC is equipped with MD as a fuel processor.

1.2 Objective

To compare the performances of the methane-fuelled SOFC systems with different fuel processors; i.e., conventional methane steam reforming and decomposition, particularly when carbon capture and storage is further demanded for CO₂ capture in steam reforming, and to perform economic analysis of the two fuel processors.

1.3 Scope of work

1.3.1 Simulate the conventional (methane steam reforming) and proposed (methane decomposition) fuel processor on the basis of 1 mol s⁻¹ of methane using ASPENTM PLUS PROGRAM to determine the characteristics of the reactions at varying temperatures.

1.3.2 Select the optimal condition for each fuel processor namely both of reaction temperature and steam to methane ratio of methane steam reforming.

1.3.3 Simulate performances of the two SOFC systems with different fuel processors to determine the amount of energy involved for all units.

1.3.4 Evaluate and compare the performances of the two SOFC systems at varying fuel utilization and operating voltage to find the thermally self-sufficient condition (at $Q_{net} = 0$) where no additional energy is demanded from an external source.

1.3.5 Calculate the overall electrical efficiency when carbon capture and storage (CCS) facility was installed in the conventional SOFC (MSR-SOFC-CCS) in order to prevent CO₂ emission to atmosphere.

1.3.6 Perform economic analysis of the three SOFC systems (SMR-SOFC, SMR-SOFC-CCS and MD-SOFC) based on a net electrical power generation of 1 MW.

1.4 Thesis organization

This thesis is organized as follows:

- Chapter I is the general introduction indicating the motivation, rationale , objective and scope of this research.
- Chapter II provides the fundamental theory for this research namely the principle of fuel cell, the specific characteristic of solid oxide fuel cell (SOFC), general characteristic of methane decomposition and conventional steam reforming, carbon capture and storage (CCS), etc.
- Chapter III reviews the previous research works on SOFC operation leading to the motivation on the proposed methane decomposition in this research. This chapter consists of the methane reforming reaction for hydrogen production, further techniques integrated with MSR processor, methane decomposition, SOFC system and CCS technologies.
- All about the research simulations methodology including the simulation program, mathematical models and calculation procedure in the performance analysis of SOFC are presented in Chapter IV.
- In Chapter V, the simulation and calculation results are presented and discussed. It is divided into three main parts; reaction characteristics of fuel processors, performance analysis of solid oxide fuel cell (SOFC) system and economic analysis.
- The overall conclusion from this research analysis and some recommendations for future research works are in Chapter VI.
- Finally, the details of thermodynamic data and properties of related composition are included in Appendices at the end of this thesis.

CHAPTER II

THEORY

2.1 Fuel cell

A fuel cell is an electrochemical device that directly transforms the chemical energy of fuel gas into electrical energy (DC), thermal energy and water without the need for direct combustion as an intermediate step, giving much higher conversion performances and lower green house gases than conventional fossil fuel power generation. As shown in Figure 2.1, the basic physical structure of fuel cell generally consists of an ion conducting electrolyte in center of a cathode (positive electrode) and an anode (negative electrode), furthermore, external circuit (load) connecting with two electrode used in the current collection and separating each unit cell in the stack by the separator (bipolar) plate.

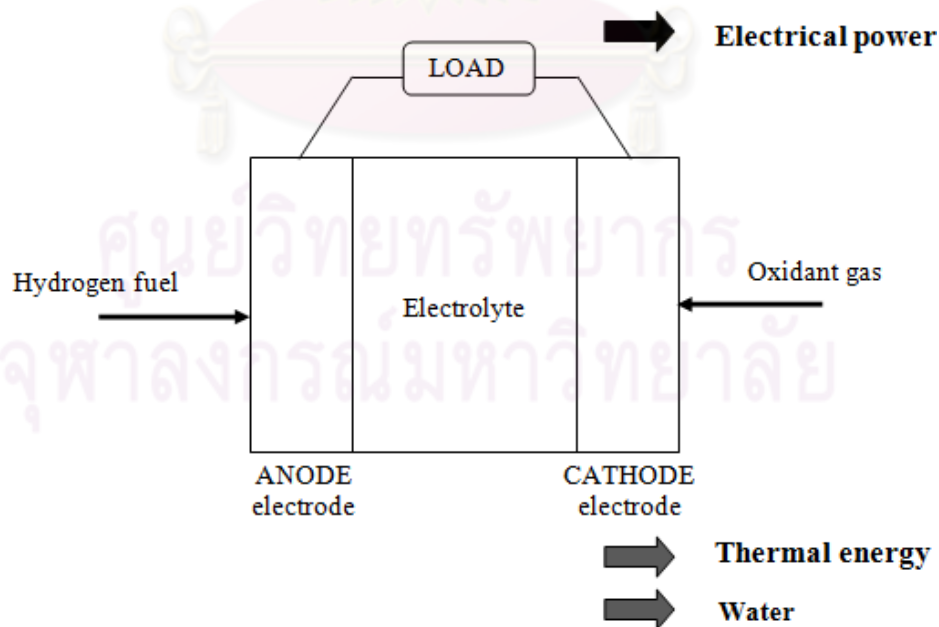


Figure 2.1 Schematic diagram of general fuel cell operation

2.1.1 Basic principles of fuel cell

The operating principle of fuel cell is quite similar to that of conventional batteries such as electrochemical conversion of reactants to generate electricity, a reaction occurs between hydrogen fuel and oxidant gas (oxygen from air) through electrodes and via an ion conducting electrolyte. However, unlike batteries, fuel cell does not run down or require recharging; it can be operated as long as both hydrogen fuel and oxygen gas are supplied into electrodes.



Generally, fuel cell operation is initially when oxidant gas and hydrogen fuel are fed into cathode and anode, respectively. The chemical reaction is shown in Eq. 2.1. When the electrochemical reaction occurs, the electrons flows pass the external circuit (load) and the ions are conducted across the electrolyte. Thus, electrical current is created while the by-products are generated in the forms of water and thermal energy.

2.1.2 Major components of fuel cell

The typical fuel cell (Figure 2.1) is mainly composed of two electrodes (anode and cathode), an electrolyte and interconnector. Separator plates, extra components, are needed when more than one unit cell of fuel cell is required. The required properties can be concluded as follows:

2.1.2.1 Electrodes

Electrodes (Boudghene Stambouli and Traversa, 2002) play an important role as their main function is to provide a reaction between the reactant and the electrolyte, without themselves being damaged or corroded. It must also contact the three phases, i.e., the gaseous fuel, electrolyte and electrode itself, when total components of fuel cell assemble to operate in power generation. The basis requirement properties of electrode are typically porous and made of an electrically conductive material.

Anode

Anode is operated in the reducing atmosphere, oxidation reaction has an effect to release the electrons. Therefore, high electronic conductivity is needed as electrons transfer to create current into the external circuit. Furthermore, it also should tolerate under the reducing atmosphere. Several requirement properties of anode are different from cathode due to difference in function. In some cases, anode also has the catalytic properties such as using in catalytic reforming in hydrocarbon fuelled fuel cell system.

Cathode

In order to conduct the electron from anode, cathode also has the high electronic conductivity and enough porosity. Generally, cathode is operated in the oxidizing atmosphere at a high temperature, hence, properties of material in cathode must have high chemical and structural stability. When it is fitted together with electrolyte and interconnector, it should have the suitable of thermal expansion and less reactivity with vicinity components.

2.1.2.2 Electrolyte

The electrolyte is used to prevent the two electrodes to come into electronic contact by blocking the electron. It must permit the flow of charged ions from one electrode to the other to maintain the overall electrical charge balance. The required properties of electrolyte are:

- High ion conductivity
- Less electronic transfer for avoidance of voltage loss
- Dense electrolyte to prevent gas mixing
- Thermal stability during operation

2.1.2.3 Interconnector

Interconnector is installed to collect the current from fuel cell. It is located to link the anode with external circuit, and its required properties are:

- High electronic conductivity
- Chemical and structural stability during operation
- Appropriated thermal expansion
- Less reactivity with vicinity components

2.1.3 Types of fuel cell

Generally, fuel cells are mostly classified by the type of electrolyte used in the fuel cells. The chemical characteristics of electrolyte affect to the selection of fuel and operating condition. The choice of electrolyte dictates the operating temperature range of the fuel cell. The operating temperature and useful life of fuel cell dictate the physicochemical and thermomechanical properties of the material used in the cell components (i.e., electrodes, electrolyte, interconnect, current collector, etc.). Aqueous electrolytes are limited to operating temperature of 473K or lower because of their high vapor pressure and rapid degradation at high operating temperature.

Nowadays, six major types of fuel cell are available as shown:

1. Proton-exchange membrane fuel cell (PEMFC)
2. Direct methanol fuel cell (DMFC)
3. Alkaline fuel cell (AFC)
4. Phosphoric acid fuel cell (PAFC)
5. Molten carbonate fuel cell (MCFC)
6. Solid oxide fuel cell (SOFC)

Each types of fuel cell have the difference of specific characteristic and basic requirement as shown in Table 2.1. They are also classified on the basis of operating temperature into 2 groups; low temperature (PEMFC, DMFC, AFC, PAFC) and high temperature range group (MCFC, SOFC). In the low operating temperature group, all the fuel must be firstly converted to hydrogen prior to entering the fuel cell. The anode catalyst in this low operating temperature of fuel cell should be strongly poisoned by CO. In addition, the high operating temperature, it allows the ability of internal fuel processing, therefore, they (MCFC, SOFC) supply fuel flexibility and offer high electrical efficiency.

Table 2.1 Summary of characteristics and basic requirement of fuel cell types

(Rayment and Sherwin, 2003; Haile, 2003; Andujar and Segura, 2009; Neef, 2009 and Kirubakaran *et al.*, 2009)

Fuel cell type	PEMFC	DMFC	AFC	PAFC	MCFC	SOFC
Electrolyte	Hydrated Polymeric Ion Exchange Membrane	Polymeric Ion Exchange Membrane	Mobilized or Immobilized Potassium Hydroxide in asbestos matrix	Immobilized Liquid Phosphorus Acid in SiC	Immobilized Liquid Molten Carbonate in LiAlO ₂	Ceramic
Operating temperature (K)	313-353	333-393	338-493	433-473	903-923	873-1273
Fuels	H ₂	CH ₃ OH or alcohol solution	H ₂	H ₂	H ₂ , CO, CH ₄ , etc	H ₂ , CO, CH ₄ , etc
Oxidants	O ₂ , air	O ₂ , humid air	O ₂ , air	O ₂ , air	O ₂ , air, CO ₂	O ₂ , air
Diluents	CH ₄ , H ₂ O, CO ₂	CH ₄ , H ₂ O, CO ₂	-	CH ₄ , H ₂ O, CO ₂	H ₂ O, CO ₂	H ₂ O, CO ₂
Poisons	CO, H ₂ S, COS	CO, H ₂ S, COS	CH ₄ , H ₂ O, CO ₂ , CO, H ₂ S, COS	CO, H ₂ S, COS	H ₂ S, COS	H ₂ S, COS
Applications	mobile, laptop, low power generation	mobile, laptop, other potable electronic application	transportation and space shuttle	medium to large power generation with CHP system	medium to large power generation	medium to large power generation with CHP system
Electrical power range (kW)	0.01-250	0.001-100	0.1-50	50-1,300	200-200,000	0.5-2,500
Electrical efficiency (%)	40-55	40	50-55	40-45	50-60	40-60

2.2 Solid oxide fuel cell (SOFC)

With the longest continuous development period starting in the late 1950s, SOFC promises to be extremely useful in large scale application over another type of fuel cell. It shows the desirable characteristic of power generation which can be considered for a wide range of applications including stationary power generation, mobile power, auxiliary power for vehicles and specialty applications (Boudghene Stambouli and Traversa, 2002; Fuel cell Handbook, 2004). Some prominent points of SOFC are concluded as listed below:

- SOFC is composed of all solid-state materials.
- The solid-state character of all SOFC components indicates that there is no fundamental limitation on the cell configuration. The cells are being installed in two main configurations, i.e. tubular cells or rolled tubes, and planar flat-plates configuration as shown in the Figure 2.2 a) and b) respectively.

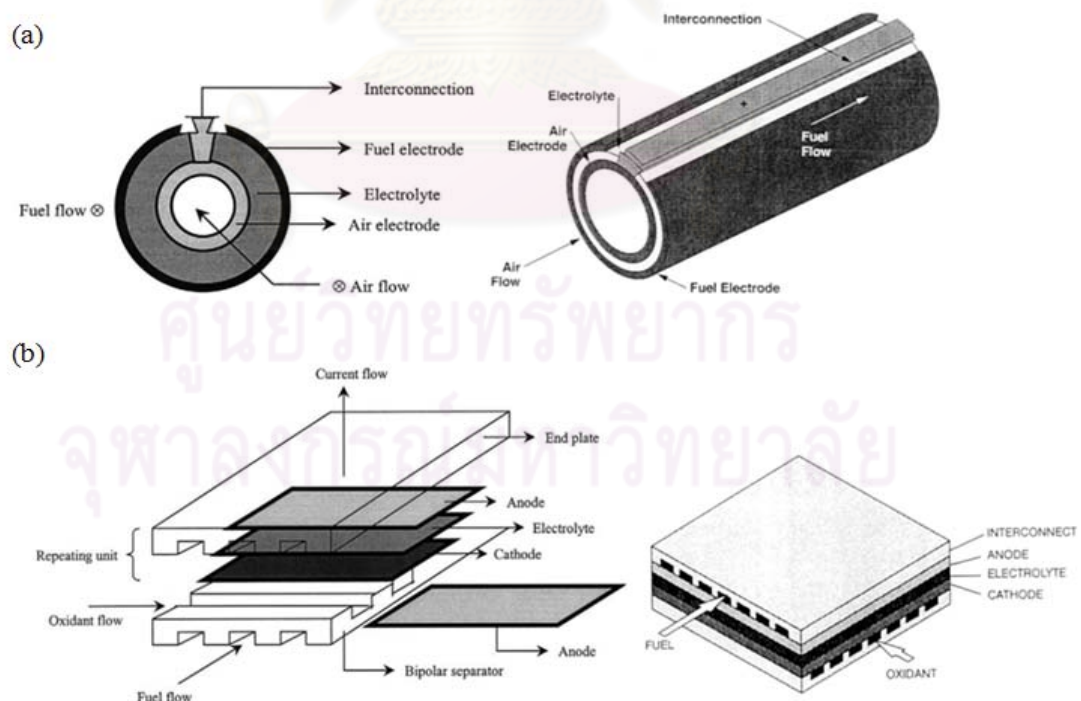


Figure 2.2 Typical SOFC configurations (a) tubular cell (b) planar flat-plate (Hammou and Guindet, 1997 and Boudghene Stambouli and Traversa, 2002)

- Particularly rigid ceramics electrolyte, it has more chemical and physical durability than other types of fuel cell resulting in the high operating temperature and endurance in corrosion problem.
- Its cells can operate at temperatures as high as 1273K, significantly higher than any fuel cell type as mentioned in the Table 2.1.
- With its extremely high temperature operation range (873-1273K), SOFC can utilize various types of fuel (e.g. alcohol, natural gas, coal and petroleum based substances), allows internal reforming, promotes electrocatalysts with non-precious metals, has fast chemical reaction and produces high quality electrical power with thermal energy.

2.2.1 Principle of solid oxide fuel cell (SOFC)

SOFCs are divided into two operations based on the type of conducted ion such as SOFC with oxygen-ion conducting electrolyte (SOFC-O²⁻) and SOFC with proton-ion conducting electrolyte (SOFC-H⁺). Major differences between two types of SOFC are the direction of ion flowing through the ceramic electrolyte and the location of produced water by-product occurring in the opposite cell sides as shown in Figure 2.3 (Boudghene Stambouli and Traversa, 2002; Andujar and Segura, 2009).

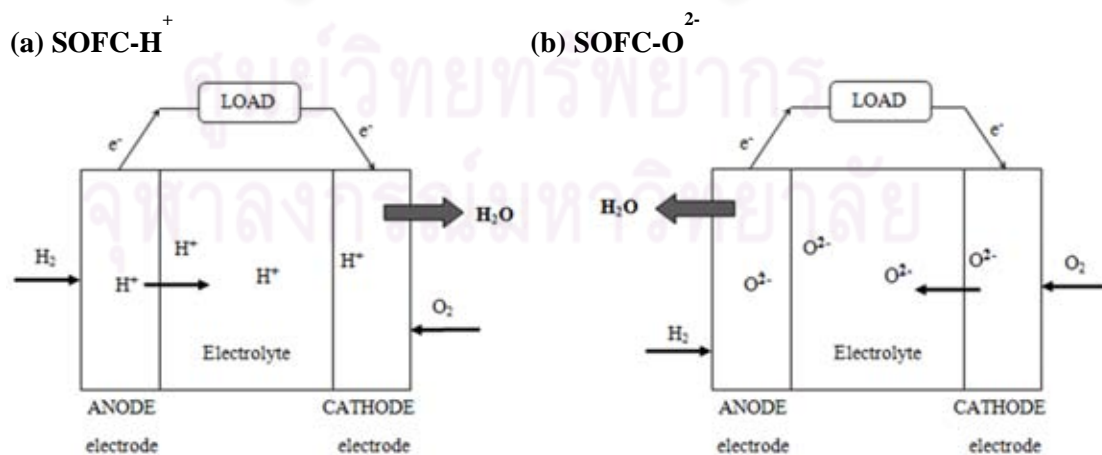
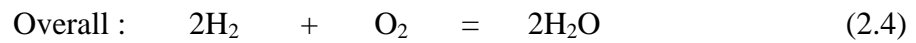
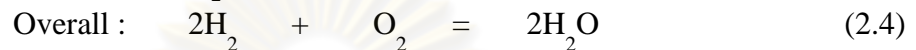
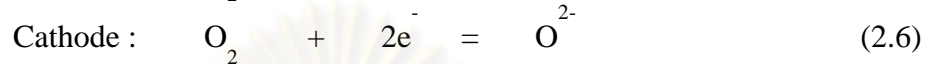
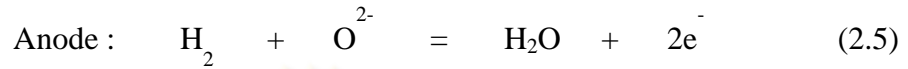


Figure 2.3 Basic principle of SOFC operation (a) SOFC-H⁺ (b) SOFC-O²⁻

The electrochemical reaction in the SOFC-H⁺



The electrochemical reaction in the SOFC-O²⁻



2.2.2 Fuel gas for SOFC

SOFC requires only a single fuel processor to pre-reform their fuel, which can be gasoline, diesel, alcohol, natural gas, coal, hydrocarbon and petroleum based substances (Assabumrungrat *et al.*, 2005; Hussain *et al.*, 2006; Naser and Timothy, 2007; Sangtongkitcharoen *et al.*, 2008; Patcharavorachot *et al.*, 2010 and Arponwichanop *et al.*, 2010). The nature of overall pollutions from the fuel cell must vary correspondingly with the fuel gas mixture. Using hydrocarbon, for which a supporting infrastructure is recently available, proposed a variety of advantages over using hydrogen.

Firstly, hydrocarbons are much easier to transport and to store since they are in a stable state which requires no processing before use. They are also more efficient at producing energy. Methane is an attractive and convenient hydrocarbon fuel for the SOFC system (Ermakova *et al.*, 2000; Boudghene Stambouli and traversa, 2002; Vivanpatarakij *et al.*, 2007 and Serrano *et al.*, 2010), it offers the large amount of hydrogen to carbon ration. In the electrochemical benefit, methane for example yields eight electrons per molecule whereas hydrogen only yields two electrons energy. This large amount of electrons must affect on the amount of electrical energy production. This advantage could be magnified with the indirect feed of more complex hydrocarbons.

2.2.3 Basic requirement of SOFC cell component

2.2.3.1 Specific component requirement of SOFC

The identification of SOFC component kinds should consider the specific function of each component of SOFC with the characteristic of SOFC operating condition. Therefore, the total component of SOFC stack cell must meet the basic requirement to provide long operation life time of power generation such as (Nguyen, 1993; Song, 2002 and Kirubakaran *et al.*, 2009):

- Suitable stability (chemical, phase, morphological and dimensional) and conductivity.
- Chemical compatibility with other components
- Similar thermal expansion all over the cell operation to avoid cracking
- Dense electrolyte to avoid gas mixing
- Porous anode and cathode to consent gas transport to the reaction sites
- High strength and toughness properties
- Fabricability and amenable to particular fabrication conditions
- Low overall cost
- Compatibility at higher operating temperatures at which the ceramic structures are fabricated.

2.2.3.2 Materials for SOFC cell components

(Boudghene Stambouli and Traversa, 2002)

- Electrolyte
The extensively used electrolyte of SOFC is a dense or non-porous ceramic material which has the excellent properties of oxygen ion-conductivity at high operating temperature such as stabilized zirconia, especially yttria (Y_2O_3)-stabilised zirconia (ZrO_2) or YSZ.
- Anode
Anode material must be metals due to the reduction condition of fuel gas. Furthermore, this metal material should be non-oxidized, even if the composition of fuel shifts during the operation of cell. The anode structure should be fabricated with a little porous to assist mass transfer of reactant

and product gases. SOFC anode is mostly fabricated from the composite powder mixtures of electrolyte material (YSZ) and nickel oxide (NiO) at which NiO subsequently being reduced to nickel (Ni) metal prior to operation. Hydrocarbons can be directly reformed in SOFC anode where the Ni/YSZ catalyzes the reaction kinetic coupled with oxygen ionic carrying. It should be notes that the state of art SOFC nickel anode can perform sufficient activity for the conventional SOFC without the need additional catalyst (Clarke *et al.*, 1997 and Dick, 1998). And it can be achieved the internal reforming or auto reforming inside SOFC cell.

- Cathode

Similar properties to the anode, cathode is a porous structure at which allows the rapid mass transfer of reactant and product gases. Under the high operating temperature of SOFC, noble metal or electronic conducting oxide is required to use as cathode material. Perovskite-type lanthanum strontium manganite (LSM) and lanthanum calcium manganite (LCM) present the excellent thermal expansion match with zirconia electrolyte and provide a good performance at SOFC temperature range. Generally, Strontium (Sr)-doped lanthanum manganite (LaMnO_3) is widely used to be SOFC cathode (Yamamoto, 2000).

2.2.4 SOFC operating characteristics

2.2.4.1 Open circuit voltage (OCV) or theoretical voltage

OCV is an ideal voltage in the electrochemical reaction based on thermodynamic equilibrium between H_2 fuel and oxidant gas. This value is obtained at specific operating condition such as temperature, pressure and reactant composition. Especially in reactant compositions, the difference in concentrations of components between anode and cathode electrode, namely H_2 pure at anode feed and O_2 pure at cathode feed, provide a maximum ideal difference potential at both of electrodes resulting in OCV of the SOFC cell. The OCV plays an important role to be the

driving force in taking electron transport from one electrode to another and generates the current passing complete circuit.

2.2.4.2 Actual cell potential

The actual cell potential is decreased from its ideal potential (OCV) because of the irreversible potential losses as shown in the Figure 2.4. These losses are often referred to as polarization, overpotential or overvoltage which can be categorized as followed:

- Activation overpotential

Activation overpotential is the one type of voltage loss which occurs from electrochemical reaction at the electrodes. This reaction requires some energy to overcome its activation energy (E_a), for example, adsorption energy of reactant on the electrode surface and desorption energy of product out of surface. Generally, this loss dominates at low current density, the V - I diagram exhibits non-linear. The main variable controlling this loss is operating temperature in order to affect the reaction rate of electrochemical. At high operating temperature of SOFC, the rate-determining step is very fast resulting in the decreasing of activation overpotential and the V - I diagram becomes linear.

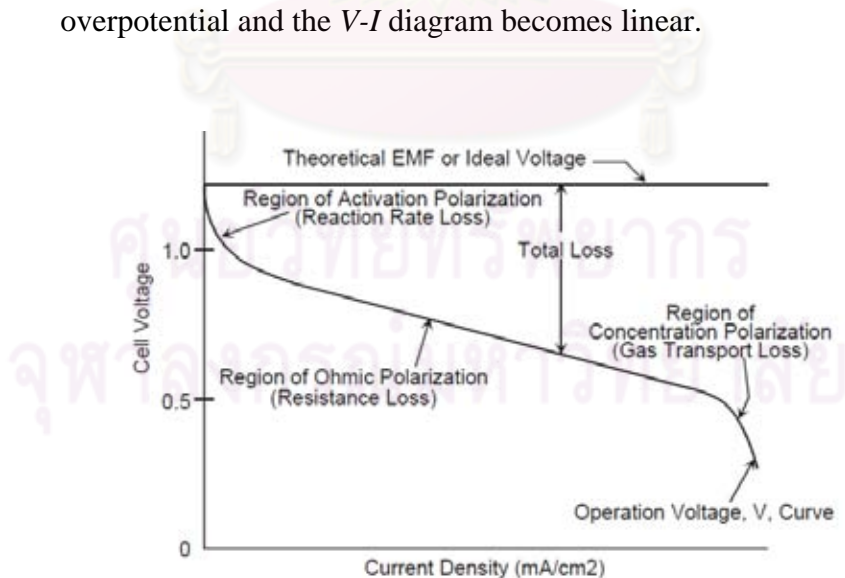


Figure 2.4 Ideal and actual fuel cell voltage on various current density (V - I diagram) (Fuel cell Handbook, 2004)

- Concentration overpotential or mass-transport-related loss
The SOFC operation under high current densities or high fuel utilization has more difference in concentrations of H₂ fuel and oxidant between bulk and electrode surface. Significantly, the larger concentration gradient in this region can cause the concentration overpotential. At lower current densities from Figure 2.4 and fuel utilization, this loss is very small.
- Ohmic overpotential or resistive loss
This ohmic overpotential is a major loss in the SOFC operation, caused by ionic resistance in the electrolyte and electrodes, electronic resistance in the electrodes, current collector and interconnect. This loss is directly proportional to current density and *V-I* diagram shows the linear trend at intermediate current density.
- Internal current overpotential or fuel cross over
Internal current overpotential or fuel crossover occurs by the fuel crossing or electron leakage through an electrolyte, however, this loss is very small.

2.2.5 SOFC advantages and some drawbacks

Although SOFC is the most promising fuel cell type with many advantages (Hammou and Guindet, 1997; Boudghene Stambouli and Traversa, 2002; Fuel cell Handbook, 2004; Andujar and Segura, 2009) as well as utilized in both of compact application and the large scale-commercial power generation as previous mentioned. However, there are some drawbacks SOFC currently being developed to be the commercialized fuel cell system under the challenges of ground-breaking technology (Hammou and Guindet, 1997; Song, 2002 and Fuel cell Handbook, 2004).

2.2.5.1 SOFC advantages

- SOFC is the most efficient fuel cell providing the high ratio of fuel input to electricity output.

- SOFC is flexible in terms of size. It can be applied in both of small home-scale power generator and large commercial-scale power plant.
- SOFC is flexible to use various types of fuel gas such as alcohol, natural gas, coal and petroleum based substances, even though it operates with or without fuel processor or reformer.
- SOFC system can reduce the CO₂ emission when compared with the conventional combustion of fossil fuel.
- High human's life qualities are presented due to eliminating the danger of carbon monoxide toxic in exhaust gases, as CO produced is transformed to CO₂ at the high operating temperature.
- The internal reforming of fuel gas can possibly operated in the SOFC cell with the rapid reaction rate. Thus, the use of precious catalysts such as platinum or ruthenium is not necessary.
- The high operating temperature of SOFC generates the thermal energy byproduct which can be utilized for co-generation systems or combined cycle applications.
- SOFC does not face the dilemma with electrolyte management liked the liquid electrolyte such as the corrosive and difficult to handle.
- SOFC is quite enough to be constructed indoor, because its configuration is set in the kind of modular with the solid state construction and no moving part.
- SOFC can be steadily operated more than 40,000-80,000hours.
- Low operating and maintenance cost can be achieved under the SOFC power generation. The efficient operation of the SOFC system will significantly decrease the energy bill (mass production) and affects on the lower maintenance cost.
- The addition of external reformer corrects the problem of difficult infrastructure of hydrogen fuel such as transportation from natural source and storage.

2.2.5.2 Some drawbacks of SOFC

- With the high operating temperature, SOFC stack is restricted the material flexibility and selection. Hence, the cost of this material fabrication and stack assemblage is higher than another fuel cell types.

- The fragility of its cells is hardly fabricated to a large size when the SOFC system is scaled up to megawatt size.
- The operating voltage loss or overpotential of cell due to the low electrolyte conductivity is still too high, even if it operates at high operating temperature.
- The high temperature operating system wastes the long operating time resulting in the slow start up and shut down.

2.3 SOFC system for sustainable energy

Although high operating temperature SOFC can produce the electrical power and usable thermal energy, the SOFC system requires the integration of many components beyond the SOFC stack itself. Various system components are incorporated into power system to allow operation with conventional fuels, to transform produced electrical power into the AC power, and often, to utilize rejected excess thermal energy to achieve high efficiency and to removal CO₂ in the exhaust gas. This incorporation of various system components is called “Balance of Plant (BoP)” (Fuel cell Handbook, 2004).

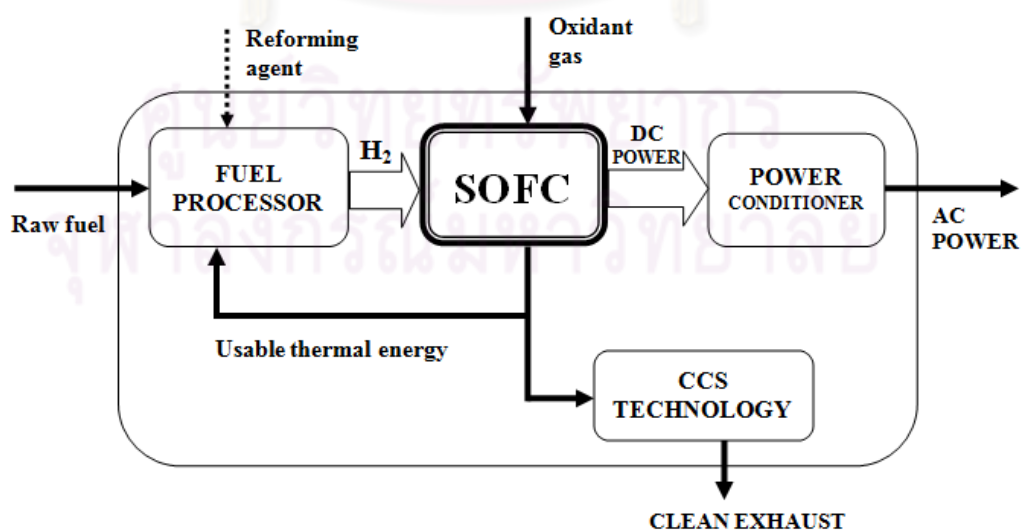


Figure 2.5 SOFC system for sustainable energy

In the rudimentary form, SOFC power systems consist of a fuel processor, SOFC unit, power conditioner, thermal energy recovery unit and CO₂ separator unit. Recently, CCS technology has been performed to capture and storage CO₂ from the exhaust gas. Although, fuel cell technology is proposed to generates electricity with eco-friendly technology, the little amount of green house gas emissions are also produced when other fuels are applied in the fuel processor. The simple schematic of this basic system and their interconnections is presented in Figure 2.5 with the integration with CCS facility.

2.3.1 Fuel processing unit

Hydrogen (H₂) is the most desired fuel for electricity generation in fuel cell because it offers high cell performance having low potential loss and coke formation. Therefore, the fuel processing should be performed to convert the various fuels via the fuel processor at the proper condition to generate the H₂ for SOFC. Although SOFC has high chemical and physical durability, fuel processor is also necessary to use in order to save the maintenance cost of SOFC stack and provide long life operation. Methane (CH₄), the main component of natural gas, is considered as a suitable and convenient raw fuel for the SOFC system due to its availability, highest hydrogen to carbon ratio in hydrocarbon substances and low cost (Ermakova *et al.*, 2000; Vivanpatarakij *et al.*, 2007 and Serrano *et al.*, 2010).

In the fuel processor, the reforming reactions are generally provided to generate H₂ from CH₄ such as steam reforming, partial-oxidation reforming and autothermal reforming. Concerning in the H₂ yield and the energy balance of SOFC system, methane steam reforming (MSR) is almost performed in the fuel processor of the conventional SOFC. Because methane steam reforming produces more H₂ yield and can efficiently utilize the generating thermal energy from SOFC stack due to nature of endothermic reaction. On the contrary way, partial-oxidation reforming and autothermal reforming provide the lower yield of H₂ and higher amount of carbon oxides (CO_x) especially in partial-oxidation reforming.

MSR is suitable for SOFC stack in terms of H₂ yield and the energy balance of conventional SOFC system; however, its system also produces the CO₂ at the afterburner step. Alternative reaction proposed to replace the conventional fuel processor is methane decomposition (MD). This reaction generated high purity of H₂ fuel can directly flow into SOFC system, and the first advantage from conventional SOFC system is to eliminate the CCS facility and can save in more cost. However, MD may be the preferred fuel processor option for SOFC system, therefore, the both of reaction should be investigated the performance with the operation of SOFC system.

2.3.1.1 Methane steam reforming (Conventional fuel processor)

Methane steam reforming (MSR) has been investigated for several decades as an effective H₂ production and was implemented in real industry in 1930 (Barelli *et al.*, 2008). MSR is the endothermic reversible reaction and normally reaches equilibrium over an active catalyst, as at such high temperatures the rates of reaction are very fast. Nickel-based catalysts are usually used in MSR. Platinum, cobalt and noble metals are also active, but more expensive. Over mentioned catalysts that are active for MSR nearly always occurs as well, however, this reaction can operate with or without a catalyst.

MSR is the mature technology, practiced industrially on the large scale for H₂ production. The basic generic hydrocarbon C_nH_m and reforming reactions for CH₄ are:

Generic hydrocarbon reforming reaction



Methane steam reforming reaction



Water-gas shift reaction



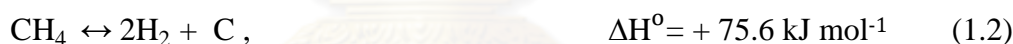
The reforming reactions (Eqs.1.1 and 2.7), more correctly termed oxygenolysis reactions, and the associated water-gas shift reaction (WGS) (Eq.2.8) are carried out normally to provide the overall methane steam reforming (Eq.2.9) at elevated temperature, typically 773 K (Dick, 1996; King *et al.*, 2005; Holladay *et al.*, 2009).

Overall methane steam reforming (MSR in fuel processor)



Therefore, the MSR in conventional fuel processor refers to the overall methane steam reforming which combined the methane steam reforming and water gas shift reaction. With the chemical equilibrium, two sub-reactions in MSR favor the H_2 at the different temperature range. Methane steam reforming significantly generates H_2 at the high operating temperature whereas water gas shift reaction is lower than methane steam reforming. Hence, the MSR fuel processor should be operated at temperature of the ensured high H_2 yield.

Methane decomposition reaction



Boudouard reaction



Carbon gasification



Consideration in the further side reaction related with compositions of MSR, carbon solid like coke and soot can be occurred via direct decomposition of methane (Eq.1.2) or by the boudouard reaction (Eq.2.10) (Dicks, 1996 and Sangtongkitcharoen *et al.*, 2005). This side reactions significantly affected both in fuel processor and SOFC due to its clogging or plugging tube, blocking the active site of catalyst. However, the increasing temperature or reacting with steam can reduce this coke or

carbon formation in MSR (Eq.2.11) (Fuel cell Handbook, 2004 and Piroonlerkgul *et al.*, 2009)

2.3.1.2 Methane decomposition (Proposed reaction in fuel processor)

Decomposition reaction can be used with the variety of gaseous and liquid hydrocarbon fuels and ideally suit to simple hydrocarbon structure. Consequently, this reaction is appropriate for methane because its simple structure has only C-atom with the H- single chemical bonds. This process of hydrogen generation is to simply heat methane in the absence of the oxidant substance (H_2O , CO_x and air). The methane is thermally decomposed to H_2 and solid carbon as shown in Eq.1.2.

Methane decomposition reaction (MD)



Methane is directly decomposed to separated H_2 gas phase and solid carbon. It is reasonably proposed to be the alternative fuel processor, because high purity of H_2 can be achieved to be the fuel of SOFC stack and CO_2 is totally captured in the form of solid carbon. This solid carbon can be used as a commodity product in the various fields (e.g. adsorption material, membrane, catalyst, electrical devices and fuel cell) or sequestered (or stored) for future use (Muradov, 2001; Meyer, 2009 and Muradov *et al.*, 2010) as shown in Figure 2.6. Many researchers have reported that this solid carbon can be precious carbon types such as carbon nanotubes and carbon nanofilaments (Piao *et al.*, 2002; Suelves *et al.*, 2005 and Makris *et al.*, 2005).

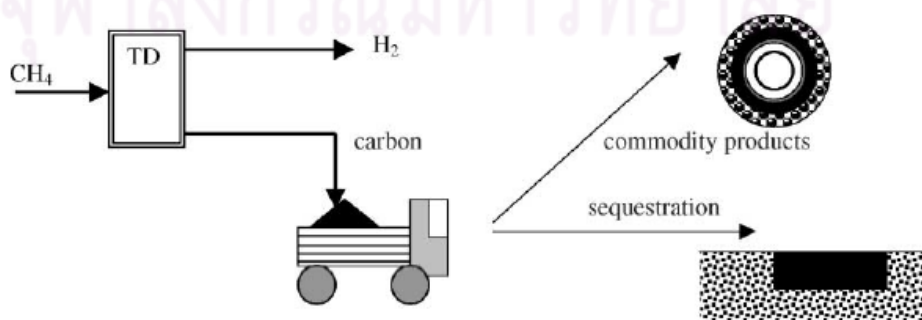


Figure 2.6 Products of methane decomposition reaction (Muradov, 2001)

On the general thermodynamics view point, methane decomposition is an endothermic reaction and also a feasible reaction at temperature over 823 K. Due to its high favorable temperature, catalyst is necessary to accelerate reaction and also reduced the maximum temperature in the reaction. Common catalysts used are noble and transition metals such as Ni, Fe, Cu, Pd, etc., supported on high surface area ceramic substrate such as Al_2O_3 and SiO_2 , etc. Especially, Nickel-based catalyst has higher activities compared to other transition metals as well as high yields of products. Bimetallic catalysts were more active and produced higher yields of H_2 compared to monometallic catalysts (Ahmed *et al.*, 2009).

2.3.2 SOFC unit

SOFC unit plays an important role in the power generation system and supplied thermal energy. H_2 rich gases produced from 2 kinds of fuel processor are fed in to the SOFC unit. Then the DC electrical power and by product thermal energy are generate via the electrochemical with oxidant gas.

2.3.3 Power conditioner

Power conditioner is an enabling technology that is necessary to convert DC electrical power generated by a SOFC into usable AC power for stationary loads, automotive application, and interfaces with electrical utilities. It should be noted that this unit is not considered in this study.

2.3.4 Thermal energy recovery unit

This thermal energy recovery unit consists of an afterburner where the unutilized fuel from the electrochemical reaction at the SOFC stack is combusted, and heat exchangers. Thermal energy generated in this combustion is recovered and distributed to other energy consumption units and equipments such as preheaters, fuel

processor, so that the demand of external thermal energy source is reduced. High performance of SOFC system can be achieved from this unit.

2.3.5 CCS unit

For a SOFC system with MSR, an additional CCS facility is installed after the afterburner in order to avoid the CO₂ emission to the environment. The CO₂ emission has significant effects on ozone layer depletion, human toxicity and fresh water aquatic eco-toxicity. The operation of CCS for SOFC includes 3 main steps as shown in Figure 2.7 as follows (Simbeck, 2004; Damen *et al.*, 2006; 2007, Abu-khader, 2006 and Koornneef *et al.*, 2008);

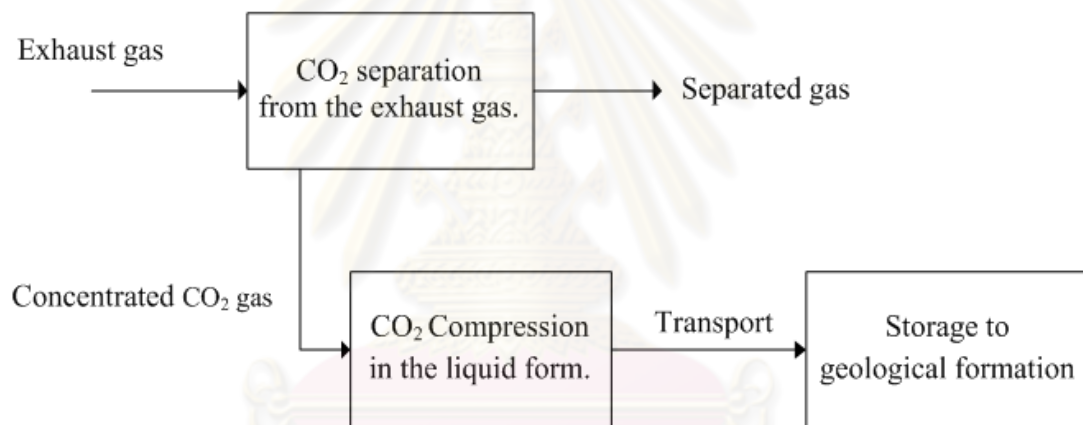


Figure 2.7 Carbon capture and storage facility (CCS).

- **CO₂ separation**
CO₂ is separated out of the exhaust gas with the various methods (mentioned in the literature review), and the remained gas such as the air is also brought back to utilize in the SOFC system.
- **CO₂ compression to the liquid phase and transportation**
Concentrated CO₂ gas from the previous step should be compressed under the critical pressure (7.4 MPa; Koornneef *et al.*, 2008) into liquid phase due to the easy transport to storage. The important concern in this step should

be considered in the pressure loss along the pipeline transportation, therefore, the compressed pressure should be higher than the critical pressure of CO₂. Moreover, this pressure loss occurring in this step, it will indentify the injected pressure in the next step.

- CO₂ storage into a geological reservoir.

This step must consider 3 main issues; the storage place, injected pressure and the depth of storage place form the Earth's surface. First, the storage places, geological informations, are proposed for this CCS process such as underground, under the sea, oil reservoirs, abandoned gas field and deep saline aquifers (Gibbins and Chalmers, 2008). Second, injected pressure is still considered more than critical pressure of CO₂ in order to easy storage and overcome the reservoir pressure. At last with the depth of the injected pressure, the depth should be enough distance due to avoidance of CO₂ leakage. Therefore, it must be longer than 800 m.

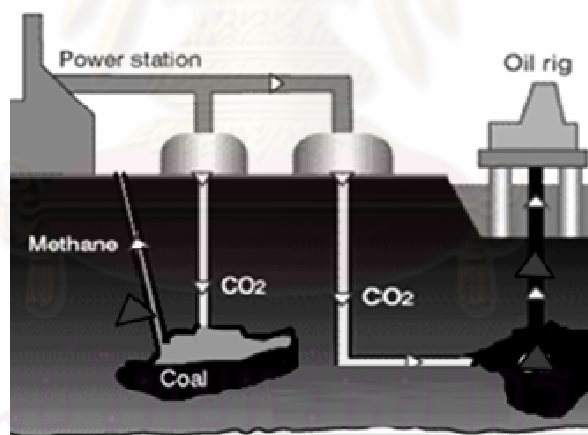


Figure 2.8 Advantage of CCS (<http://news.bbc.co.uk>)

Furthermore, CCS advantages are not only to prevent the CO₂ emission emitted out to our world, but also to utilize the CO₂ in the enhancement oil and gas recovery as shown in the Figure 2.8. By pumping CO₂ into an oil and gas reservoir, previously unrecoverable oil and natural gas can be pushed up to where they can be reached. Once all of the recoverable natural resources have been reached, the depleted reservoir can act as a storage site for the CO₂ (IEA, 2006).

CHAPTER III

LITERATURE REVIEWS

In this chapter, the literature reviews are divided into five parts. From the first part, the previous works on methane reforming reaction for H₂ production are presented especially on methane steam reforming. This part aims to show that methane steam reforming is the available choice for high efficiency H₂ production. Then the further techniques which improve the efficiency of methane steam reforming are also reviewed in the second part. The various techniques are developed in order to generate the higher yield and purity of hydrogen.

Next, methane decomposition reaction is proposed and also compared with the conventional steam reforming in the third part. Then, the fourth part is about the previous interesting SOFC system such as the effect of the composition of fuel gas, the SOFC efficiency development. At last, the new carbon capture and storage (CCS) technology is studied in the characteristics and requirement in each step.

3.1 Methane reforming reaction for H₂ production

There are three main conventional methane reforming reactions to produce H₂ fuel including steam reforming, partial oxidation and autothermal reforming. Table 3.1 compares the pros and cons and also shows the efficiency of the three reforming reactions.

Table 3.1 Comparison of three reforming reactions
(King *et al.* 2005; Holladay *et al.*, 2009 and McHugh, 2005)

Hydrogen production	Advantage	Disadvantage	Efficiency
Steam reforming	-Oxygen not required -Lower process temperature -Best H ₂ /CO ratio -Most extensive industrial experience	-High air emission with more green house gas	85%
Partial oxidation	-No catalyst required -Compact	-Low H ₂ /CO ratio -Very high processing temperatures -Soot formation/handling adds process complexity	60-75%
Autothermal reforming	-Lower process temperature than partial oxidation	-Limited commercial experience -Required air or oxygen	60-75%

3.1.1 Methane steam reforming

Steam reforming is the most well-established H₂ production technology and the highest performance of reforming reaction in terms of the amount of H₂ produced per mole of reactant feed and the ratio of H₂ to undesired CO (McHugh, 2005; King *et al.* 2005 and Holladay *et al.*, 2009). As the previous mentioned, the combined steam reforming and water-gas shift is the endothermic reaction so the large extent of external thermal source is required. At intermediate and high operating temperatures (Holladay *et al.*, 2009), the major problem affecting on the deceasing of activity in methane steam reforming is the coke deposition on the catalyst surface due to blocking the pore of catalyst surface. Thus, this reaction continuously enhanced by improving the catalysts, operating conditions and heat transfer to achieve better performance (Yanbing *et al.*, 2007).

In the real commercial process, the steam to carbon ratio is usually set to a value higher than 1.4 in orders to maintain the catalyst activity and improve cycle efficiency (Fuel cell Handbook, 2004).

Methane steam reforming reaction

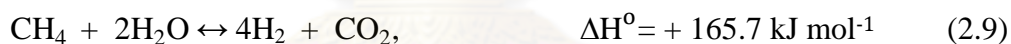


In equilibrium consideration of the side reaction (WGS), the steam to carbon molar ratio should be 2 or higher (Palsson *et al.*, 2000; Sangtongkitcharoen *et al.*, 2005 and Arpornwichanop *et al.*, 2010). The excess steam is used to force the reaction to completion. Air is further added to improve the resistance of coke formation (Eqs. 2.11 and 1.2) and supply the energy demanding (Dias and Assaf, 2004; Sangtongkitcharoen *et al.*, 2005).

Water-gas shift reaction



Overall methane steam reforming (MSR in fuel processor)



Due to nature of endothermic reaction, basis of required condition is high temperature and low pressure. Atmospheric operating pressure has been suggested in the economic consideration (Holladay *et al.*, 2009). Although this reaction can operate with or without a catalyst (Larminie and Dicks, 2000), methane can be highly converted itself at temperatures above 1173 K (Anderson and Garcis, 2005). Furthermore, methane can be converted to the H₂ over a nickel-based catalyst at the temperature about 773 K (Dick, 1996 and Hoogers, 2003). Therefore, catalysts are necessary to reduce this high operating temperature. The properties of the methane steam reforming catalyst should resist coking and decomposition by steam, be inactive for side-reaction, maintain the activity at high temperature and have high mechanical strength as well as good heat transfer properties (Oliveira *et al.*, 2009).

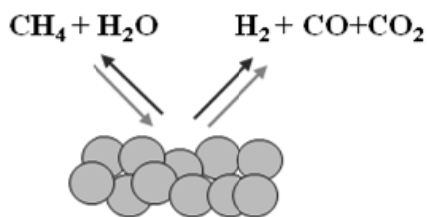


Figure 3.1 Function of catalyst besides from catalyzed reaction.

The methane steam reforming catalyst can be divided into two groups: non-precious metal (typically nickel) and precious metals from group VIII elements (typically platinum or rhodium based). The advantage of using precious metals from group VIII elements is about less coke formation. Due to the severe mass and heat transfer, the activity of the catalyst does not affect the limiting conversion. So less expensive nickel-based catalysts are used almost universally in industry (Rostrup-Nielsen, 2001). Rakass *et al.* (2006) also examined that unsupported nickel powder catalysts as a catalyst in internal or external reforming exhibited the high methane conversion of $98 \pm 2\%$, no coke was generated at the steam to carbon ratio of 2 and temperature of 973 K.

Some additives such as magnesia, potassium or other alkaline (Ross, 1974; Takeguchi *et al.*, 2002) are almost added into the nickel-based catalysts to enhance the activation of steam, and dissociation of steam into OH and H species. Carbon deposits can lead to active site blocking and affect the catalyst reactivity and stability. The support can also play a role in suppressing carbon deposition. Ceria (Kusakabe *et al.*, 2004 and Laosiripojana *et al.*, 2005) has been known to be able to oxidize and inhibit the deposited carbon.

Several works have evaluated the performance of methane steam reforming based on equilibrium reactions (Temkin, 1979; Hufton *et al.*, 1999; Ding and Alpay, 2000) and also determined the kinetics of this reaction. It is very fast on the range of high temperature of 1173-1273 K and may be affected by mass transfer phenomena (Achenbach *et al.*, 1994). Both of Joensen and Rostrup-Nielsen (2002) mentioned about the effect of operating condition on a typical equilibrium conversion of steam reforming of methane against temperature and pressure and steam/carbon ratio. In

order to maintain a high methane conversion, it is necessary to operate the system at high temperature, low pressure, and relatively high steam to carbon ratio.

3.1.2 Methane Partial oxidation

Methane partial oxidation reaction



Partial oxidation converts methane to H₂ fuel by partial oxidization (combustion of methane with non-excess oxygen or substoichiometric amount of air). A low oxygen-to-fuel ratio favors higher hydrogen yield. This reaction is highly exothermic, and raises the reactant to a high temperature, thus, it is not necessary to use a catalyst for operation (Doctor and Lamm, 1999 and Holladay *et al.*, 2009). It can express that oxygen suppresses the hydrogen production; however the energy requirement from external thermal sources would be decreased. The thermal energy in this reaction is only provided in the fuel processor for the “controlled” combustion. Generally, partial oxidation can handle much heavier petroleum fraction or larger hydrocarbon structure than other catalytic reactions and is therefore suitable in case of gasoline or other logistic fuels.

The amounts of desired hydrogen from partial oxidation per mole of reactant feed are less than from steam reforming reaction. The H₂/CO product ratio is favored for the feeds to hydrocarbon synthesis reactors such as Fisher-Tropsch (Holladay *et al.*, 2009). Moreover, some soot actually occurs in the high operating temperature, but the separate scrubber can remove it out (Joensen and Rostrup-Nielsen, 2002). However, the non catalytic methane partial oxidation also needs the high combustion temperature of 1573-1773 K to ensure complete conversion and to reduce carbon or soot formation (Rostrup-Nielsen and Horvath, 2003). This causes relatively the most significant CO₂ emission (Turpeinen *et al.*, 2008).

Although catalysts hardly provide long operation because the coke and more hot spot take place in the fuel processing reactor due to exothermic nature of this

reaction, several works (Song, 2002 and McHugh, 2005) have demonstrated the use of catalyst to reduce the operating temperature. This reaction is called catalytic partial oxidation. It provides sufficient thermal energy internally to maintain the operating temperatures of 873-1473 K capable of achieving equilibrium product concentrations at millisecond residence times (Dauenhauer *et al.*, 2006). Nickel and Rhodium based catalysts are mostly used, but nickel has a strong tendency to coke via the consumed CO in boudouard reaction and Rhodium cost has significantly increased. Torniainen *et al.* (2006) also reported that these two catalysts can be achieved around 90% in methane conversion and more than 90% in hydrogen selectivity. Lower temperature conversion increases system efficiency and leads to less CO. At last, methane partial oxidation has a good reaction characteristic in little amount feed of O₂ to provide more complete reaction, it should be of concern on the safety in exothermic operation and the thermal management to supply the system.

3.1.3 Autothermal reforming of methane

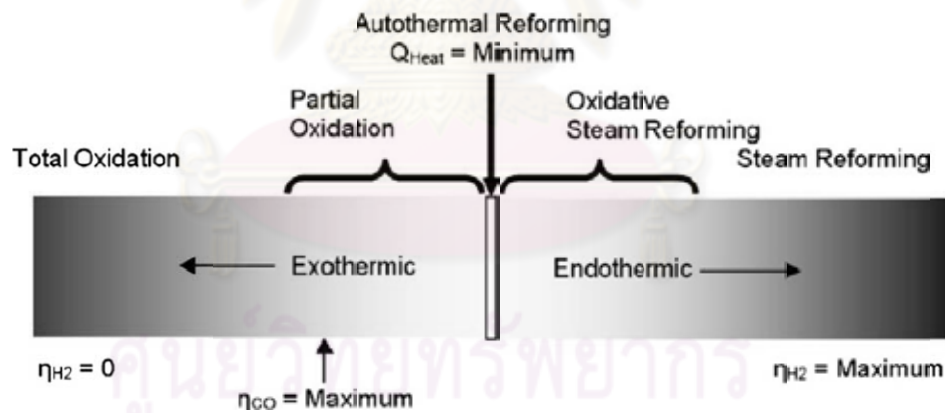


Figure 3.2 Different operating conditions for fuel reforming
(Rabenstein and Hacker, 2008)

The improvement on the hydrogen production of partial oxidation need steam addition to the reactant mixture in order to prevent coke formation, control operating temperature and composition of product (Bellows, 1999; Joensen and Rostrup-Nielsen, 2002). With the proper air (O₂) to carbon ratio and steam, an adiabatically or thermally neutral point (net thermal energy of the reformer equals zero) can be

presented that is called Autothermal reforming as shown in Figure 3.2. Methane can be converted faster at which no external thermal source.

As mentioned previously, excess of steam (water), oxygen and catalyst can be also utilized to prevent the carbon formation at high temperature. The great configuration in thermal management can be achieved in this reaction. It consists of two extremely different zones at which a thermal zone of partial oxidation is used to generate the heat needed to drive the down steam reforming reaction in catalytic zone. An advantage partial oxidation over methane steam reforming is about the rapid reaction start while producing larger amount of H_2 than partial oxidation.

Dvorak *et al.* (1998) examined the relation of methane steam reforming and partial oxidation and the results showed that the oxidation reaction takes place to equilibrium faster than the steam reforming reaction over the nickel based catalyst. But in ruthenium based, both reactions occur in parallel. This can be expressed that it combines from endothermic steam reforming and exothermic partial oxidation. However, for the real operation, it may be difficult to control at adiabatic condition without external thermal source. It should be kept under slightly exothermic reaction (Xuan *et al.*, 2008).

3.2 Further techniques integrated with MSR processor

Regarding overall products of methane steam reforming (MSR), the combination of hydrogen, carbon oxides, water and unconverted methane are presented at the outlet steam of fuel processor or reactor. The improvement of the reforming reaction is needed when the large amount of CO_x was produced.

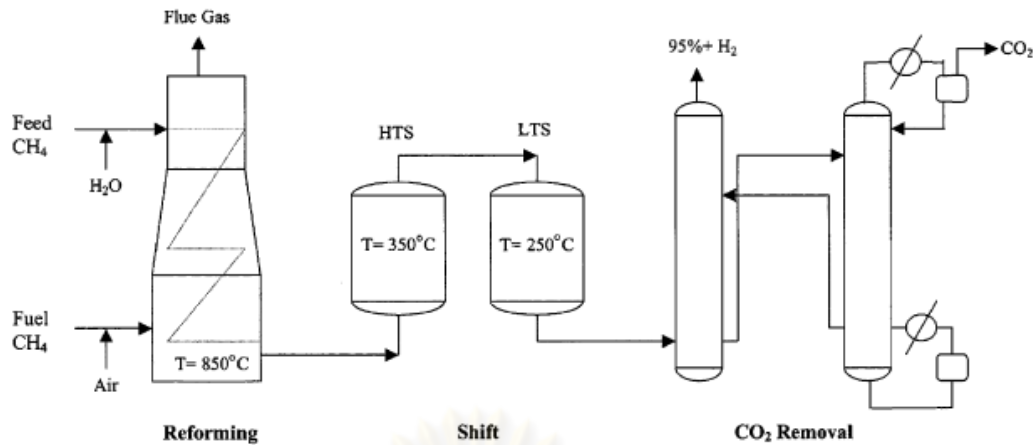


Figure 3.3 Complex configuration of development of MSR (Barelli *et al.*, 2008)

Firstly, one or more water-gas shift (WGS) reactors - typically a high temperature reactor (HTS) and low temperature reactor (LTS) (Figure 3.3) (King *et al.* 2005 and Holladay *et al.*, 2009) are proposed to utilize the equilibrium of WGS as shown in Eq. 2.8. High and low temperature WGS reactors generally use the iron and copper catalyst, respectively. Barelli *et al.* (2008) illustrated in these complex configuration of MSR in order to achieve large amount and high purity of H_2 production. The supplemental CH_4 is combusted to supply the high thermal energy at the bottom of MSR fuel processor. At higher temperature of 623 K, the reaction has the fast equilibrium, but is limited by thermodynamics to the amount of CO that can be shifted. This high temperature stage can reduce 7% of the total amount CO (Choudary and Goodman, 2002). Then, a lower temperature reactor (483-603 K) has a role to convert the CO back, and then the amount of CO declined to around 0.5% of the total amount of CO. And not only is the additional shift reactor further integrated to provide the WGS in the increasing of H_2 product, but also the CO_2 removal unit such as pressure swing adsorption, temperature swing adsorption and amine scrubbing is desired in order to achieve more than 95% purity of H_2 .

Next, sorption enhanced MSR is a new field of research to operate MSR fuel processor with in situ CO_2 separation. This addition of CO_2 sorbents to a hydrocarbon-reforming reactor was first described in 1868 by Roster-Nielsen (Rostrup-Nielsen, 2001) in order to reduce the complexity of the set of the WGS

reactor. CO₂ sorbents such as calcium oxide, dolomite are added in the MSR to enhance and shift the reaction resulting in the fast kinetics of reaction and high purity of H₂ (Rawadieh and Gomes, 2009; Fernandez *et al.*, 2009). These types of CO₂ sorbents are inexpensive, easy to find and characterized by high adsorption ability. Moreover, this process is simplified, there is no need for WGS reactor, therefore, and the investment cost can possibly be reduced. Balasubramanian *et al.* (1999) presented a H₂ rich gas product from the sorption enhanced MSR by CaO, the CH₄ conversion was improved to 88% and high purity of 95% can be achieved at temperature of 773-923 K at atmospheric pressure. Lopez Ortiz and Harrison (2001) applied dolomite into the Ni-based catalyst in the mass ratio of 2.2-2.7 with an aim to use CO₂ sorbents to substitute the catalyst support. Dolomite plays an important role to remove the CO₂ and increase CH₄ conversion in the multi-cycles.

However CO₂ sorbents need the high temperature (over 923 K) to regenerate the inactive state of their sorption which leads to less stability (Barelli *et al.*, 2008). The advantage of combining of CO₂ sorbent in the MSR is about lower operating temperature which may reduce catalyst coking and sintering. And it is also used as the catalyst support. Some disadvantages should be considered; more energy is required to regenerate the sorbent. The exothermic energy is produced along the sorption step, more thermal durability in reactor or fuel processor is needed to be aware of about the hot spot. However, this method is only the best for the improvement of MSR reaction, CO₂ is produced back in the generating step. It cannot totally eliminate CO₂ and CO based on this method. Another concern in this MSR with sorption enhancement techniques is the content of CO in the product gas, especially for some application such as fuel cell that may be poison for the catalyst. When this process is applied to use in the fuel cell system, more than one unit in CO₂ sorption is required at the fuel processor and the after afterburner due to consideration in global warming crisis.

Lastly, palladium (Pd) inorganic membrane is the further technique applied into the MSR fuel processor which called Pd membrane reactor-fuel processor (Basile *et al.*, 2003; Galucci *et al.*, 2004; Fernandes and Soares Jr, 2006; Patel and Sunol, 2007). Although some polymeric membranes can provide the good result of hydrogen selectivity, they cannot be operated at high temperatures necessary for MSR. Pd membrane is a preferred choice (Lu *et al.*, 2007) due to high stability, H₂ permeability

and selectivity. Roys *et al.* (1998) has succeeded in the use of Pd membrane under the severe condition of MSR fuel reformer in the high endurance as 1600 h and 30 cycles. The simultaneous of generation and separation in the one unit can be achieved, when the forward shifting of MSR equilibrium is done by the Pd membrane, the operating temperature can be lower to 773-823 K. This further advantage of Pd membrane fuel processor is about to modify the system less complicated comparing with the further integration of shifting reactor. However, this MSR integrated with Pd membrane have been operated with high operation and investment cost because of desired high operating pressure and high Pd membrane cost, respectively (Galucci *et al.*, 2004 and Piroolerkgul *et al.*, 2009).

3.3 Methane decomposition

In general hydrogen production such as steam reforming, partial oxidation, auto-thermal reforming as mentioned in the previous part, they require more than one applications to give the high purity and large amount of hydrogen such as WGS reactor, pressure swing adsorption unit, temperature swing adsorption unit, amine scrubbing unit, sorption enhanced MSR unit and Pd membrane reactor.

Decomposition reaction is an alternative hydrogen production. The decomposition reaction is suitable to use for a variety of gaseous and liquid hydrocarbon fuels. It is an attractive method to produce hydrogen-main product and also give more valuable by-products-carbon nanotubes and filiments (Suelves *et al.*, 2005).

Overall methane steam reforming (MSR fuel processor)



Methane decomposition reaction (MD fuel processor)



Regarding economic point of view, more researches have studied on other processes to substitute conventional hydrogen production processes (Muradov, 2001; Muradov *et al.*, 2005; Abbas and Wan Daud, 2009 and Ahmed *et al.*, 2009). Methane steam reforming (MSR) was mostly selected on the hydrogen production because of high efficiency, high amount of hydrogen product (Ahmed *et al.*, 2009). Comparing between the reaction (Eq. 2.9) and decomposition (Eq. 1.2), the thermal energy requirement per mole of H₂ for methane decomposition (MD) is less than that of MSR (37.8 and 41.4 kJ mol⁻¹ H₂, respectively). The amount of CO₂ emissions from the process could potentially be as high as 0.43 mol CO₂ mol⁻¹ H₂ for steam methane reforming compared to 0.05 mol CO₂ mol⁻¹ H₂ for methane decomposition. More than 10% of the methane heating value is needed to drive the endothermic process.

The decomposition accomplishes the removal and separation of carbon in a single-step. Consequently, this process offers significant emission reduction. It can potentially produce a stream of H₂ with the purity up to 95 vol.% (Takenaka *et al.*, 2001; Villacamp *et al.*, 2003 and Suelves *et al.*, 2005). From the point of view of carbon sequestration, it is easier to separate, handle, transport, and store solid carbon than gaseous CO₂. The major drawback of the thermal decomposition method is the energy loss associated with the sequestration of carbon. Thus, decomposition may be the preferred option for natural gas and other hydrocarbons with high H₂/C ratio.

Non-catalytic thermal decomposition of methane requires temperature higher than 1573 K to achieve the reasonable yield due to the strong bonds of carbon and hydrogen atoms (Holmen, 2009). By using catalyst, the temperature can be significantly reduced, depending on type of catalyst. Abbas and Wan Daud (2009) and Ahmed *et al.* (2009) suggested the selection of catalyst as shown in Table 3.2.

There are various parameters to decide the selection of catalyst such as operating temperature, stability and carbon product; moreover, the precious carbon product must be in the form of filament which has the hollow shape and nanometer size. General decomposition of methane also investigated reaction over Ni-based and Fe-based catalyst. Ni-based catalysts as the combination Ni with more stable metals were more active and produced higher yields of H₂. But the main product was CNTs not H₂; some research used the Fe-based catalyst. Fe metal has the opposite properties

of Ni metal. The properties of Fe are more stability and less activity. Then, it can use in high temperature reaction, but their low activity affected on the accumulation of various type of carbon product.

Table 3.2 Summary of catalysts generally used for CH₄ decomposition and their suitable operation temperature and carbon product characteristics. (Abbas and Wan Daud, 2009 and Ahmed *et al.*, 2009)

Parameter	Temperature range (K)				
	773-973	923-1223	1123-1223	923-1523	> 1473
Catalysts	Ni-based	Fe-based	Carbon-based	Ni, Co, Fe, Pd, Pt, Cr, Ru, Mo	Thermal/plasma
Carbon product	Filament	Filament	Turbostratic filament	Graphitic turbostratic/filament	Amorphous

Effect of type of support was investigated; the support also plays an important role to affect on the reaction activity and the size of carbon solid. The high dispersion of metal of the good support can be achieved the small size of metal resulting in the carbon nanotube and filament growth and long life catalyst (Nakamura, 1999). The sizes of metal particles were approximately the same as the diameters of the carbon nanotube and filament, were much larger than the particle size of the catalysts before reaction one may believe that the decrease of the carbon nanotube and filament rate is caused by the sintering of the metal particles. The metal-support interactions are found to play a determinant role for the growth mechanism. Weak interactions yield tip-growth mode whereas strong interactions lead to base-growth. Both growth modes are schematically shown in Figure.3.4.

Takenaka *et al.*(2004) operated this reaction at 823 K and subsequent dry reforming of the carbon-filament product with CO₂ into CO at 923 K over supported Ni catalysts (Ni/F-SiO₂, Ni/SiO₂, Ni/TiO₂, Ni/Al₂O₃). Among various supports, catalyst activity varied on the kind of support according to the following trend: TiO₂~Al₂O₃ >> F-SiO₂, SiO₂. Their results indicated that TiO₂ and Al₂O₃ were excellent supports for the repeated cycles of the methane decomposition, compared

to SiO_2 . TiO_2 and Al_2O_3 supports inhibited serious aggregation of Ni metal particles and maintained the size of Ni particles at the range favorable (60-100 nm) for methane decomposition, while Ni metal particles in Ni/ SiO_2 aggregated into ones larger than 150 nm with the repeated cycles.

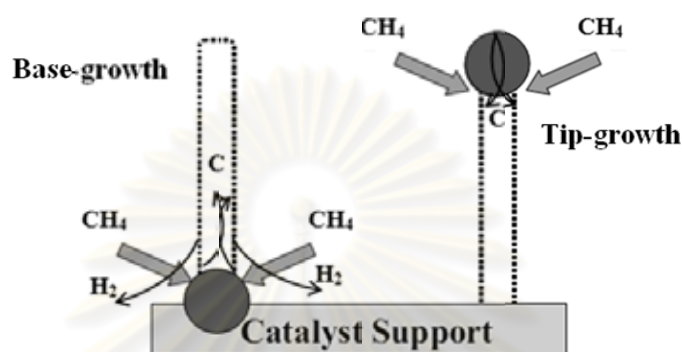


Figure 3.4 The two growth modes of filamentous carbon (Anne, 2005)

The systems with a greater metal surface area are more stable, resulting in a longer lifetime to catalyze the CH_4 decomposition was presented by Bonura *et al.* (2006). By varying types of Ni-base support catalysts such as Ni/MgO, Ni/ SiO_2 , Ni/ ZrO_2 and Ni/LiAlO₂, it was found that Ni/MgO gave the best activity on CH_4 conversion (around 60%) due to their high active surface to react the decomposition of CH_4 , high dispersion of Ni metal and low Ni mean particle size. Catalyst activity was compared according to the following reactivity scale: Ni/MgO > Ni/ SiO_2 >> Ni/LiAlO₂ > Ni/ ZrO_2 . Consideration in the carbon purification, Bai *et al.* (2007) and Yusuke *et al.* (2009) presented the alternative way to neglect the purification step of carbon solid. By the use of carbon type support with small loading of metal, CH_4 decomposition showed high activity, and carbon nanotubes and filament can be achieved at the high operating temperatures.

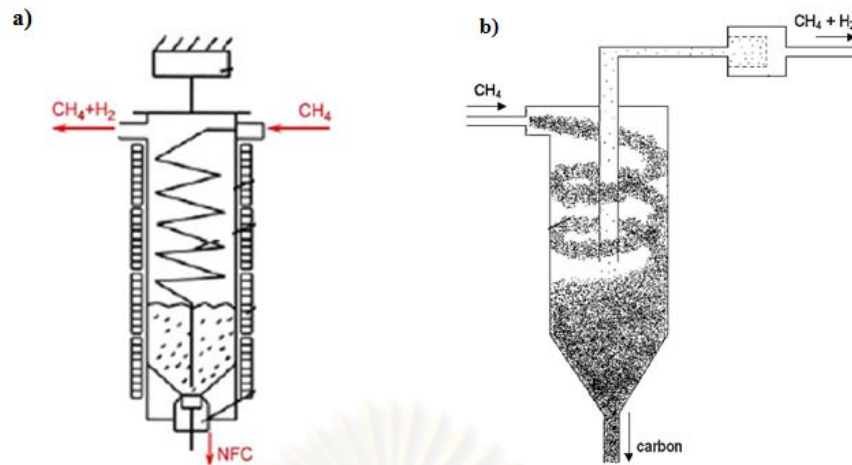


Figure 3.5 Schematics of fluidized bed reactor with further mode in the study of
 a) Ahmed *et al.* (2009) b) Muradov *et al.* (2010)

Ahmed *et al.* (2009) and Muradov *et al.* (2010) suggested the way to separate the carbon solid out of the MD reactor for continuous operation. This proposed system can lead to the application of MD fuel processor into the fuel cell system in order to separate carbon solid before the H_2 rich gas was fed into fuel cell stack as shown in Figures 3.5a) and b), respectively. Fluidized bed reactors applied with the vibration mode (Figure 3.5a) are utilized to separate out of capture carbon solid by the gravimetric force. These schematics can reduce the carbon clogging problem not only in the fuel processor, but also in the anode of fuel cell. Moreover, it can be the possible path to avoid the carbon oxides generation via the side reaction (such as Boudouard reaction) from solid carbon in the power generation (Piroonlerkgul *et al.*, 2009).

3.4 SOFC system

SOFC performance actually depends on the composition of fuel gas fed into the anode side of SOFC. In the conventional SOFC with MSR fuel processor, this steam reforming system gave the higher performance with high power density than

another reforming system (i.e. reforming with air, reforming with combined air and steam) (Piroonlerkgul *et al.*, 2008). However, the general direct feed compositions from the MSR fuel processor are normally consisted another gas products with desired hydrogen such as unconverted methane, excess water and carbon oxides (CO₂ and CO) (Suwanwarangkul *et al.*, 2006; Sangtongkitcharoen *et al.*, 2005; Piroonlerkgul *et al.*, 2009; Barelli *et al.*, 2008 and Holladay *et al.*, 2009). The steam to carbon ration mainly plays an important role to determine the composition in fuel gas. Due to the larger steam to carbon ratio, the fuel gas (hydrogen rich gas) is diluted with the excess steam in the anode side (Arpornwichanop *et al.*, 2010; Dokmaingam *et al.*, 2010 and Patcharavorachot *et al.*, 2010) leading to the lower fuel utilization. Thus, the power generation is decreasingly produced resulting in lower performance of SOFC. For the low steam to carbon ratio, unconverted methane is also present in the fuel gas. Dick (1996) and Sangtongkitcharoen *et al.* (2005) have reported that the presence of unconverted methane in the SOFC feed also decreases the SOFC performance because of carbon formation and partial blocking of anode pore. The anode is likely to rapidly break down at last.

Similarly, the performance of SOFC also declines when the amount of carbon monoxide in the anode feed gas increases according to increases in the activation and concentration overpotential losses (Eguchi *et al.*, 2002; Baron *et al.*, 2004 and Dalle Nogare *et al.*, 2007). Furthermore, carbon dioxide produced via the WGS also has an effect on the lower performance of SOFC system (Suwanwarangkul *et al.*, 2006 and Dokmaingam *et al.*, 2010). Carbon monoxide and carbon dioxide has relation in each other via Boudouard reaction which performs more carbon solid at the lower temperature. Assabumrungrat *et al.* (2005) and Sangtongkitcharoen *et al.* (2008) suggested the possibility to prevent carbon formation at the anode by raising the SOFC temperature. However, the durability in anode material should be considered to operate at the high temperatures.

Pure hydrogen theoretically seems to be the right fuel for SOFC power generation (Fuel cell Handbook, 2004). The superior SOFC performance with high power density and electrical efficiency has been reported, when pure hydrogen instead of a MSR fuel gas is fed to the anode side of SOFC (Eguchi *et al.*, 2002; Baron *et al.*, 2004; Suwanwarangkul *et al.*, 2006 and Piroonlerkgul *et al.*, 2009). Therefore, the

further applications in MSR fuel processor were developed to provide high purity of hydrogen as previously mentioned in Section 3.2. Dalle Nogare *et al.* (2007) examined the natural gas reforming processes for fuel cell. They proposed the installed the WGS reactors including high and low shift reactor over the FeO-based catalyst at operating temperature of 643 K and over CuO-based catalyst at operating temperature of 473 K, respectively. After that the pressure swing adsorption is also required to purify the hydrogen fuel at operating temperature of 973 K, and then fed into the fuel cell. They showed that high purity of hydrogen product can be achieved about 80 mol% at the WGS reactor. PSA unit has taken place to remove carbon dioxide out; the fuel cell efficiency has been improved to 43%.

Membrane reactor technology (the combination of membrane and steam reforming reactor) (Powell and Qiao, 2006; Damen *et al.*, 2006) is the promising pre-carbon capture technology in power generation. Especially palladium type has been widely examined the selective of hydrogen (Basile *et al.*, 2003; Galucci *et al.*, 2004; Fernandes and Soares Jr, 2006; Patel and Sunol, 2007) and proposed to install in the fuel processor, this method can perform high purity of hydrogen, increase the methane conversion. Vivanpatarakij *et al.* (2009) presented the upgrading of SOFC system with the applied the various operation modes in membrane reactor considering the combined compressor and vacuum pump. Three operation modes of membrane reactor are high pressure compressor, combined low pressure compressor and vacuum pump and combined high pressure compressor and vacuum pump. The economic analysis of this study revealed that the total capital cost/net electrical power is dependent on hydrogen recovery, net electrical efficiency and operation mode. This results showed that the replacement of conventional fuel processor with membrane reactor become attractive at high electrical efficiency. And the combined high pressure compressor and vacuum pump is the best operation mode to be the fuel processor with SOFC system, because of more increasing of driving force. However, this work did not provide the thermal energy utilization integrating in the SOFC system.

Piroonlergkul *et al.*, (2009) examined the improvement of driving force by vacuum pump and also compared the performance and economic profit with the conventional SOFC system under the thermal energy utilization operation. This

condition is called “thermally self-sufficient” which means is the recovery of thermal energy generating from SOFC. They proposed that the high performance of SOFC can be achieved at this operating condition due to no external thermal source. The palladium membrane reactor integrating with additional vacuum pump gave the higher power density more than that of conventional SOFC system, which power density is around 0.4398 W/cm^2 . However, this system is hardly provided in the real operation due to high cost of membrane material and high operating pressure (Sangtongkitcharoen *et al.*, 2008 and Piroonlergkul *et al.*, 2009).

Considering in other techniques, the CaO-CO₂ acceptor can provide the higher purity of hydrogen, since it is constructed after the fuel processor. The removal of CO₂ from fuel prior to be fed in SOFC can improve SOFC performance (Iordanidisa *et al.*, 2006 and Vivanpatarakij *et al.*, 2009) Nevertheless, this system configuration is not suitable from an environmental view point since CO₂ produced via WGS reaction is found at the afterburner and cannot be captured. Piroonlergkul *et al.* (2010) has developed this SOFC system with the application of second CO₂ capture unit. The second CO₂ capture unit such as palladium membrane reactor is located after the first unit in order to achieve highest purity of hydrogen. Although this system can provide the high performance, reduce the stack area and prevent CO₂, negative net cost saving was shown. Little amount of CO₂ also occurs at the exits of the afterburner, consequently, the conventional SOFC system should be equipped with a carbon capture and storage (CCS). CCS has a role in the reducing of global warming problem, because it prevents the CO₂ emitted to the atmosphere.

According to the discussion above, more complexity and not much eco-friendly in the conventional SOFC system should be improved with the alternative fuel processor. The reaction in the fuel processor should give the separated phase of product, no mix with desired hydrogen. Methane decomposition (MD) (Eq. 1.2) is proposed for hydrogen production as it requires lower energy consumption than conventional MSR (Muradov, 2001; Muradov *et al.*, 2005; Choudhary *et al.*, 2006; Ahmed *et al.*, 2009; Abbas and Wan Daud, 2009). It has performed more advantages for the SOFC.

When pure hydrogen generated by MD has applied to be the fuel, the performance of this SOFC is improved better than conventional SOFC (Eguchi *et al.*, 2002; Baron *et al.*, 2004; Suwanwarangkul *et al.*, 2006; Damen *et al.*, 2006; Bonura *et al.*, 2006; Yusuke *et al.*, 2009 and Piroonlerkgul *et al.*, 2009). Considering their by-product, MD produces a separated phase by-product as it only capture the carbon in to the valuable solid form. So that no carbon oxides is presented in the SOFC, resulting in a long operation life time of the catalyst and SOFC stack (Dick, 1996; Sangtongkitcharoen *et al.*, 2005). Furthermore, this solid carbon can be used as a commodity product in the various fields (e.g. adsorption material, membrane, catalyst, electrical devices and fuel cell) or sequestered (or stored) for future use (Muradov, 2001; Meyer, 2009 and Muradov *et al.*, 2010).

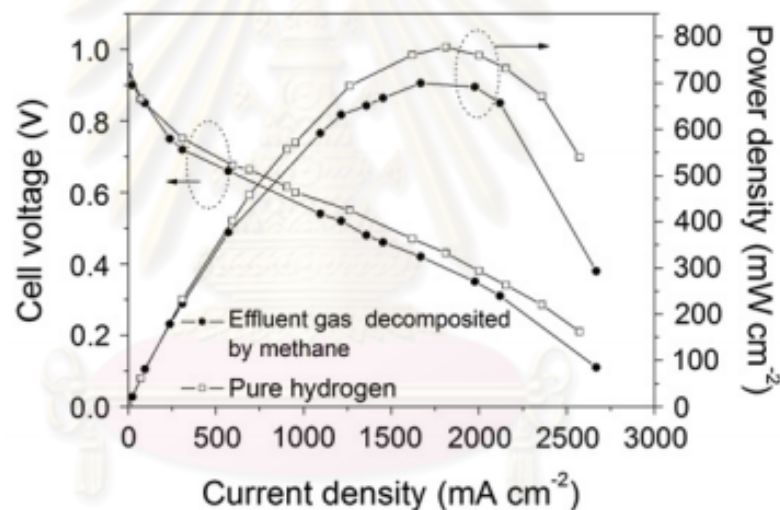


Figure 3.6 PEMFC experiment's result with the MD fuel processor (Sun *et al.*, 2010)

However, MD fuel processor is not widely studied in the SOFC system (Liu *et al.*, 2010 and Muradov *et al.*, 2010), this MD is mostly interesting to improve operating condition to receive the high purity of hydrogen for fuel gas of SOFC. The new proposed on the MD fuel processor integrated in PEMFC experiment is presented as shown in the Figure 3.6 that the maximum power density of fuel gas feed from MD fuel processor showed the value nearly pure H₂ (0.7 W cm⁻² for fuel gas form MD and 0.78 for pure H₂) (Sun *et al.*, 2010). It should be noted that the fuel gas feed from MD

fuel processor passes the high purity hydrogen's restriction of the PEMFC and it also shows the equivalent of efficiency liked pure hydrogen fed in PEMFC.

Importantly, the comparison of MD and MSR in terms of performance and economic analysis should be the interesting parameters to decide that MD or conventional MSR is appropriate for SOFC system.

3.5 Carbon capture and storage technologies (CCS)

Although, the separation processes have been developed to capture totally CO₂, somehow, CO₂ is not diminished out except that further using in another process such as dry reforming, water-gas shift reaction, acid process, etc (Holmen, 2009). In recent years, CCS has achieved much attention for its potential to receive the major CO₂ reduction especially in the operation of fuel processor and power generation plant (Calin, 2009; Naser and Timothy; 2008). CCS plays an important role not only to separate CO₂ out of the system, but also it can prevent the CO₂ pollution emitted to the atmosphere.

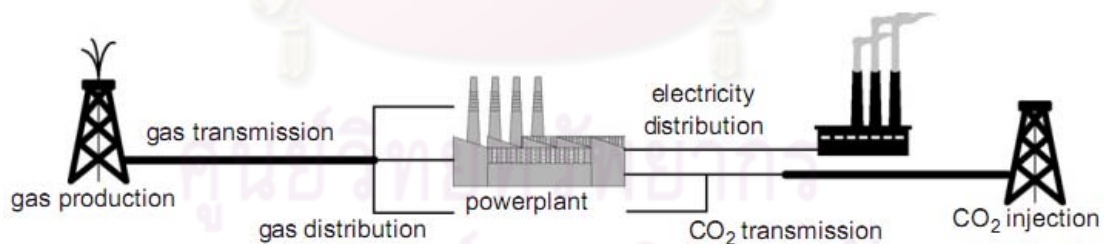


Figure 3.7 CCS The power plant with CCS technology (Damen *et al.*, 2007)

CCS could enable large reduction of CO₂ emissions from power generation plant by more than 85% of total amount, and only reduce the power plant efficiency around 8-12% (IEA, 2006). Generally, CCS consists of 3 main steps of an exhaust gas from the power plant; 1) CO₂ separation, 2) CO₂ compression to the liquid phase and transportation (usually via pipelines or tankers), and 3) CO₂ storage into a geological

reservoir (more than 800m) as shown in Figure 2.7 and 3.7 (Damen *et al.*, 2006; 2007; Abu-khader, 2006 and Kurt *et al.*, 2009).

3.5.1 CO₂ capture or separation technology

There are several methods for CO₂ capture or separation from gas stream such as the use of chemical solvent, adsorption on the solid, membrane (Abu-khader, 2006 and Figueroa *et al.*, 2008). This section showed further contents as revealed in the following sections.

Adsorption technology on the solid, especially CaO, is developed in the CO₂ removal performance liked beyond mentioned. CO₂ has been removed by the carbonation of CaO to CaCO₃. Two stages of this process are carbonator and calciner operated for different functions. At the carbonator, the circulating fluidized bed prefers to be the carbonation reactor, when the CO₂ capture continuously takes place with the exhaust gas. CaO solid particles can easily attach this exhaust gas feed and can be recycled (Grasa *et al.*, 2008). This first stage is operated at 873-973K and must lower than the regeneration stage (973-1150K) (Vivanpatarakij *et al.*, 2009; Piroonlergul *et al.*, 2010 and Romeo *et al.*, 2010). Nevertheless, make-up CaO is required to be fed to the carbonator due to the sintering of CaO solid since these CO₂ capture operates several cycles of carbonation-calcination (Abanades, 2002; Grasa *et al.*, 2008 and Vivanpatarakij *et al.*, 2009) and affects on the operating cost. Lee *et al.* (2006) study on the kinetics of carbonation reaction which present two regimes; chemical reaction control regime and diffusion control regime. They showed that the values of activation energy of two regimes are 72 kJ kmol⁻¹ for chemical reaction control regime and 102.5 kJ kmol⁻¹ for diffusion control regime in the carbonation of the mesoporous CaO and CO₂. The CO₂ capture by this technology performs more benefit when installed in the fuel processor. The removal of CO₂ shifts the forward reaction of WGS, hence, the partial pressure of H₂ can be improved resulting in higher purity and larger amount of H₂ fuel (Balasubramanian *et al.*, 1999; Lee *et al.*, 2006; Wang *et al.*, 2006 and Chen *et al.*, 2008). Furthermore, the exothermic energy from the carbonation could compensate the thermal energy demand in the MSR fuel processing reaction.

Membrane separation technology is expected to provide high performance CO₂ capture from the exhaust gas of a power generation plant (Abu-khader, 2006). The component technologies of the membrane separation technology include various kinds of CO₂ separation membrane and the vacuum pumps applicable to physical adsorption technology (Teramoto *et al.*, 2003 and Figueroa *et al.*, 2008). This technology has been extensively test and presently applied in the capture of CO₂ in natural gas (Bredesen *et al.*, 2004; Granite and O'Brien, 2005). Membrane technology performs more advantages over conventionally used of chemical absorption technology. It can be flexibly operated in handling feed steams with variable flow rates and composition. Bracht *et al.* (1996) presented the range of energy consumption using in membrane technology, its range is 6.33-11.09 kJ mol⁻¹ CO₂ in case of a shift coal-derived fuel gas. Furthermore, CO shift reaction (in WGS reactor) couple with this technology can diminish the problem of energy losses because of the lower steam demand in the syngas processing part. In the CO₂ selective membrane, polymer is one of interesting material choice due to its low capital costs compared with other types of membrane (Alexander Stern., 1994). The production process of polymeric membrane is also simple and easy to handle. However, it should be noted that the common problem of this polymeric membrane use is the instability of the membrane at the high operating temperature (Amelio *et al.*, 2007). Permeability and permselectivity are the two important variables to decide the optimal operating membrane for gas separation. The most attractive type of polymeric membrane in this area is polyimide membrane because it offers higher permeability and permselectivity (Shekhawat *et al.*, 2003). Harasimowicz *et al.* (2007) investigated the capability of this type of membrane by the capillary module. The CH₄ concentration in mixture of biogas can be improved from 55-85% to 91-94.4%, this showed that CO₂ can be significantly separated out of CH₄. Poly-1-trimethylsilyl-1-propyne (PTMSP) and Poly-dimethylsiloxane (PDMS) also give high selectivity of CO₂/H₂ (Merkel *et al.*, 2001), therefore, these two types must be installed after a fuel processor.

Chemical absorption technology is selected to be the capture unit in this research in order to receive separation efficiency more than 90% (Herzog., 1999; IPCC., 2005 and Koornneef *et al.*, 2009). CO₂ is captured by using a chemical absorbent such as amine solution. Thermal energy is consumed to operate this capture in the absorber at temperature range of 320-340 K and to regenerate the chemical

absorbent in the stripper around 400 K so that the net electrical power output of the SOFC system is reduced (Bolland and Undrum, 1998 and Kurt *et al.*, 2009).

Monoethanolamine (MEA) is the most used absorbent in this system (Freguia and Rochelle, 2003; Wang *et al.*, 2004). MEA is mostly used at the 30% concentration (Singh *et al.*, 2010) and consumed at the rate of 1.5-3.1 kg ton⁻¹ CO₂ removed (Chakma, 1995; Chapel *et al.*, 1999; Rao *et al.*, 2006; Knudsen *et al.*, 2006; IEA GHG., 2006; Koornneef *et al.*, 2009 and Singh *et al.*, 2010). Then, it is compressed to adsorb CO₂ from the exhaust gas, and then pumped into the stripper. At this stage, the energy demand comprises of compression and pumping of solvent which consume in the range of 2.63-4.83 kJ mol⁻¹ CO₂ removed from the gas (Condorelli *et al.*, 1991; IPCC., 2005 and Koornneef *et al.*, 2008) while the energy consumption in the regeneration stage (stripper) consumed in the range of 34.23-38.02 kJ mol⁻¹ CO₂ removed (Chapel *et al.*, 1999; Alie *et al.*, 2005; Knudsen *et al.*, 2006; RaO *et al.*, 2006; Abu-Zahra *et al.*, 2007 and Koornneef *et al.*, 2009).

3.5.2 CO₂ compression to the liquid phase and transportation

After CO₂ was separated out of the exhaust gas, the concentrated gas CO₂ is also provided to the compression stage to be in liquid form. Thus, the liquid form of CO₂ can be easily transported via the pipeline to storage, but this method is high cost (Damen *et al.*, 2007). The basic requirement in this stage is the compressed pressure of CO₂. The pressure should be more than the critical pressure of CO₂ (7.4 MPa; Koornneef *et al.*, 2008) in order to have the enough pressure supporting the CO₂ liquid flow along the pipe line transportation. The compressed pressure which prevents the two phases flow of CO₂ is in the range of 11-17 MPa for 50-500 km of transported distance (Hattenbach *et al.*, 1999; Wong and Bioletti, 2002; Damen *et al.*, 2007; Koornneef *et al.*, 2008; House *et al.*, 2009 and Singh *et al.*, 2010) Isentropic compression or reversible adiabatic compression is the basis assumption to calculate the energy requirement for this step (Damen *et al.*, 2007 and Koornneef *et al.*, 2008). For example, minimum work required in this stage is obtained at 14 MPa and 50 km distance; a typical value is about 13 kJ mol⁻¹ CO₂ transported (Kurt *et al.*, 2009).

Koornneef *et al.* (2008) also derived the energy requirement for compression from Damen *et al.* (2007), this stage consumed energy of $17.6 \text{ kJ mol}^{-1} \text{ CO}_2$ transported basis on the pressure of 11 MPa and distance of 50 km. After the compression step, the pressure loss calculation should be provided to identical the initial pressure of the next step.

3.5.3 CO₂ Storage

This stage also required the energy in order to inject to the storage place (<http://www.osler.com/newsresources/Details.aspx?id=1324>) such as the ocean, underground. In the petroleum industry, liquefied CO₂ must be injected to the deep saline, depleted oil and gas reservoirs to recover this valuable natural recourse with the CO₂ injection. Minimum of required distance of the depth is more than 800 m (IEA, 2006). Pressure of this step is around the hydrostatic pressure of the ground water at the well head. This step is assumed to overcome the physical barriers which are gravity and surface tension. Minimum work is about the power from the change of pressure and concerned on the injection lifetime due to the increasing of reservoir pressure (Damen *et al.*, 2006; 2007). A typical value of the minimum work over the life time of the injection is approximately $2 \text{ kJ mol}^{-1} \text{ CO}_2$ storage at 2km. depth and 20 MPa (Kurt *et al.*, 2009), where as Koornneef *et al.* (2008) presented this stage consumed $1.11 \text{ kJ mol}^{-1} \text{ CO}_2$ storage at 3km. depth and 15 MPa.

CHAPTER IV

SIMULATION

This chapter presents all about the research simulations methodology including the simulation program, mathematical models and calculation procedure in the performance analysis of solid oxide fuel cell (SOFC). At first, two types of fuel processing reaction, conventional steam reforming (MSR) and decomposition (MD), are simulated by the AspenTM Plus program in order to study and analyze on the characteristics of fuel processing reactions. This simulation can justify the appropriate condition in each fuel processor to obtain into the performance analysis of SOFC system. Mathematical models written in Visual Basic are employed to analyze the SOFC system performance under the thermally self sufficient condition. It should be noted that the carbon capture and storage (CCS) is demanded for CO₂ capture in MSR fuel processor.

Thus, SOFC system are considered in the three kinds with the further integration in its system such as the MD fuel processor (called MD-SOFC), conventional MSR fuel processor (called MSR-SOFC), conventional MSR fuel processor and the CCS (called MSR-SOFC-CCS). At last, the economic analysis of all the SOFC systems is performed with the same basis of electrical power generation. The costing model and related information used in this analysis is also presented in this chapter.

4.1 SOFC systems overview description

The schematic diagrams of the SOFC systems with MSR, with MSR and CCS, and with MD are shown in Figures 4.1- 4.3, respectively. It should be noted that the overall of SOFC system operating pressure are set at the atmospheric pressure due to the economics consideration (Holladay *et al.*, 2009). Furthermore, isothermal

condition is performed in overall equipments and system. The major components in the systems include heat exchangers, a fuel processor, an SOFC stack, and an afterburner.

For the conventional SOFC system with MSR (Figure 4.1), steam is generated in a heat exchanger and mixed with the heated methane. Then the gas mixture is fed into the fuel processor where the steam methane reforming (Eq.1.1) and water-gas shift reaction (Eq.2.8) take place to generate H_2 -rich gas (reformed gas) for SOFC fuel. The H_2 -rich gas and air are introduced into the SOFC stack at the operating condition of 1073 K and atmospheric pressure (Piroonlerkgul *et al.*, 2008; 2009). After electricity and useful thermal energy were produced, the exhaust gases are then combusted in the afterburner to generate thermal energy for utilizing in the system. The exhausted gases are cooled and discharged from the SOFC system at 483 K. Furthermore, the addition of CCS is only required in the case of the MSR-SOFC system (Figure 4.2), the CCS is placed after the afterburner for CO_2 capture. For our proposed SOFC system with MD (Eq.1.1), the operation is less complicated as there is no steam input to the reactor and no the additional CCS (Figure 4.3).

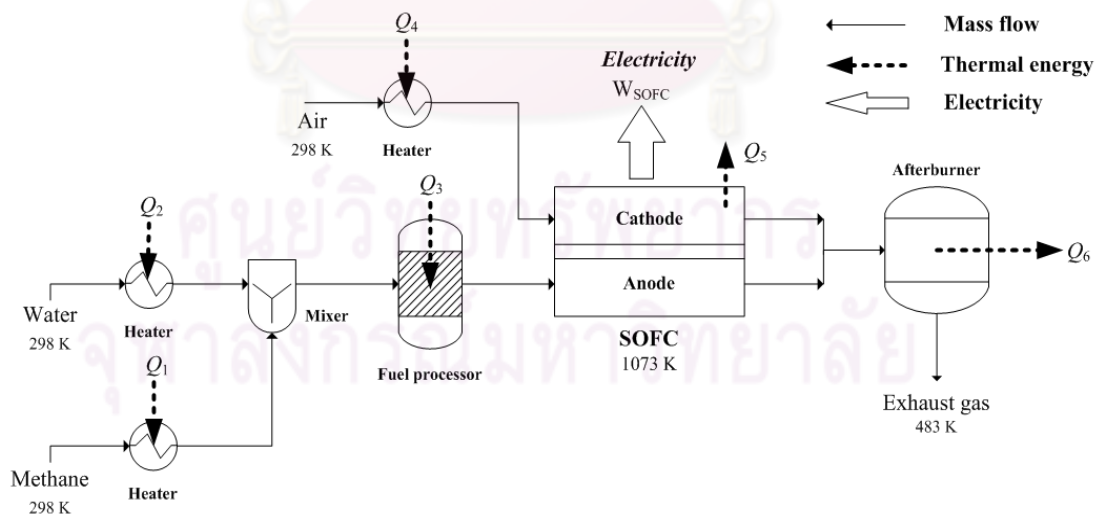


Figure 4.1 The conventional SOFC system configuration (with MSR in fuel processor).

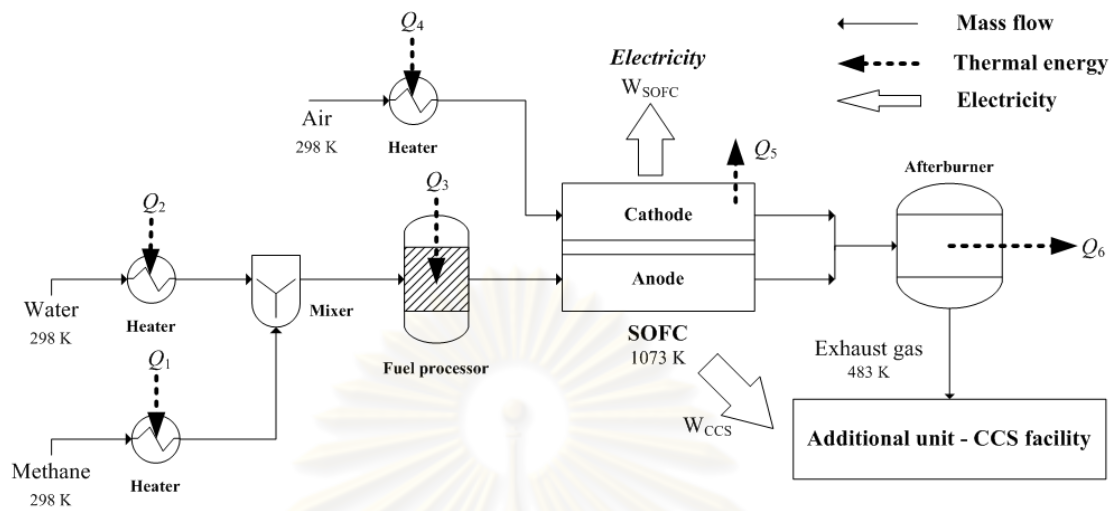


Figure 4.2 The conventional SOFC system configuration integrated with CCS facility.

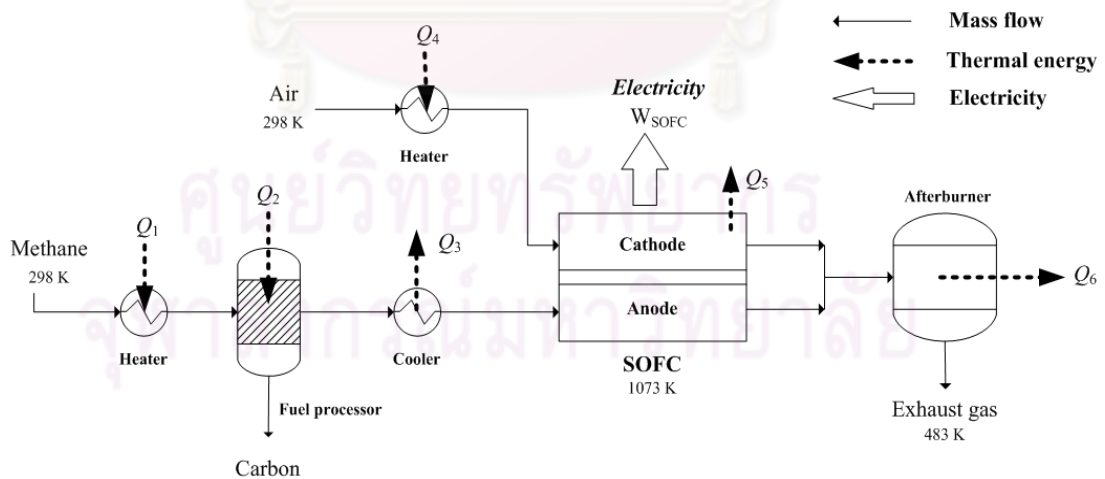


Figure 4.3 The proposed SOFC system configuration (with MD in fuel processor).

4.2 Fuel processors

Two types of fuel processor which are methane steam reforming (MSR) and methane decomposition (MD) fuel processor as shown in Figure 4.4 a) and b), respectively are simulated using AspenTM Plus program and the basic assumptions are listed as follows:

- Steady state operation with negligible friction loss.
- All gasses, e.g. CH₄, CO, CO₂, H₂O, H₂, N₂ and O₂, are ideal gases.
- In order to accept the mechanism of MSR (related with Eqs. (2.1) and (2.8)), MSR contains only five components which are CH₄, CO, CO₂, H₂O, H₂ (King *et al.*, 2005; Dalle Nogare *et al.*, 2007; Barelli *et al.*, 2008).
- The air contains 21 mol% O₂ and 79 mol% N₂.
- Due to nature of endothermic reaction basis of the *Le Chatelier's* principle, atmospheric pressure is set to be the operating pressure.
- Isothermal condition.
- For the performance analysis, 1 mol s⁻¹ of methane is set at the inlet fuel processor.

The fuel processing reactions are investigated under the thermodynamic equilibrium, thus, the *RGibbs* reactor is chosen to be the fuel processor model in this program. Consequently, the exit gas in each fuel processor reaches its equilibrium composition. Beginning with the 1 mol s⁻¹ of methane feed at the fuel processor, the heat exchangers need to pre-raise temperature up for reduction of the slow start up problem at the fuel processor (Abbas and Wan Daud, 2009 and Ahmed *et al.*, 2009).

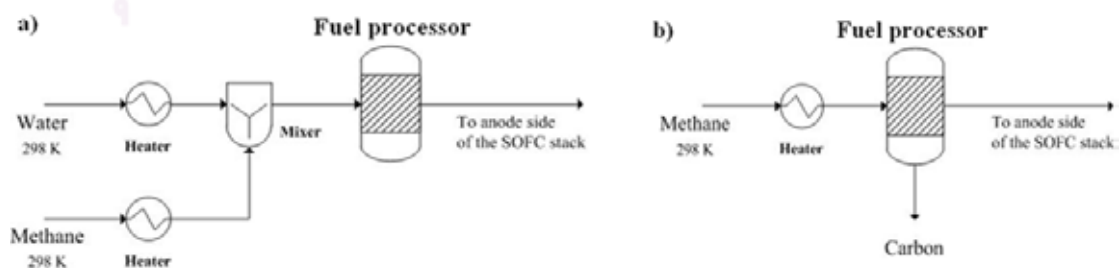


Figure 4.4 Schematic diagrams of fuel processors: a) MSR b) MD.

In order to study and analyze the characteristics of fuel processing reactions, CH_4 conversion, H_2/CH_4 mole ratio, purity of H_2 fuel in the gas phase and the energy requirement of fuel processing reaction are obtained by adjusting the operating parameters. The operating temperature of both fuel processors are varied in the range of 273 to around 2000 K and the MSR reaction is further varied with the steam to carbon molar ratio in its reaction. However, the amount of steam should consider in the equilibrium restriction of the side reaction (WGS), the steam to carbon molar ratio should be 2 or higher due to avoidance of coke formation and faster complete reaction (Palsson *et al.*, 2000; Sangtongkitcharoen *et al.*, 2005 and Arpornwichanop *et al.*, 2010).

Finally, the appropriate operating conditions in each fuel processor namely both of reaction temperature and steam to carbon molar ratio of MSR are selected to analyze the product distribution, then provided this appropriate fuel processor to integrate with SOFC system.

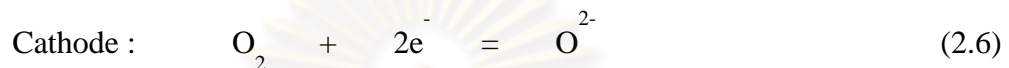
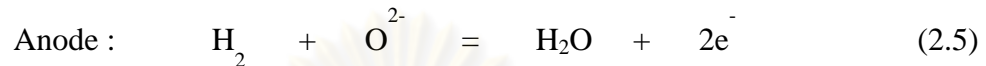
4.3 SOFC STACK MODEL

A fuel processor is installed prior to the SOFC unit. With appropriate conditions, the H_2 rich gas or reformed fuel gas is fed to the anode of the SOFC stack while the heated excess air (100% based on the methane equivalent flow) is introduced in the cathode side. After that the electrochemical reaction occurs to generate electricity and useful thermal energy as mentioned in Section 4.1. The SOFC systems are operated as shown in Figures 4.1-4.3 for MSR and MD, respectively.

The analysis in the SOFC stack cell unit should employ the reliable SOFC model. Therefore, the modeling of SOFC stack is based on the researches of Piroonlerkgul *et al.* (2008; 2009) to investigate the performance of SOFC system integrated with different fuel processors. This type of SOFC model is oxygen-ion conducting electrolyte (SOFC- O^{2-}) as well as it is more attractive than the proton-ion conducting electrolyte (SOFC- H^+) due to less steam requirement and less carbon

activity (Sangtongkitcharoen *et al.*, 2005). The electrochemical mechanism in this SOFC type is shown in the Eqs. (2.4)-(2.6). Only hydrogen is assumed to react electrochemically with oxygen ions. The SOFC stack component's materials; the anode, electrolyte, and cathode are made of Ni-YSZ, YSZ, and LSM-YSZ, respectively.

The electrochemical reaction in the SOFC-O²⁻



Importantly, this SOFC model has been verified with the three experiment result's cases; high purity of hydrogen case (mole fraction of hydrogen =0.97; Zhao and Virkar, 2005), MSR reformed fuel case (mole fraction of hydrogen =0.4; Tao *et al.*, 2005) and low concentration of hydrogen case (mole fraction of hydrogen =0.26; Petruzzi and Fineschi, 2003). Model validation in the high purity of hydrogen case (Zhao and Virkar, 2005) and MSR reformed fuel case (Tao *et al.*, 2005), the simulation showed the good result with the high accuracy of the experiment data, especially at the operating temperature of 1073K. And with the experiment data using low concentration of hydrogen case, the model also showed the good agreement with those from the literature (Petruzzi and Fineschi, 2003).

The high operating temperature of SOFC significantly promotes the reaction rate and the fast kinetics. It was reported at high temperature that the electro-oxidation of H₂ is much faster than of CO (Khaleel *et al.*, 2004), and the reaction rate of WGS is faster than any rate of oxidation (Blom *et al.*, 1994; Swaan *et al.*, 1994; Bradford and Vannice, 1996). Hence, it is also assumed that the methane remaining from the fuel processor is consumed via the overall methane steam reforming in the stack and the anode compositions always reach their equilibrium along the cell length.

4.3.1 Electrochemical model

Equations using for SOFC performances analysis namely open circuit voltage, overpotentials, power density, power and electrical efficiency are considered in this model. The related parameters in this model are presented in the Table 4.1.

4.3.1.1 Open circuit voltage

Open circuit voltage or theoretical voltage (E) can be calculated from the Nernst equation, at which the value depends upon the reversible potential (E^0), temperature, and gas compositions. Such open circuit voltage can be obtained by:

$$E = E^o + \frac{RT}{2F} \ln \left(\frac{P_{H_2} P_{O_2}^{\frac{1}{2}}}{P_{H_2O}} \right) \quad (4.1)$$

4.3.1.2 Actual cell potential

Actual cell potential (V) as expressed in Eq. (4.2) is always less than the open-circuit voltage (E) (Eq. 4.1) due to appearance of overpotentials. Three major overpotentials are involved in the system, including ohmic overpotential (η_{ohm}), activation overpotential (η_{act}), and concentration overpotential (η_{conc}).

$$V = E - \sum \eta_{loss} = E - \eta_{act} - \eta_{ohm} - \eta_{conc} \quad (4.2)$$

4.3.1.3 Overpotentials

In the calculation, there are three major overpotentials type namely ohmic overpotential (η_{ohm}), activation overpotential (η_{act}), and concentration overpotential (η_{conc}). The internal current overpotential can be neglected due to its small value.

- The ohmic overpotential (η_{ohm}) is the most concerned overpotential in the SOFC stack when compared to others, and it has directly related to current density (i) as shown in Eq. (4.3)

$$\eta_{ohm} = 2.99 \times 10^{-11} i L \exp\left(\frac{10300}{T}\right) \quad (4.3)$$

This loss causes from the higher electronic conductivity of the electrodes compare to the electrolyte. It has an effect on the resistance of ion flow in electrolyte and the resistance of electrons flow through the electrodes (Ferguson *et al.*, 1996).

- The activation overpotential (η_{act}) is controlled by the kinetics of electrochemical reaction at the electrode surface. High temperature operation in SOFC promotes the fast reaction rate, leading to a reduction of this loss. In this work, the Butler-Volmer equation is performed to compute the activation overpotential. And F is the *Faraday's* constant which is equal to $96,485.34 \text{ C mol}^{-1}$.

$$i = i_0 \left[\exp\left(\frac{\alpha z F \eta_{act}}{RT}\right) - \exp\left(\frac{(\alpha - 1) z F \eta_{act}}{RT}\right) \right] \quad (4.4)$$

In case of SOFC, α and z are set to be 0.5 and 2 according to Chan *et al.* (2001). Consequently, the activation potential at each electrode from the Eq. (4.4) can be simplified as:

$$\eta_{act,j} = \frac{RT}{F} \sinh^{-1}\left(\frac{i}{2i_{0,j}}\right), \quad j = a, c \quad (4.5)$$

The exchange current density (i_0) in each electrode is related to partial pressure and operating temperature. The expression for the anode and cathode electrodes can be computed from the following equations (Fleig, 2003):

$$i_{0,a} = \gamma_a \left(\frac{P_{H_2}}{P_{ref}} \right) \left(\frac{P_{H_2O}}{P_{ref}} \right) \exp \left(- \frac{E_{act,a}}{RT} \right) \quad (4.6)$$

$$i_{0,c} = \gamma_c \left(\frac{P_{O_2}}{P_{ref}} \right)^{0.25} \exp \left(- \frac{E_{act,c}}{RT} \right) \quad (4.7)$$

- The concentration overpotential (η_{conc}) is a loss occurring from a slow mass transfer. While the electrochemical reaction takes place over the stack, the reactant gases diffuse to the pore of the catalyst, resulting in the difference concentration of gas between the bulk and the reaction site. Therefore, this loss can be computed by the relation between gas diffusion coefficients and operating temperature as shown in Eqs. (4.8)-(4.9):

$$\eta_{conc,a} = \frac{RT}{2F} \ln \left[\frac{\left[1 + \left(\frac{RT}{2F} \right) \left(\frac{l_a}{D_{a(eff)} P_{H_2O}^I} \right) i \right]}{\left[1 - \left(\frac{RT}{2F} \right) \left(\frac{l_a}{D_{a(eff)} P_{H_2}^I} \right) i \right]} \right] \quad (4.8)$$

$$\eta_{conc,c} = \frac{RT}{4F} \ln \left[\frac{P_{O_2}^I}{(P_c - \delta_{O_2}) - ((P_c - \delta_{O_2}) - P_{O_2}^I) \exp \left[\left(\frac{RT}{4F} \right) \left(\frac{\delta_{O_2} l_c}{D_{c(eff)} P_c} \right) i \right]} \right] \quad (4.9)$$

where δ_{O_2} , $D_{a(eff)}$ and $D_{c(eff)}$ can be expressed by:

$$\delta_{O_2} = \frac{D_{O_2,K(eff)}}{D_{O_2,K(eff)} + D_{O_2-N_2(eff)}} \quad (4.10)$$

$$D_{a(eff)} = \left(\frac{P_{H_2O}}{P_a} \right) D_{H_2(eff)} + \left(\frac{P_{H_2}}{P_a} \right) D_{H_2O(eff)} \quad (4.11)$$

$$\frac{1}{D_{c(eff)}} = \frac{\xi}{n} \left(\frac{1}{D_{O_2,K}} + \frac{1}{D_{O_2-N_2}} \right) \quad (4.12)$$

and related with:

$$\frac{1}{D_{H_2(eff)}} = \frac{\xi}{n} \left(\frac{1}{D_{H_2,K}} + \frac{1}{D_{H_2-H_2O}} \right) \quad (4.13)$$

$$\frac{1}{D_{H_2O(eff)}} = \frac{\xi}{n} \left(\frac{1}{D_{H_2O,K}} + \frac{1}{D_{H_2-H_2O}} \right) \quad (4.14)$$

The correlation between the effective parameter and the normal parameter can be expressed by Eq. (4.15).

$$D_{(eff)} = \frac{n}{\xi} D \quad (4.15)$$

Knudsen diffusivity can be computed by the correlation below:

$$D_{i,K} = 9700r \sqrt{\frac{T}{M_i}} \quad (4.16)$$

Ordinary diffusivity can be calculated by Chapman-Enskog equation (Eq. (4.17)) (Massman, 1998):

$$D_{A-B} = 1.8583 \times 10^{-3} \left(\frac{T^{\frac{3}{2}} \left(\frac{1}{M_A} + \frac{1}{M_B} \right)^{\frac{1}{2}}}{P \sigma_{AB}^2 \Omega_D} \right) \quad (4.17)$$

where σ_{AB} (collision diameter; Å) and Ω_D (collision integral; Yakabe *et al.*, 2000) of each gas is computed as follows:

$$\sigma_{AB} = \frac{\sigma_A + \sigma_B}{2} \quad (4.18)$$

$$\Omega_D = \frac{1.06036}{T_k^{0.1561}} + \frac{0.193}{\exp(0.47635 \cdot T_k)} + \frac{1.03587}{\exp(1.52996 \cdot T_k)} + \frac{1.76474}{\exp(3.894 \cdot T_k)} \quad (4.19)$$

As well as T_k is equal to $\frac{T}{\varepsilon_{AB}}$.

Total related parameters of this model are concluded in the Table 4.1.

Table 4.1 Summary of model parameters (Ni *et al.*, 2007).

Parameters	Values
l_a	750 μm
l_c	50 μm
L	50 μm
n	0.48
ξ	5.4
γ_a	$1.344 \times 10^{10} \text{ A m}^{-2}$
γ_c	$2.051 \times 10^9 \text{ A m}^{-2}$
$E_{act,a}$	$1 \times 10^5 \text{ J mol}^{-1}$
$E_{act,c}$	$1.2 \times 10^5 \text{ J mol}^{-1}$
σ_{H_2}	2.827 \AA
σ_{H_2O}	2.641 \AA
σ_{N_2}	3.798 \AA
σ_{O_2}	3.467 \AA
ε_{H_2}	59.7
ε_{H_2O}	809.1
ε_{N_2}	71.4
ε_{O_2}	106.7

4.3.2 SOFC calculation procedure

The most variables which are employed to decide the optimal SOFC system are the electrical efficiency, power density and the stack area. Then, the mathematical models in the section 4.3.1 are managed and ordered to the step of the calculation (called the algorithm as shown in the Figure 4.5) before the Visual basic is set up to calculation. The calculation procedures are shown as below;

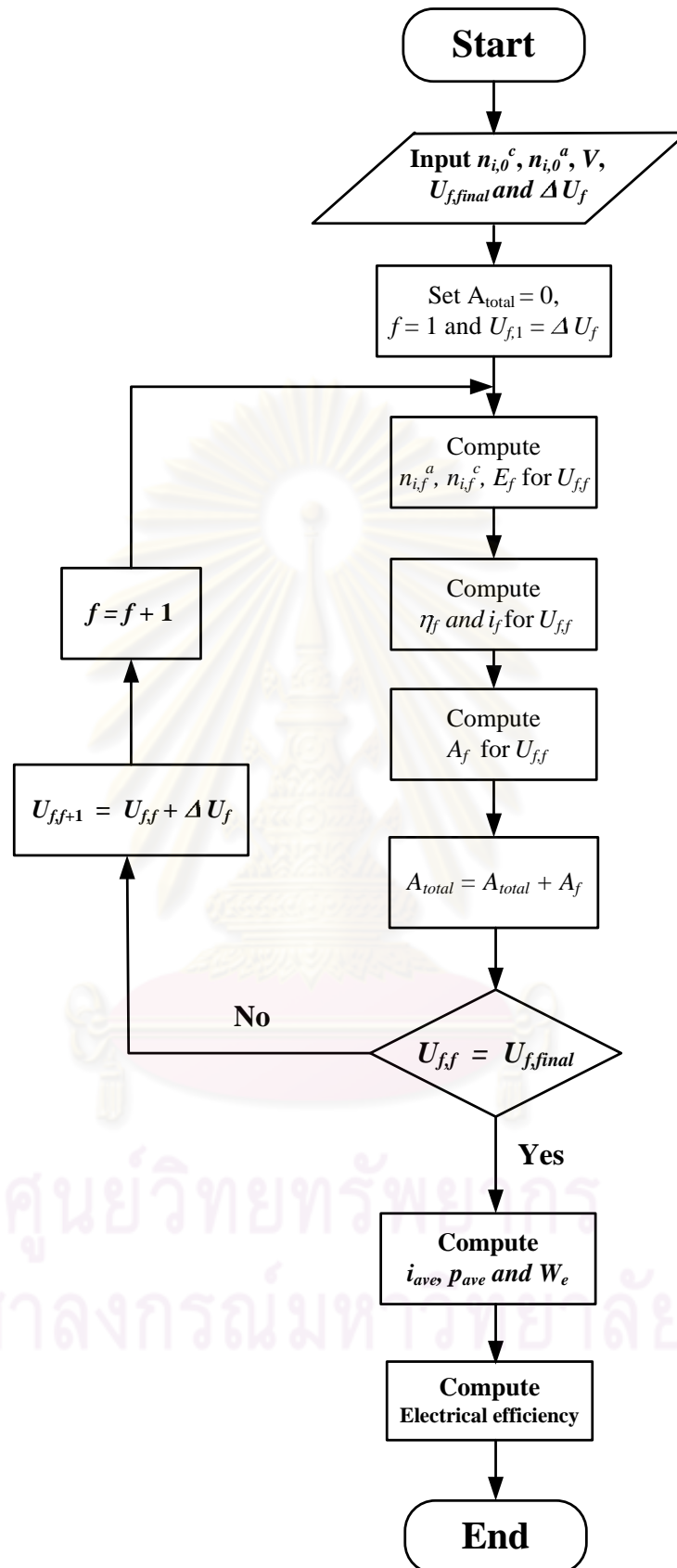


Figure 4.5 The flowchart of the calculation procedure in the program.

4.3.2.1 The desired values of anode and cathode inlet molar flow rate of each composition ($n_{i,0}^a$ and $n_{i,0}^c$), operating voltage (V), final fuel utilization ($U_{f,final}$), fuel utilization step (ΔU_f) are initially input to the program at the ensured operating condition (temperature of 1073 K and atmospheric pressure).

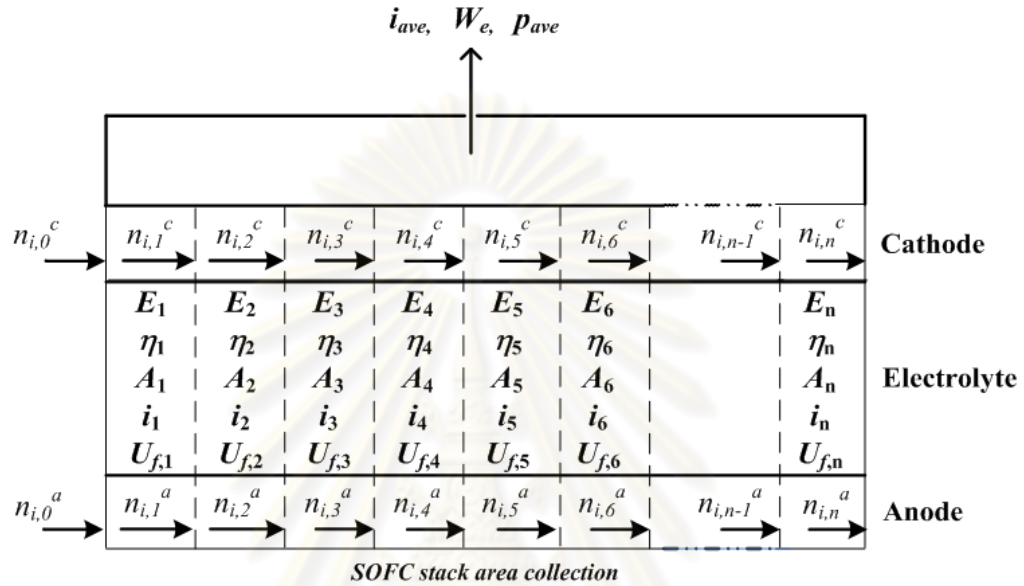


Figure 4.6 The SOFC stack area separation for the electrochemical calculation.

Some definitions, formulas or information of important parameters are presented;

- The available SOFC fuel includes of hydrogen, carbon monoxide and methane (Andujar and Segura, 2009; Neef, 2009 and Kirubakaran *et al.*, 2009).
- Fuel utilization (U_f): The measurement of the amount of fuel is consumed in the stack cell based on the inlet fuel feed at the of fuel cell.

$$U_f(\%) = \frac{H_{2, \text{equivalent}} \text{ consumption in SOFC stack}}{H_{2, \text{equivalent}} \text{ fed to the SOFC system}} \times 100 \quad (4.20)$$

- Hydrogen equivalent ($n_{H_2, eq}$): The other gas compositions can be influenced the electricity generation like hydrogen gas such as carbon

monoxide and methane (Palsson *et al.*, 2000; Zhang *et al.*, 2005; Piroonlerkgul *et al.*, 2009 and Arpornwichanop *et al.*, 2010).

$$n_{H_2,eq} = n_{H_2} + n_{CO_2} + (4 \times n_{CH_4}) \quad (4.21)$$

- Fuel utilization step (ΔU_f): The fuel consumption which refer to the used oxygen atom in the electrochemical is divided into steps for simplistic calculate and accuracy results (Piroonlerkgul *et al.*, 2009).

$$\Delta U_f = U_f \times n_{H_2,eq} \quad (4.22)$$

$$= \frac{\text{Total current (I)}}{2 \times F} \quad (4.23)$$

4.3.2.2 The equation set of the electrochemical model from Section 4.3.1 is used in the calculations. Open circuit voltage (E) is initially calculated from Eq.(4.2) and then provided to set the equivalent following in Eq.(4.3). The trial and error of current density (i) takes place until the difference between E and total overpotential (η) is equal to the operating voltage (V).

- The current density of SOFC system is achieved, then, the SOFC stack area of this fuel utilization region (A_f) is calculated using the following equation. A_f derived from the calculation at each fuel utilization region are added up to achieve total SOFC stack area (A_{total}) as shown in Figure 4.6.

$$A_f = \frac{2F(\Delta U_f)}{i_f} \quad (4.24)$$

4.3.2.3 After the area of SOFC in the step size of the fuel utilization is collected, next, the value of $U_{f,f}$ is checked with the desired fuel utilization ($U_{f,final}$) whether it reaches the $U_{f,final}$ or not.

- If $U_{f,f}$ is still lower than $U_{f,final}$, thus the calculations which increased the step of fuel utilization (U_f iteration) are recomputed until $U_{f,f}$ is equal to $U_{f,final}$.

4.3.2.4 Average current density (i_{ave}), average power density (p_{ave}) and total electricity (W_e) are also calculated with Eqs. (4.39) - (4.41), respectively.

$$i_{ave} = \frac{2F(U_{f,final})}{A_{total}} \quad (4.25)$$

$$p_{ave} = i_{ave}V \quad (4.26)$$

$$W_e = \frac{p_{ave}}{A_{total}} \quad (4.27)$$

4.3.2.5 Finally, the electrical efficiency calculations; overall electrical efficiency and stack cell electrical efficiency take place to further compare the performance of the interesting SOFC system.

Overall electrical efficiency (%)

$$= \frac{\text{Net electrical power generated}}{(\text{LHV of methane} \times \text{methane feed rate}) + \text{Required external energy}} \times 100 \quad (4.28)$$

Stack cell electrical efficiency (%)

$$= \frac{\text{Net electrical power generated}}{(\text{LHV of fuel} \times \text{fuel feed rate})_{\text{at anode side}}} \times 100 \quad (4.29)$$

4.4 Supplementary equipments

4.4.1 Heat exchanger

Thermal energy requirement for each unit can be calculated using conventional energy balances. It is assumed that the heat exchangers in the SOFC system are operated under adiabatic condition (no energy loss).

4.4.2 Afterburner

The anode and cathode exhaust gases are fed to the afterburner unit, where the exhaust gas is completely combusted to eradicate the composition of methane, carbon monoxide and hydrogen. It also generates thermal energy for supplying to all energy-demanding units in the SOFC system. The thermal energy can be extracted from the combusted gas without energy loss and the final exhaust gas emits to the environment at 483 K excepting in the case of MSR-SOFC-CCS.

4.5 Carbon capture and storage unit

For the conventional SOFC system with MSR, an additional CCS facility (Figure 4.7) is installed after the afterburner (called MSR-SOFC-CCS) in order to prevent CO₂ emission to the environment (Simbeck, 2004; Damen *et al.*, 2006; 2007 and Abu-khader, 2006).

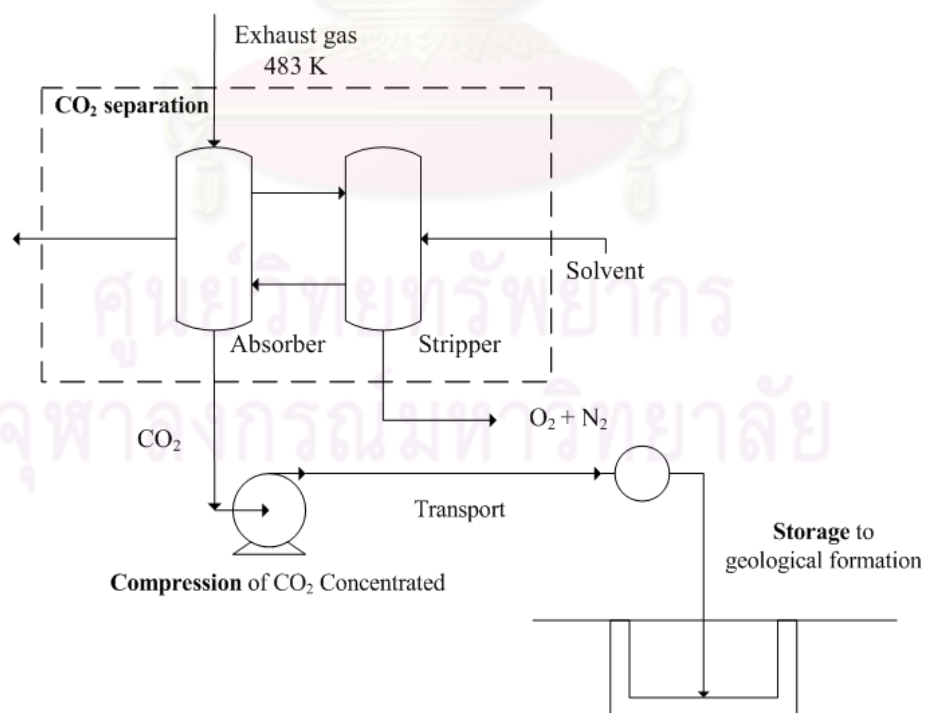


Figure 4.7 Three important steps in the CCS facility

The operation of CCS employs the power generation of the SOFC to utilize in its steps as shown in the Figure 4.2. There are 4 main assumptions for this unit, including:

- No water is prior separated out from the exhaust gas,
- Operation is under the isothermal and isobaric condition
- The ideal gas state is still the basis assumption.
- CO₂ and air do not chemically interact.

The energy requirement in the CCS facility can be calculated as follows:

4.5.1 CO₂ separation from the exhaust gas

The exhaust gas from the afterburner is transported to the CCS facility. The selected capture method is the chemical absorption by the methyl ethanolamine absorbent (MEA) (Freguia and Rochelle, 2003 and Wang *et al.*, 2004). This capture method offers more CO₂ separation efficiency than 90% (Herzog., 1999 and Koornneef *et al.*, 2009) and only use MEA approximately 1.96 kg ton CO₂⁻¹ (average from Chapel *et al.*, 1999; Koornneef *et al.*, 2009; Knudsen *et al.*, 2006; IEA GHG., 2006 and Singh *et al.*, 2010.). With the 30%wt of MEA solution, CO₂ is initially absorbed at the absorber unit (Singh *et al.*, 2010) with the operating condition; temperature of 323 K and atmospheric pressure (Gibbins and Chalmers, 2009). At this stage, the electricity is required around 23.55 kWh ton CO₂⁻¹ in order to use in the pump and fan. This function of the pump and fan are to carry MEA absorbent and to overcome the pressure drop at the absorber unit. After the CO₂ is absorbed until the MEA solution will saturate. MEA solution is fed to regenerate at the stripper for reuse in the absorber. Temperature of this stripper unit is 393 K (Gibbins and Chalmers, 2009) and the thermal energy is required around 4.12 GJ_{thermal} ton CO₂⁻¹ (average from Chapel *et al.*, 1999 (optimal) ; Alie *et al.*, 2005 (optimal); Knudsen *et al.*, 2006; RaO *et al.*, 2006; Abu-Zahra *et al.*, 2007 and Koornneef *et al.*, 2009). However, this CCS facility employs the electricity from the SOFC system to utilize, thus , the power equivalent factor (P_{ef}) is important to convert the thermal energy form into the electrical energy form. Koornneef *et al.* (2009) presented this value is about 0.2 GJ_{electrical} GJ_{thermal}⁻¹.

4.5.2 CO₂ compression and transportation

The concentrated CO₂ separated from the exhaust gas at the previous step is converted into the liquid form under the compression step. In order to easily transport and to prevent the two phases flow of CO₂ via the pipeline, the compressed pressure should be more than the critical pressure of 7.4 MPa and the temperature should be less than or equal to the critical temperature of 304 K (Koornneef *et al.*, 2008).

The compressed pressure in this study determined by averaging compressed pressure of the various literature reviews is about 14 MPa (average from Hattenbach *et al.*, 1999; Damen *et al.*, 2007; Koornneef *et al.*, 2008 and House *et al.*, 2009), furthermore, this average compressed pressure may support the transport distance of 50 km without the pressure loss (Koornneef *et al.*, 2008 and House *et al.*, 2009). The temperature is assumed at 303 K (Damen *et al.*, 2007). The calculation of the compressor is based on the fluid mechanics theory at which the compressed work under the isentropic compression (Damen *et al.*, 2007; Koornneef *et al.*, 2008 and House *et al.*, 2009) as shown in the Eq.(4.30). The N stages which are equal to 4 are determined for the reduction in the power consumption (Koornneef *et al.*, 2008).

$$W = \frac{ZRT}{M} \frac{N\gamma}{\gamma-1} \left(\left(\frac{P_{out}}{P_{in}} \right)^{\frac{\gamma-1}{N\gamma}} - 1 \right) \quad (4.30)$$

where $\gamma = \frac{C_p}{C_p - R}$ (4.31)

Finally, the actual electrical power consumption (Eq.(4.32)) can be achieved by stipulating the isentropic (η_{is}) and mechanics efficiency (η_m) of 0.8 and 0.99 (Damen *et al.*, 2007 and Koornneef *et al.*, 2008).

$$E_a = \frac{W}{\eta_{is}\eta_m} \quad (4.32)$$

4.5.3 CO₂ Storage

After liquid CO₂ transport to a promising place, it also needs the enough pressure in order to inject to the 3km. depth of the well (Koornneef *et al.*, 2008) and to overcome the physical barriers which are gravity and surface tension (House *et al.*, 2009). Pressure of this step which is around the hydrostatic pressure of the ground water at the well head is 20 MPa (average from Hattenbach *et al.*, 1999; Damen *et al.*, 2007; Koornneef *et al.*, 2008 and House *et al.*, 2009). The calculation of the compressor is similar to the section 4.5.2, but the N stages are equal to 2 (Koornneef *et al.*, 2008).

4.5.4 SOFC efficiency with the further CCS application

The overall electrical efficiency alters from the Eq.(4.28), when CCS facility is integrated to the conventional SOFC. The CCS facility doesn't relate with the thermally self sufficient operation in terms of zero net energy's balance, but, it only provides the electrical power generation of SOFC to utilize in its driving operation. SOFC efficiency with CCS application is shown in Eq.(4.33).

Efficiency of MSR-SOFC-CCS (%)

$$= \text{Efficiency of MSR-SOFC} - \frac{W_{\text{Capture}} + (Q_{\text{Capture}} \times P_{\text{ef}}) + W_{\text{Compression}}}{(\text{LHV of methane} \times \text{methane feed rate})} \times 100 \quad (4.33)$$

4.6 Thermally self-sufficient operation ($Q_{\text{net}} = 0$)

The SOFC systems in this study are focused on an operation at the thermally self-sufficient condition) (Palazzi *et al.*, 2007; Vivanpatarakij *et al.*, 2007 and Piroonlerkgul *et al.*, 2009). At this condition, the value of Q_{net} is equal to zero, indicating that the total generated thermal energy from the SOFC system is performed to supply the overall thermal energy-demanding units without external energy input.

The thermally self-sufficient condition can be achieved by tuning of fuel utilization (U_f) at various operating voltages (V).

From the system configuration in Figures 4.1-4.3, there are main units which play an important role in releasing thermal energy namely; SOFCs (Q_5) and afterburner (Q_6). But the MD requires a further cooler due to its high temperature in fuel processor. Therefore, this proposed system with MD will have three generated thermal energy units, Q_3 , Q_5 , and Q_6 . In term of thermal energy demand, this value consists of the energy consumption in heaters and fuel processors. The Q_{net} in the thermally self-sufficient operation is calculated by:

SOFC system with MSR

$$Q_{net} = (Q_1 + Q_2 + Q_3 + Q_4) - (Q_5 + Q_6) \quad (4.34)$$

SOFC system with MD

$$Q_{net} = (Q_1 + Q_2 + Q_4) - (Q_3 + Q_5 + Q_6) \quad (4.35)$$

For the CCS facility (Figure 4.3), only conventional MSR is necessary to add the CCS facility (MSR-SOFC-CCS) due to capture and storage the CO_2 . Because of thermally self-sufficient operation, there are no external energy and electrical input; hence, this unit has merely the effect on the electrical power produced from the SOFC system to separate CO_2 , compress, transport and storage.

4.7 Economic analysis

Not only the performance analysis is the method to justify the optimal SOFC system, but also the economic analysis should be analyzed couple with performance in the real process system. For the economic analysis, the deviation in the value of money with time is neglected. Hence, the interest rate and the inflation rate are assumed to be zero. Under the economic analysis, the net electrical power generation of three SOFC systems; MSR-SOFC, MSR-SOFC-CCS and MD-SOFC are set to be identical to 1 MW.

It should be noted on this analysis that

- Under the thermally self-sufficient operation, external energy and electricity are not required.
- CCS is only constructed with MSR due to CO₂ capture, thus, higher produced electrical in MSR-SOFC-CCS will be need due to the similar 1MW of net electrical power generation.
- Other costs without mention are assumed to be similar to conventional case (MSR-SOFC).

The overall cost is provided to analyze consisting of the SOFC stack capital cost, supplementary equipment, raw material fuel and receiving product cost and CCS capital cost. Five variables used to justify the SOFC system which provide more economic benefit are saving in capital cost in SOFC stack, saving in additional cost of supplementary equipment, saving of raw material fuel, return profit from by product and additional cost of CCS. And the final result is shown in the form of net cost saving in the Eq. (3.36).

Net cost saving (\$)

$$= \text{Saving in capital cost in SOFC stack} + \text{Saving in additional cost of supplementary equipment} + \text{Saving of raw material fuel} + \text{Return profit from by product} - \text{Additional cost of CCS} \quad (3.36)$$

Where the word of “saving” is refer to the comparison this interesting value with the conventional case. For example, saving in capital cost in SOFC stack is equal to the fuel cost of conventional case minus the interested case. Under this result of economic analysis, positive net cost saving indicates that the interested case is economically superior to the conventional case. The costing models and parameters used in the economic analysis are listed in Table 4.2.

Under the consideration of environmental with economic analysis, two carbon captur cases; MSR-SOFC-CCS and MD-SOFC are performed to evaluate in term of “effective cost of carbon capture” as shown in the Eq. (3.37).

Effective cost of carbon capture (\$ ton⁻¹)

$$= \frac{\text{Net cost saving (\$)}}{\text{Rate of carbon capture (ton year}^{-1}\text{) } \times \text{Plant life time (year)}} \quad (3.37)$$

Table 4.2 Costing models and parameters used in the economic analysis.

Costing model and parameters	
SOFC* (Piroonlerkgul <i>et al.</i> , 2009)	
- Cell cost (\$)	$C_{\text{cell}} = A_{\text{single cell}} \times 0.1442^*$
- Number of cells	$N_{\text{cell}} = A_{\text{total}} / A_{\text{single cell}}$
- Number of stacks	$N_{\text{stack}} = N_{\text{cell}} / 100$
- Fuel cell stacks cost (\$)	$C_{\text{stack}} =$ $2.7 \times [(C_{\text{cell}} \times N_{\text{cell}}) + (2 \times N_{\text{stack}} \times A_{\text{single cell}} \times 0.46425)]$
Heat exchanger (\$ kW ⁻¹)	100 (Steinberg, 2009)
Capture capital cost (\$ ton ⁻¹ CO ₂)	42.33 (Herzog., 1999)
Compressor (\$)	$C_{\text{compressor}} = 1.49 \times HP^{0.71} \times 10^3$ (Piroonlerkgul <i>et al.</i> , 2009)
Pipeline cost in CCS (\$ ton ⁻¹ CO ₂ 100km ⁻¹)	2.35 (average cost; http://www.arc.ab.ca)
Raw material fuel cost (\$ (1000 ft ³) ⁻¹)	9.36 (IEA Natural gas, 2010)
Carbon selling cost (\$ lb ⁻¹)	0.5 (http://www.icispricing.com)
MEA cost (\$ ton ⁻¹)	1950 (average cost; http://www.alibaba.com)
Project life time (year)	5

*A single cell area is fixed at 200 cm²

CHAPTER V

RESULTS AND DISCUSSION

In this chapter, the simulation and calculation results are presented and discussed by dividing into three main parts; reaction characteristics of fuel processors, performance analysis of solid oxide fuel cell (SOFC) system and economic analysis as mentioned in the previous chapter. At first, the appropriate operating condition of both fuel processors is chosen to generate a reformed gas for feeding to the SOFC system, and then the SOFC system is analyzed to find the thermally self-sufficient operating point. Carbon capture and storage (CCS) is further integrated to the integrated methane steam reforming and solid oxide fuel cell (MSR-SOFC) system in order to be environmental friendly like the integrated methane decomposition and solid oxide fuel cell (MD-SOFC) system. Under the desired condition, the optimal condition (related with the highest of power density) can be achieved via the performance analysis. Lastly, the net electrical generation is scaled up into 1MW basis for economic analysis. This part is significantly discussed to find the best fuel processor for integration with SOFC system.

5.1 Reaction characteristics of fuel processors

Under the thermodynamic consideration, two fuel processors; MSR and MD are firstly investigated to determine the characteristics of the reactions and to select appropriate operating condition of the fuel processors.

5.1.1 General characteristics of fuel processing reaction

Both of two reactions simulated in AspenTM Plus program are based on the equivalent methane flow rate of 1 mol s^{-1} at various operating temperatures and

various steam to carbon ratios (S/C) for MSR. The operating temperature of both reactions is varied on the range of 273-2000 K and the S/C ratio is varied initially at the basic requirement S/C ratio (Palsson *et al.*, 2000; Sangtongkitcharoen *et al.*, 2005 and Arpornwichanop *et al.*, 2010) of 2 until the excess steam of S/C ratio of 4.

According to the *Le Chatelier's* principle, both reactions (Eqs. 2.9 and 1.2) are favorable at low pressure. Thus, the atmospheric operating pressure is reasonably performed to operate in the overall SOFC system due to the economic consideration and the *Le Chatelier's* principle acceptance.

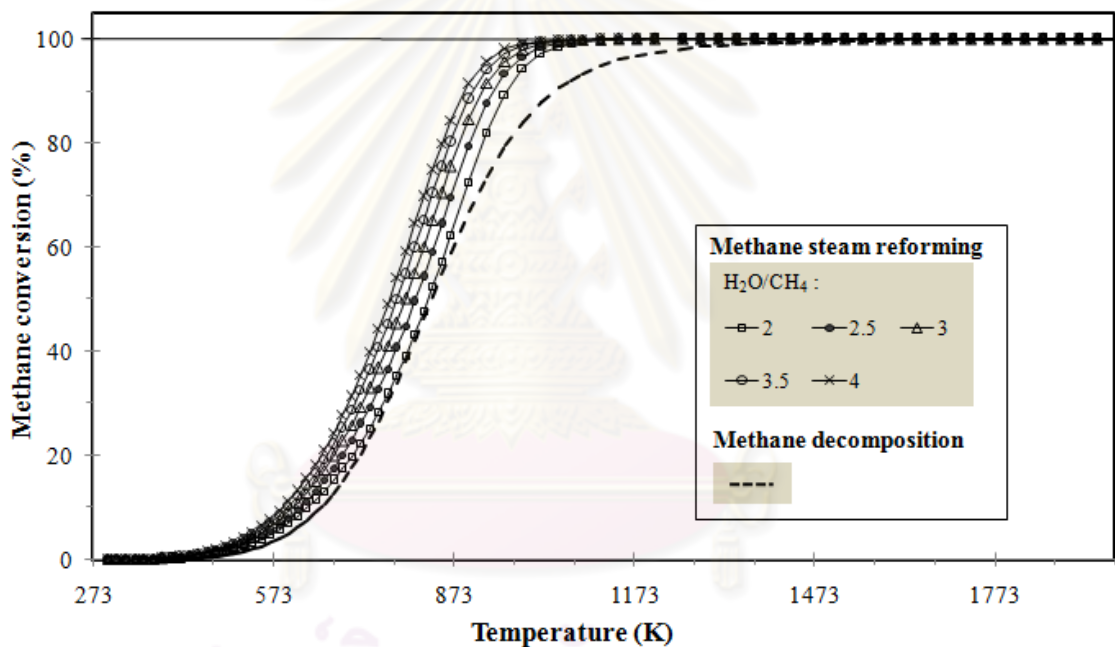


Figure 5.1 Methane equilibrium conversions between conventional methane steam reforming (solid line with marker point) and decomposition (dash line) at the atmospheric pressure and varying temperature.

Figure 5.1 shows that the methane conversion increases with the increasing operating temperature because of endothermic nature of both reactions. Water is a suitable oxygenated compound for reforming reaction (Piroonlerkgul *et al.*, 2008 and Holladay *et al.*, 2009) and methane in the MSR fuel processor can be converted to

desired hydrogen fuel at a lower temperature. The higher amount of steam can shift the forward MSR reaction to complete methane conversion at the lower temperature. Comparison with MD, methane at minimum S/C ratio of 2 in MSR is completely converted at the lower temperature (over 1000 K) than methane in MD (1400 K).

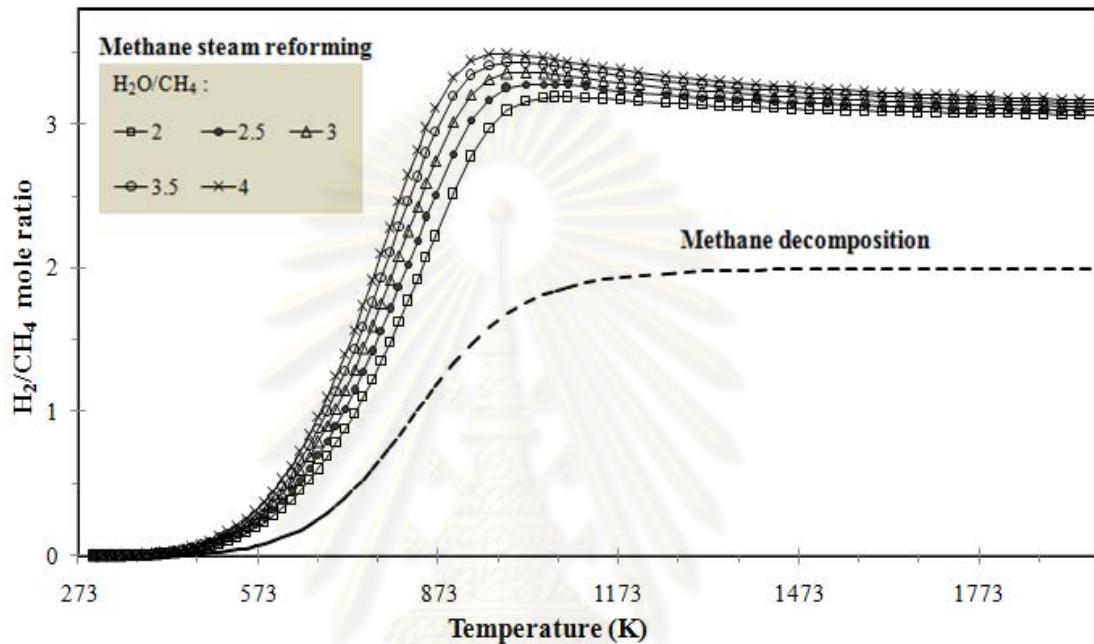


Figure 5.2 Hydrogen to methane (H_2/CH_4) mole ratio between conventional methane steam reforming (solid line with marker points) and decomposition (dash line) at the atmospheric pressure and varying temperature.

Figure 5.2 shows the hydrogen production represented by the mole ratio of H_2/CH_4 . MSR offers much higher H_2/CH_4 mole ratio than MD as part of hydrogen is obtained from the steam. Methane in MD is directly converted to hydrogen in the H_2/CH_4 mole ratio of 2 following to Eq. 1.2. In contrast, for MSR, this H_2/CH_4 mole ratio is influenced by the coupled reaction-water gas shift reaction (WGS) along the operating temperature. At the initial operating temperature, methane steam reforming reaction (Eq.1.1) as well as the WGS (Eq. 2.8) continuously generate hydrogen, so the H_2/CH_4 mole ratio curve increases and reaches the maximum hydrogen production.

After that the endothermic reverse WGS (reverse Eq. 2.8) plays an important role in the MSR at the higher temperature around 900 K, the hydrogen is consumed with the carbon dioxide in the reaction. The H_2/CH_4 mole ratio curve slowly drops to steady curve at the higher temperature.

Although the MSR fuel processing reaction shows higher methane conversion and hydrogen mole in the product compared with MD fuel processing reaction, it is obviously shown that the hydrogen purity is much lower as shown in Figure 5.3.

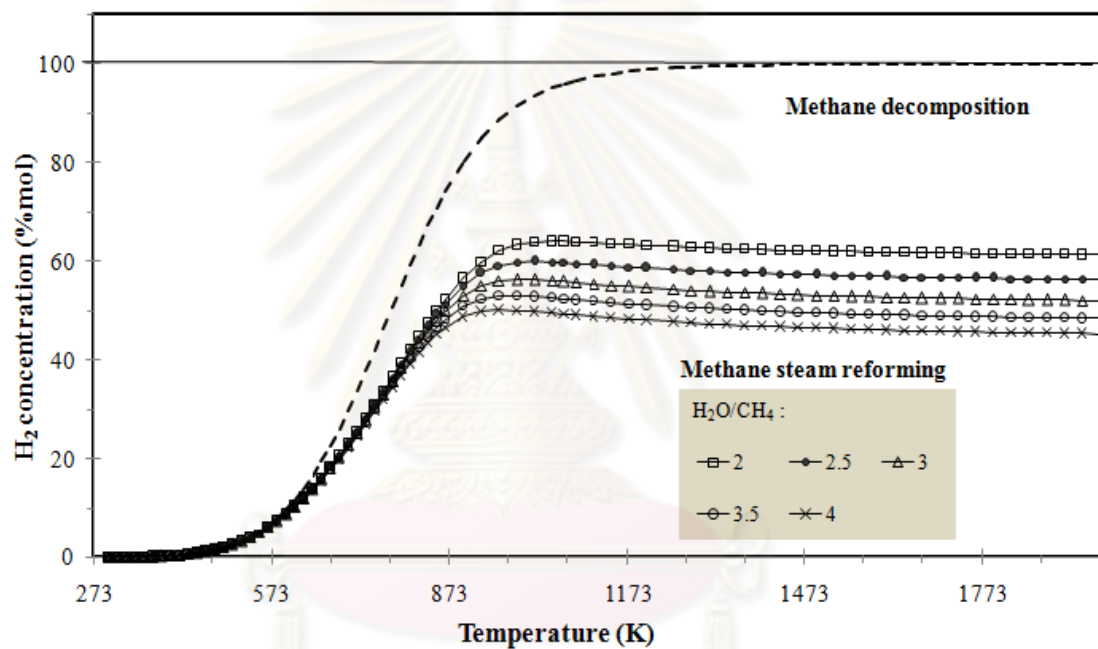


Figure 5.3 Hydrogen concentrations between conventional methane steam reforming (solid line with marker points) and decomposition (dash line) at the atmospheric pressure and varying temperature.

MSR is taken place via the two main reactions (methane steam reforming in Eq. 1.1 and water-gas shift in Eq.2.8) as previously mentioned, thus, its hydrogen concentration must be lower because of the contamination with carbon oxides (CO_x), remaining steam and methane. Even though the higher amount of steam (higher S/C ratio) can shift the forward MSR reaction, it also dilutes the hydrogen fuel with the

excess of steam (Piroonlerkgul *et al.*, 2008 and Dokmaingam *et al.*, 2010). This will be effect in future use in the SOFC (Suwanwarangkul *et al.*, 2006; Sangtongkitcharoen *et al.*, 2005; Piroonlerkgul *et al.*, 2009; Barelli *et al.*, 2008; Holladay *et al.*, 2009). For MD, hydrogen is generated without the presence of CO_x and diluted steam in the gas product. Hydrogen purity of MD can be achieved nearly 100% at operating temperatures higher than 1473 K. Furthermore, carbon can be captured as the solid form, thus, the gas composition at the exit of this fuel processor only consists of only hydrogen and the remaining methane.

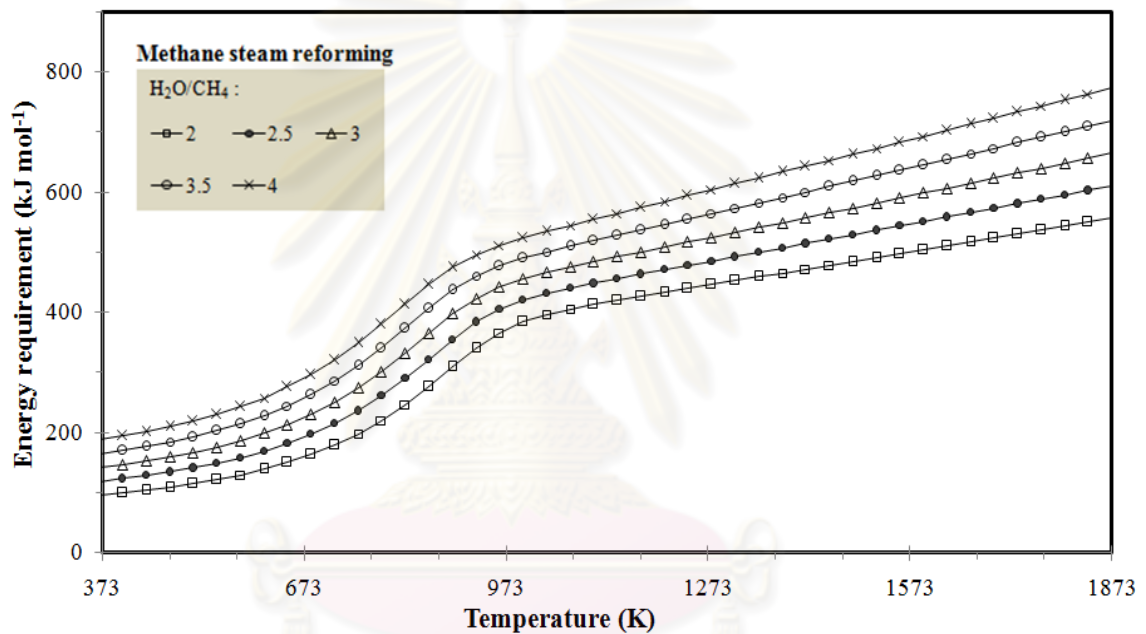


Figure 5.4 Total energy requirements of conventional methane steam reforming at the atmospheric pressure, varying temperature and steam to carbon ratio.

Considering the energy requirement as shown in the Figure 5.4, MSR fuel processor is also influenced by the thermal energy demand of the side reactions; namely methane decomposition reaction (Eq. 1.2), boudouard reaction (Eq. 2.10) and carbon gasification (Eq. 2.11). This part only analyzes the related reaction, the related product distribution will be later mentioned in the appropriate condition of fuel processor part. There are two regions on the energy profile at varying temperature; low temperature region (at room temperature to around 953K) and high temperature

region (higher than 953 K). The effect of the side reactions has significant influence on the reduction of the total energy requirement at the low temperature region.

At the low temperature region, two main reactions (Eqs. 1.1 and 2.8) generally play an important role in the generation of hydrogen fuel, resulting in the net endothermic reaction in Eq. 2.9. The energy requirement increases with the increasing temperature and the increasing S/C ratio, but the energy profile in this region does not behave like the linear curve. It can be identified that the carbon formation occurring via the Boudouard reaction (Eq. 2.10) affected to the exothermic thermal energy (Dicks, 1996). Thus, this Boudouard and WGS reaction support some energy requirement for MSR. Other side endothermic reaction which are MD reaction (Eq.1.2) and Carbon gasification reaction (Eq. 2.11) have an effect when the Boudouard and WGS reaction do not favor at the higher temperature of 696 K and 812 K, respectively (identified from Gibb's free energy). Consequently, the energy profile presents the linear tend of energy requirement at the high temperature region. It shows higher energy requirement level than low temperature region, because the summation of endothermic reations also play the role in the MSR system namely methane steam reforming (Eq. 1.1), MD reaction (Eq.1.2), reverse WGS (reverse Eq. 2.8) and Carbon gasification reaction (Eq. 2.11).

Even though Boudouard reaction can provide some exothermic energy, the long operation without the reactor clogging by coke or soot is preferable. To have high methane conversion, avoidance of many related side reactions and reduction of the excess of steam are considered to operate at the high operting tempertaure (Fuel cell Handbook, 2004 and Timmermann *et al.*, 2010) as shown in Figures 5.1-5.5. Figure 5.5 shows that S/C ratio is an important variable affecting on the total energy requirement at the varying temperatures. The basic heat of reaction at the specific temperature is the energy that the reactant can be readily converted at the state of selecting tempertature, therefore, every S/C ratio has intimately the basic heat of reaction at the one temperature. This is emphasized that higher steam feed in the reaction must require the higher pre-heating energy as shown in the defference area of total energy and basic heat of reaction (Sangtongkitcharoen *et al.*, 2005 and Dokmaingam *et al.*, 2010).

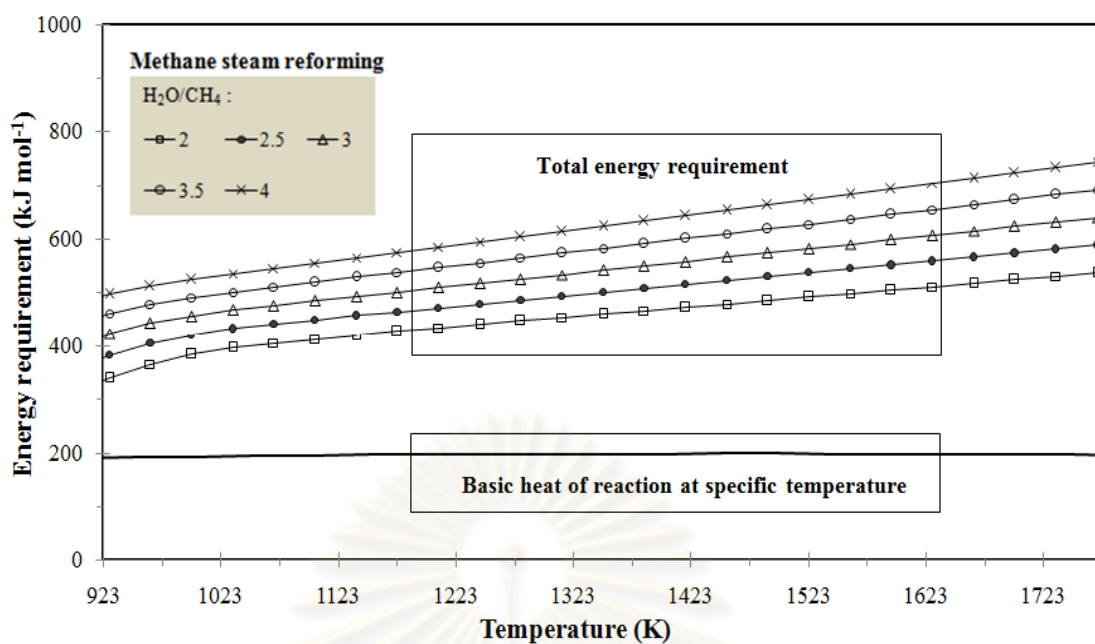


Figure 5.5 Energy requirements of conventional methane steam reforming at the atmospheric pressure, varying high temperature and steam to carbon ratio.

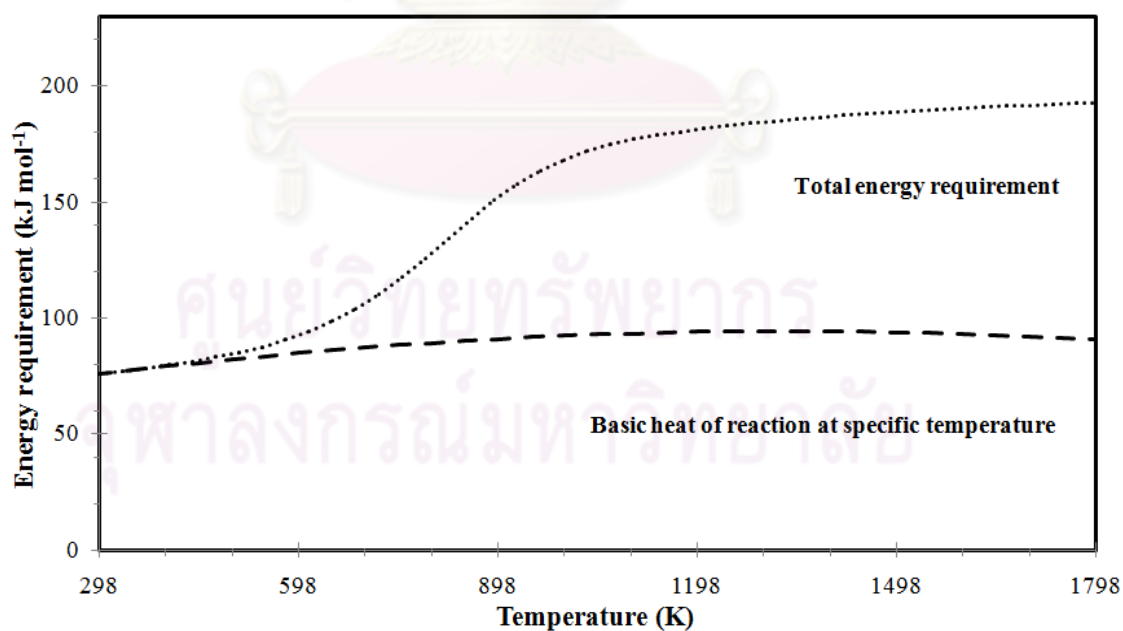


Figure 5.6 Energy requirements of methane decomposition at the atmospheric pressure, varying high temperature.

The energy requirement of MD is presented in Figure 5.6, the total energy requirement has been improved with the increasing temperature. This figure also has the difference region between total energy and basic heat of reaction like Figure 5.5, methane also required the two parts of energy in order to preheat to the reaction temperature and to convert itself into hydrogen and carbon. However, methane in MD has the equivalent methane conversion, it must require the higher operating temperature than MSR operating temperature. This is because the decomposition of methane takes place without the oxidant substance (like steam in steam reforming of methane).

5.1.2 Appropriate operating condition of fuel processor

The appropriate conditions of methane steam reforming (MSR) and decomposition (MD) fuel processors can be selected from the investigation on general characteristics of reaction. For the MSR fuel processing reaction, several works have reported a suitable amount of steam to provide long activity and reduce carbon formation. As mentioned in the literature review, conventional industrial methane steam reforming reaction is usually run under a S/C ratio of 1.4 or higher (Dick, 1996), but the equilibrium consideration of the water gas shift reaction (WGS), the S/C ratio is suggest to be 2 or higher (Renner and Marschner, 1985; Palsson *et al.*, 2000; Sangtongkitcharoen *et al.*, 2005; Vivanpatarakij *et al.*, 2009; Arpornwichanop *et al.*, 2010).

In addition, it is noted that using high excess of water in the system has some disadvantages; 1) excess steam can dilute the hydrogen concentration in the reformed gas, 2) higher thermal energy is required in the SOFC system, and 3) power density and performance of the SOFC can be lower as reported by Piroonlerkgul *et al.* (2009) and Dokmaingam *et al.* (2010). The S/C ratio of MSR is firstly selected at the ratio of 2.5 as the carbon activity at this value tends to approach zero (Piroonlerkgul *et al.*, 2009). Many researches also gave support to utilize the S/C ratio of 2.5 at the high operating temperature for MSR fuel processor (Renner and Marschner, 1985; Palsson *et al.*, 2000; Douvartzides *et al.*, 2003 and Zhang *et al.*, 2005). Next, appropriate

operating temperature is determined based on the requirements of high methane conversion, large amount and high purity of desired hydrogen in the reformed gas.

The product distribution should be firstly described before the appropriate temperature of both reactions is selected. This behavior of product distribution (Figure 5.7) under the varying temperature agrees with the related reaction explanation in the two energy profiles of Figures 5.4 and 5.6. It can be concisely enumerated that methane is increasingly consumed to produce hydrogen fuel when the operating temperature of endothermic reaction is raised. It is clearly shown that hydrogen can be more generated in the MSR due to the presence of water reagent and higher stoichiometric coefficient in the theoretical mole balance (Eqs. 2.9 and 1.2) (Dokmaingam *et al.*, 2010; Halabi *et al.*, 2010). MD reaction shows the simple reaction in order to directly crack without the side reaction, thus it shows the similar trend of hydrogen and carbon solid. The carbon solid only occurs in the main products of MD, it can be in the various forms of carbon such as nanotubes, nanofilament, fibers, and powder like carbon black or activated carbon (Suelves *et al.*, 2005; Bonura *et al.*, 2006 and Abbas and Wan Daud, 2009). The high temperature is desired in the operation of this MD for SOFC system in order to achieve the high purity and large amount of hydrogen fuel.

Whereas the MSR reaction manifests the different trend of product, two behavior of product occurs with the changing operating temperature range. At the lower temperature range, product distribution of MSR occurs under the methane steam reforming (Eq. 1.1) and WGS reaction (Eq. 2.8). The products are hydrogen and carbon oxides. The carbon formation in MSR also significantly occurs at the lower temperature via the Boudouard reaction (Eq. 2.10), so in the lower temperature the energy requirement must be lower by this exothermic reaction. However, the excessive can suppress the carbon formation in the MSR reaction (Eq. 2.10), and then the carbon in MSR is not present in this temperature range.

At the high temperature, WGS and Boudouard reaction are not favored resulting in the significant reduction of carbon dioxide. The endothermic reverse water gas shift reaction (RWGS) (reverse of Eq. (3)), in turn, plays an important role

in the MSR process, resulting in the declination of hydrogen production at temperature higher than 1100 K. The appearance of methane decomposition (Eq.1.1) and the carbon removal of gasification reaction causes the higher carbon monoxide. The side reactions occurring with methane steam reforming reaction also support that this temperature range needs higher energy requirement, and thus reduces the amount and purity of hydrogen as mentioned at the previous part.

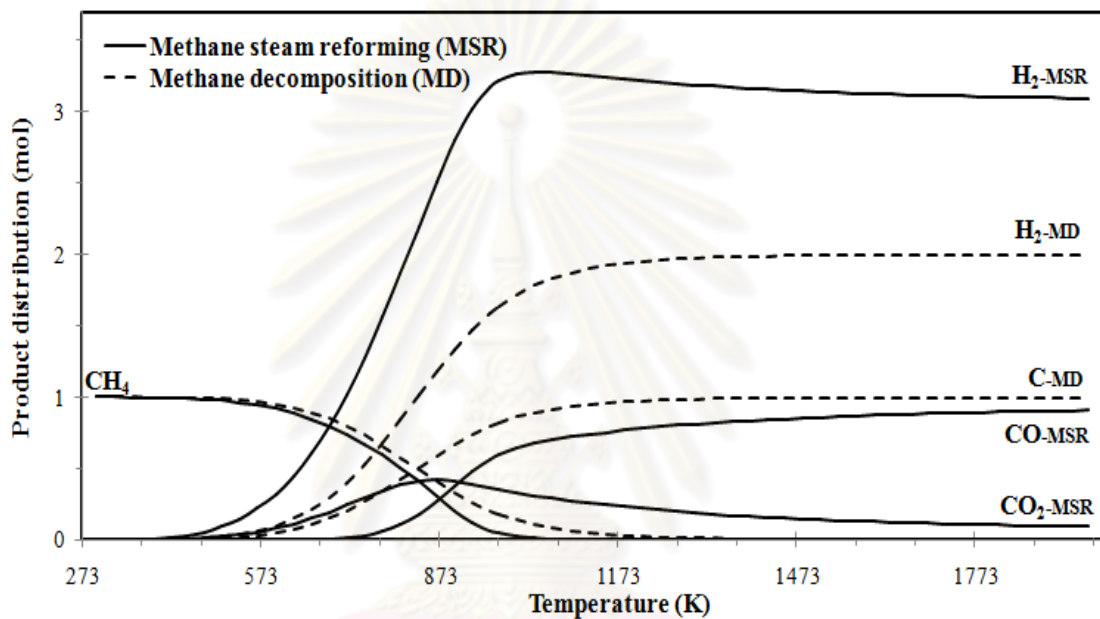


Figure 5.7 Product distribution of conventional methane steam reforming ($\text{H}_2\text{O}:\text{CH}_4=2.5$) (solid line) and of decomposition (dash line) at atmospheric pressure and varying temperature (basis on 1 mole of pure methane for both processes).

Consequently, the appropriate operating temperatures under equivalent methane conversion of two reactions are selected at 1073 K and 1523 K, respectively at the atmospheric pressure. This selected temperatures offer the suitable of S/C ratio (for MSR) and high methane conversion, H_2/CH_4 mole ratio, purity of hydrogen with the acceptable total energy requirement. In addition, the appropriate condition of MSR fuel processor at which is the atmospheric pressure, S/C ratio of 2.5 and the operating temperature of 1073 K (Piroonlerkgul *et al.*, 2009) is reasonably selected to

compare with MD fuel processor. It is suitable for the SOFC system, because this appropriate condition is in the region of CARBON-FREE-REGION of the carbon deposition mapping of methane steam reforming in the Fuel cell Handbook (Fuel cell Handbook, 2004) and the carbonization chart of Douvartzides *et al.*'s research (Douvartzides *et al.*, 2003).

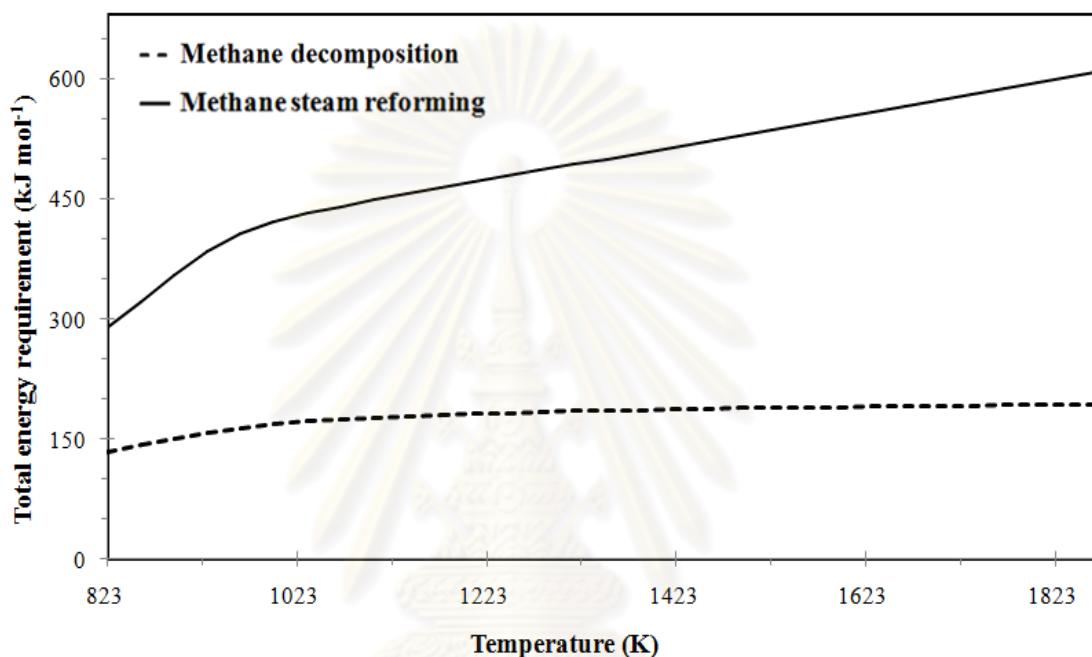


Figure 5.8 Energy requirements between methane conventional steam reforming (solid line) and decomposition (dash line) at the atmospheric pressure and varying temperature.

5.2 Performance analysis of solid oxide fuel cell (SOFC) system

Both of appropriate fuel processors; conventional methane steam reforming (MSR) and decomposition (MD) are integrated into SOFC system called MSR-SOFC and MD-SOFC, respectively. The performance analysis is initially investigated under the thermally self-sufficient condition ($Q_{\text{net}} = 0$) (Palazzi *et al.*, 2007; Vivanpatarakij *et al.*, 2007 and Piroonlerkgul *et al.*, 2009) in order to operate without external energy

requirement, and then these conditions are performed to operate the SOFC system for the high electrical efficiency.

5.2.1 Investigation of thermally self-sufficient condition ($Q_{\text{net}} = 0$)

For both MD-SOFC and MSR-SOFC, the systems are operated under the thermally self-sufficient condition ($Q_{\text{net}} = 0$) at fuel cell temperature of 1073 K, which is previously reported as a suitable SOFC operating temperature (Andujar and Segura, 2009; Neef, 2009; Kirubakaran *et al.*, 2009 and Piroonlerkgul *et al.*, 2009). To find the optimal condition at thermally self-sufficient condition, the amount of fuel processor and air heater's thermal energy can be firstly calculated which are Q_1 , Q_2 , Q_3 (fuel processor) and Q_4 (air heater) as shown in the Figures 5.9 and 5.10, respectively for MSR-SOFC and MD-SOFC. The total generated thermal energy from the SOFC (Q_5) and the afterburner (Q_6) is calculated via a trial-and-error method by tuning the fuel utilization (U_f) at fixed operating voltage of SOFC. The thermally self-sufficient condition at which this total generated thermal energy is equal to the total thermal energy consumption from the system (Eq.4.34 for MSR-SOFC and Eq.4.35 for MD-SOFC).

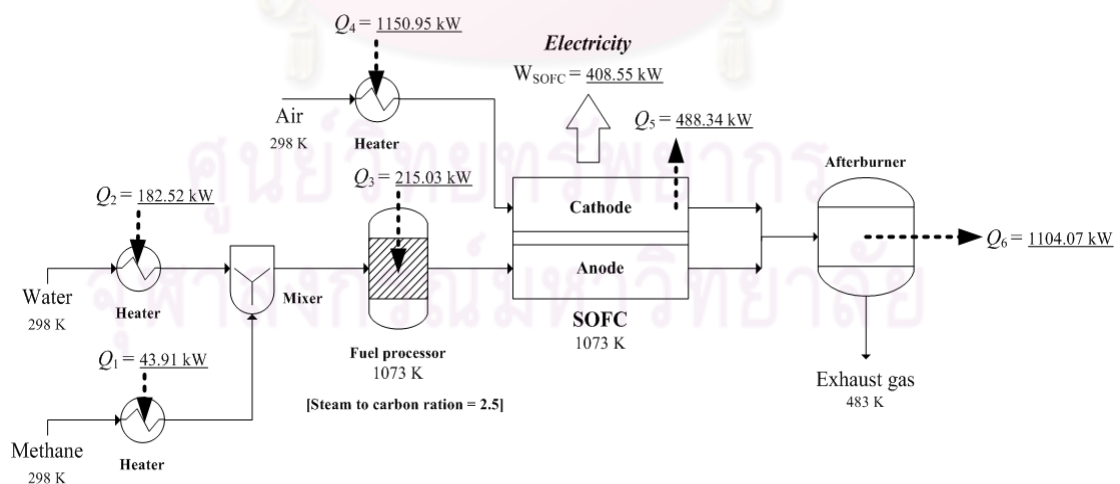


Figure 5.9 The thermally self-sufficient operation of SOFC integrated with conventional methane steam reforming fuel processor.

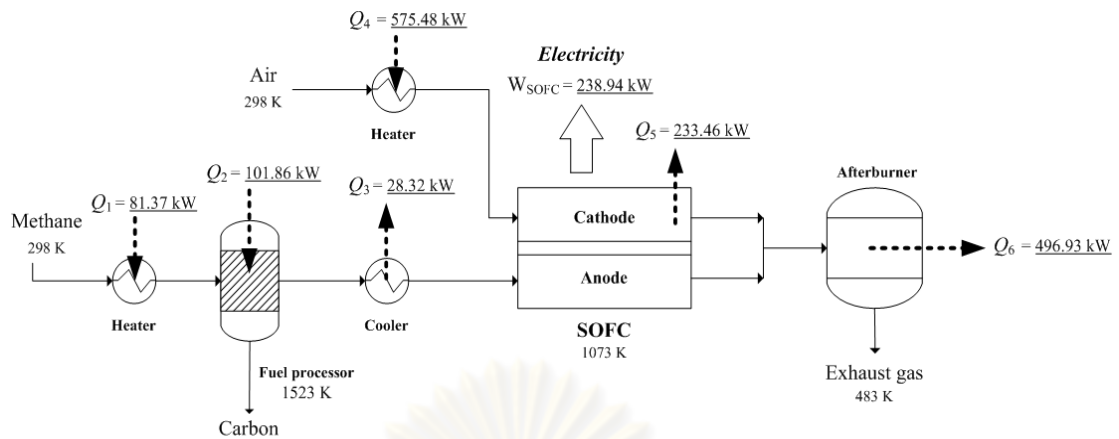


Figure 5.10 The thermally self-sufficient operation of SOFC integrated with methane decomposition fuel processor.

The results of net thermal energy (Q_{net}) under a trial-and-error method by tuning the fuel utilization (U_f) at fixed operating voltage of SOFC cell stack (V) are presented in Figure 5.11 (MSR-SOFC) and Figure 5.12 (MD-SOFC). At the same operating voltage MSR-SOFC needs to operate at lower fuel utilization than MD-SOFC, because more residual fuel or non-utilized fuel is required to supply the sufficient thermal energy requirement by combustion at the afterburner. This supports the discussion in the previous part that MSR is more endothermic reaction than MD. Not only MSR has more energy requirement in its reaction, but also in the complete combustion step at the afterburner MSR also needs to remove more unwanted exhaust gas substances before venting to the atmospheric or feeding to a CCS unit.

Consequently, the optimal condition based on 1 mol s^{-1} of pure methane feed of fuel processor presents the highest electrical power generation which are 408.55 kW for MSR-SOFC and 238.94 kW for MD-SOFC as shown in Figures 5.9 and 5.10.

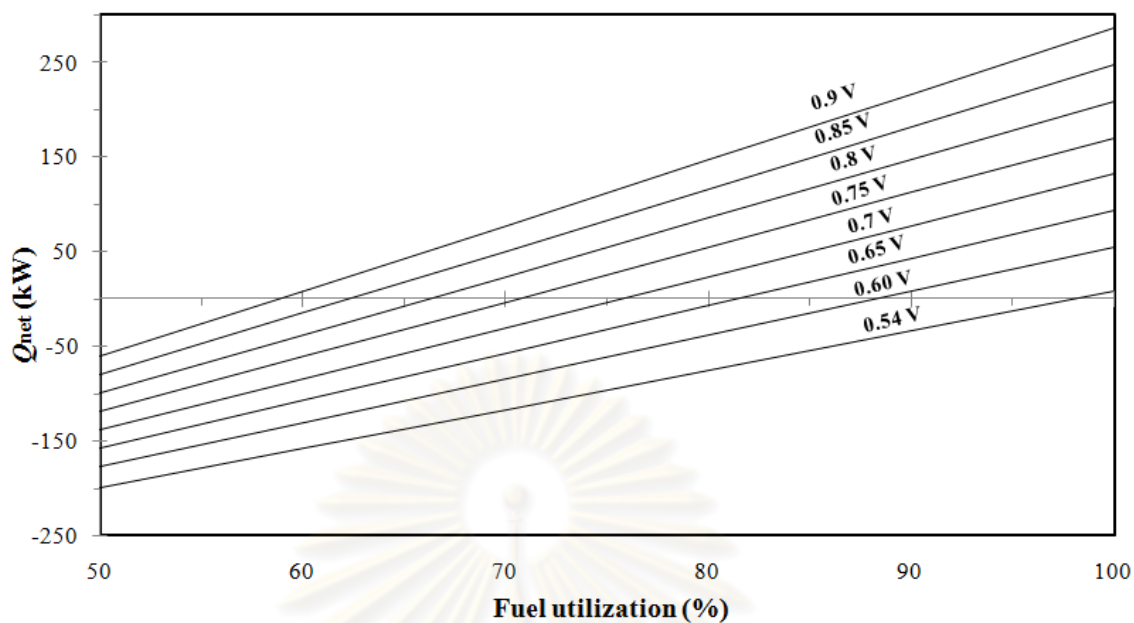


Figure 5.11 Q_{net} at different fuel utilization and operating voltage at 1073 K in conventional SOFC system with MSR, basis on 1 mole of pure methane ($\text{H}_2\text{O}:\text{CH}_4=2.5$).

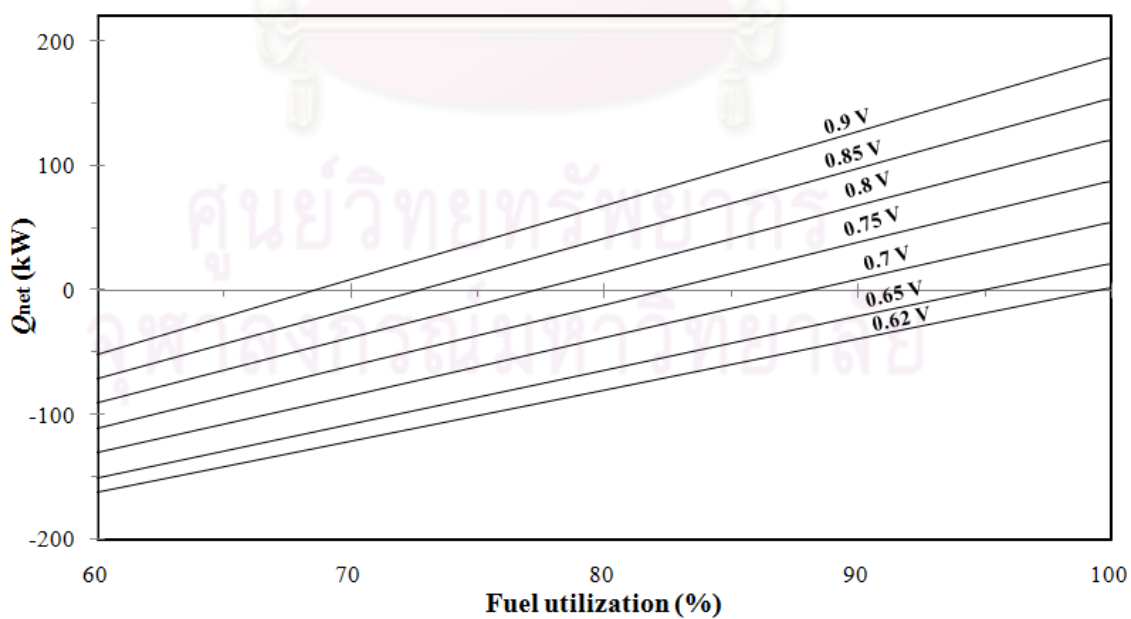


Figure 5.12 Q_{net} at different fuel utilization and operating voltage at 1073 K in proposed SOFC system with MD, basis on 1 mole of pure methane.

5.2.2 SOFC performance analysis with the different fuel processors under thermally self-sufficient condition ($Q_{\text{net}} = 0$)

Methane-fuelled solid oxide fuel cell (SOFC) via the different types of fuel processor (MSR and MD) is operated under the thermally self-sufficient operation ($Q_{\text{net}} = 0$) which was achieved from the previous part. Based on 1 mol s^{-1} of methane flow rate, methane is fed into the conventional MSR or MD fuel processor to produce hydrogen fuel at the temperature of 1523 K and 1073 K, respectively and the atmospheric pressure, and in order to compare the influence of product composition, the products of fuel processing reaction is then fed directly to SOFC system at the temperature of 1073 K to generate the high efficient electricity and useful thermal energy under the operation without external energy requirement.

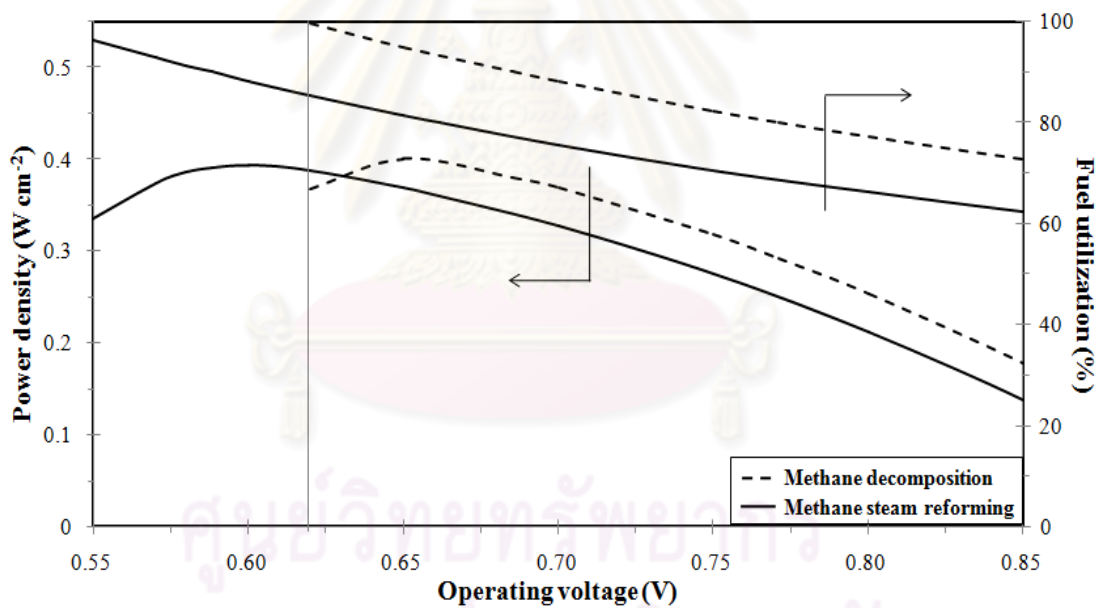


Figure 5.13 Power density and fuel utilization at various operating voltages for different SOFC systems at the thermally self-sufficient operation ($Q_{\text{net}} = 0$).

By varying operating voltage at the thermally self-sufficient operation, the SOFC performances of two different fuel processors are presented in Figure 5.13. The

optimum operating voltage (where maximum power density is obtained) for the MSR-SOFC system is at 0.60 V (0.4 W cm^{-1}) and for the MD-SOFC is at 0.65 V (3.9 W cm^{-1}). The higher power density is observed in the case of the MD-SOFC since the MD produces purer H_2 than the MSR-SOFC as is evident in the hydrogen concentration in Figure 5.3.

This optimal fuel utilization and operating voltage are reasonably chosen in the moderate values. Low operating voltage is not appropriate for SOFC system since it is difficult to control high thermal energy releasing from SOFC stack (as presented in the Figure 5.15) and may damage the cell stack due to the high fuel utilization. In contrast of high operating voltage, it is not practical for use in conventional SOFC due to the achievement of low power density (as presented in Figure 5.13).

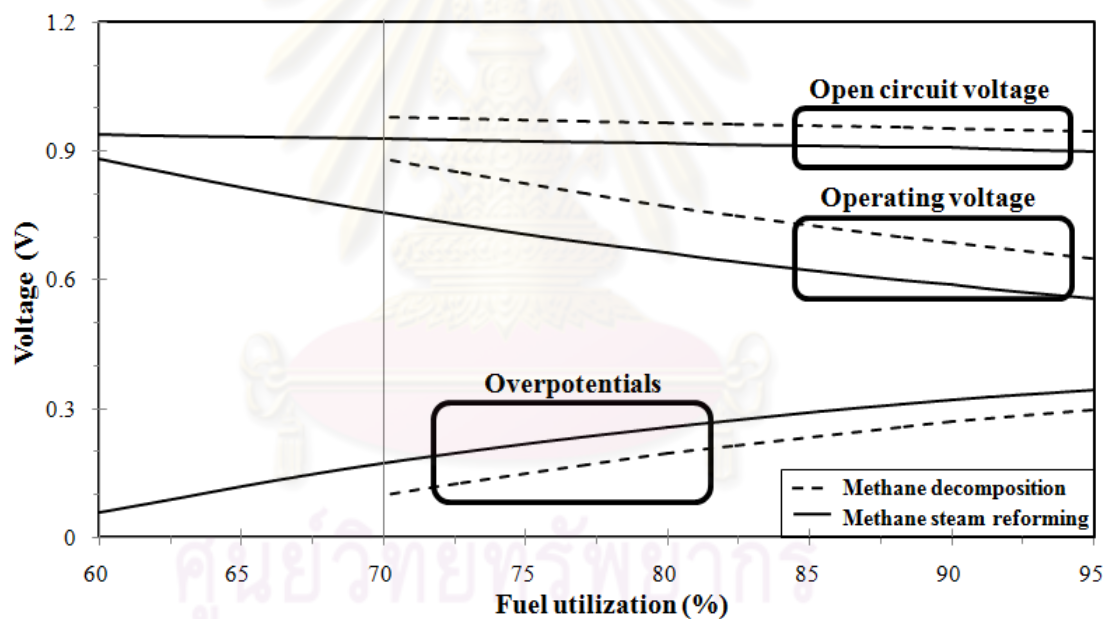


Figure 5.14 Voltage information at various fuel utilizations for different SOFC systems at the thermally self-sufficient operation ($Q_{\text{net}} = 0$).

Figure 5.14 presents open circuit (or theoretical) voltage, operating voltage and overpotentials (losses) at various fuel utilizations. The product composition produced from the fuel processor has a major effect on the cell operating voltage of SOFC (Fuel cell Handbook, 2004). MD produces high purity of the hydrogen fuel

without the dilution of another composition, thus, the open circuit (or theoretical) voltage is yielded to be higher than MSR. When the fuel utilization is larger consumed, the more depletion of fuel at the anode is, leading to an increase in overpotentials (losses). Similarly, because the impurity in hydrogen fuel in case of the MSR is higher than that of the MD, the overpotentials in the SOFC system in case of the MSR are therefore higher than that of the MD at similar fuel utilization.

This result is in good agreement with those reported by Eguchi *et al.* (2002), Baron *et al.* (2004) and Dalle Nogare *et al.* (2007), of which overpotentials in SOFC system, such as activation and concentration overpotentials, are occurred due to CO impurity in hydrogen fuel, leading to lower SOFC performance. This is also the reason why MD presents the higher operating voltage of than MSR at the same fuel utilization. The current density also increases with the increase of fuel utilization, finally, MD offers the higher power density as mentioned in Figure 5.13.

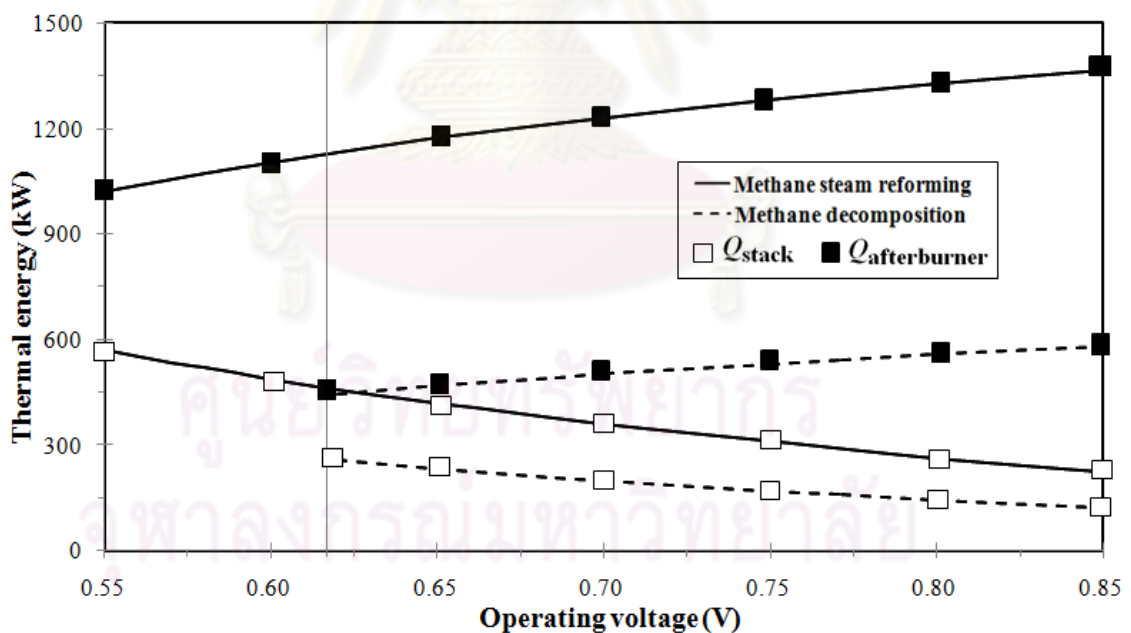


Figure 5.15 Thermal energy at various operating voltages for different SOFC systems at the thermally self-sufficient operation ($Q_{net} = 0$).

Regarding the energy consideration, the value of produced thermal to electrical ratio (TER), which is defined as the portion of fuel needed to utilize as a thermal energy to obtain an equal electricity production (Farhad *et al.*, 2010), is found to be 3.90 for the MSR-SOFC, and 2.66 for the MD-SOFC system at the thermally self-sufficient point ($Q_{\text{net}} = 0$). The higher value of TER observed in the MSR-SOFC system is because the MSR is more endothermic than the MD. Figure 5.15 has conformed to the aspect of both TER ratio of the fuel processors. Under the zero net balance of energy in the SOFC system, MSR-SOFC offers the higher thermal energy from the SOFC and afterburner to supply the total energy requirement of overall unit, especially in, MSR fuel reformer. Thus, MSR-SOFC has the lower fuel utilization at the similar operating voltage in order to get the unburned fuel utilization at the afterburner.

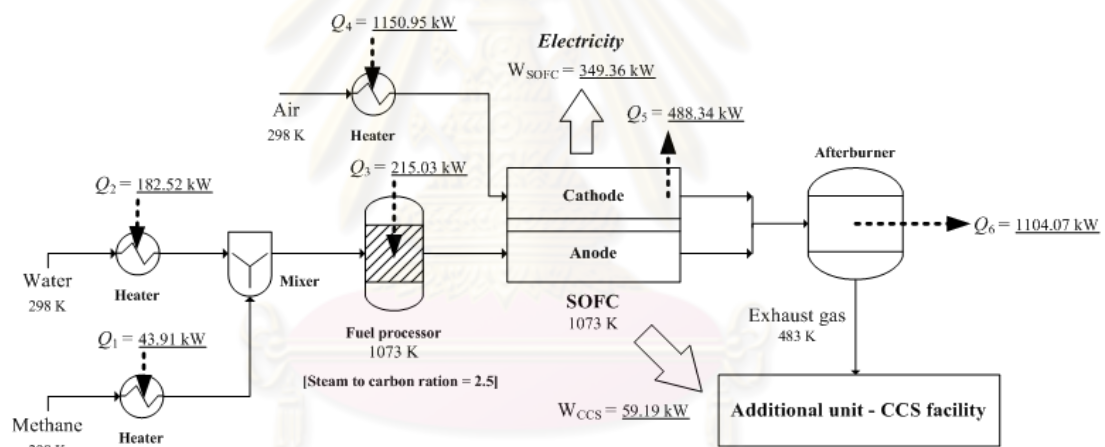


Figure 5.16 The thermally self-sufficient operation of SOFC integrated with conventional methane steam reforming fuel processor and CCS facility.

Concerning the environmental friendliness of MSR-SOFC, CCS facility is integrated into MSR-SOFC called MSR-SOFC-CCS. The CCS is applied after the afterburner in order to separate the carbon dioxide. The concentrated carbon dioxide gaseous is then compressed to convert into the liquid form and then transported to

storage as described about the details in the previous chapter. The additional CCS has no effect from either external energy or electrical input due to the operation under energy self-sufficient condition, therefore only the electrical power produced from the SOFC has an effect. Under the calculation from Section of 4.5, under the 1 mol s^{-1} of methane input to system, CCS needs the electrical power from the SOFC system to separate out CO_2 ca. 40 kW, to compress, transport, and storage approximately 18.04 and 1.15 kW, respectively.

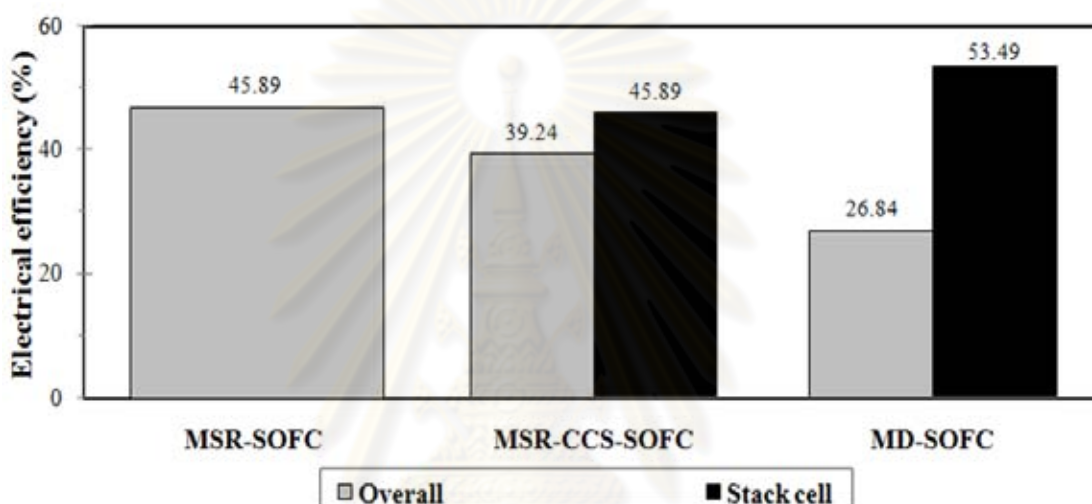


Figure 5.17 Electrical efficiency for different SOFC systems at the thermally self-sufficient operation ($Q_{\text{net}} = 0$).

At last, it can be seen that although the electricity of MD-SOFC is generated lower amount than of MSR-SOFC, based on the product composition inlet at the anode side of SOFC system the stack cell efficiency of the MSR-SOFC was found to be 45.9%, lower than that of the MD-SOFC of which is 53.5% (Figure 5.17). However, overall electrical efficiency of the MSR-SOFC system, either with or without the CCS, is much higher than that of the MD-SOFC (26.84%). This is because the flue gas in the MSR-SOFC is combusted and generates thermal energy whereas the by-product, solid carbon, is not further combusted; hence the energy in case of the MD-SOFC is stored in the system. The CCS needs the total electrical power from the MSR-SOFC system about 51.19 kW, consequently, the addition of CCS reduces the net electrical efficiency ca. 6.7%.

5.3 Economic analysis

After comparing the appropriate operating condition between two main fuel processors (MSR, MD) and performance investigation of three SOFC systems (MSR-SOFC, MSR-SOFC-CCS and MD-SOFC), it is necessary to further consider the benefit in term of economics in order to evaluate possibility in large-scale industrial operation. Economic analysis is based on 1 MW of net electrical power generation as mentioned the information in Chapter 4. It should be noted that the CCS facility is only applied in the MSR-SOFC. Under the thermally self-sufficient operation, CCS does not alter the optimal condition (optimal fuel utilization and operating voltage) because the operation of this unit utilized the produced electricity from SOFC stack. Basis on 1MW of net electricity production, thus MSR-SOFC-CCS need the higher methane feed and generates electricity more than 1 MW in order to provide enough electricity in the CCS facility.

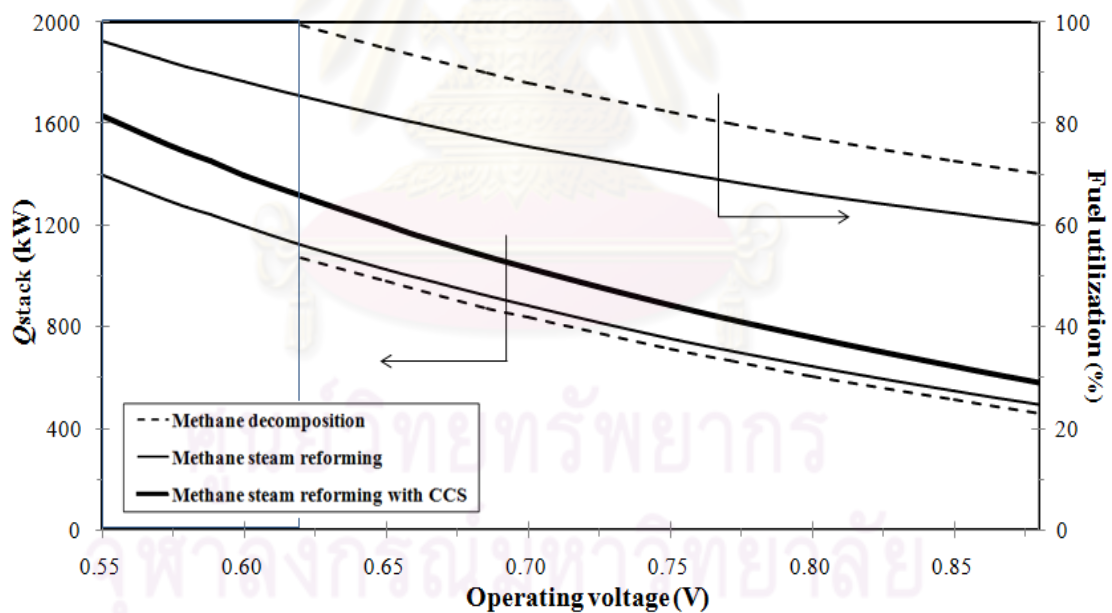


Figure 5.18 Q_{stack} and fuel utilization for different SOFC systems at the thermally self-sufficient operation ($Q_{net} = 0$).

Under the 1MW of net electrical generation, when the fuel is increasingly consumed to supply the thermally self-sufficient operation as shown in Figure 5.18,

the more overpotentials occur affecting to lower operating voltage. With the higher fuel utilization, thermal energy at the SOFC stack cell should be considered due to the physical properties (thermal stability) of stack cell.

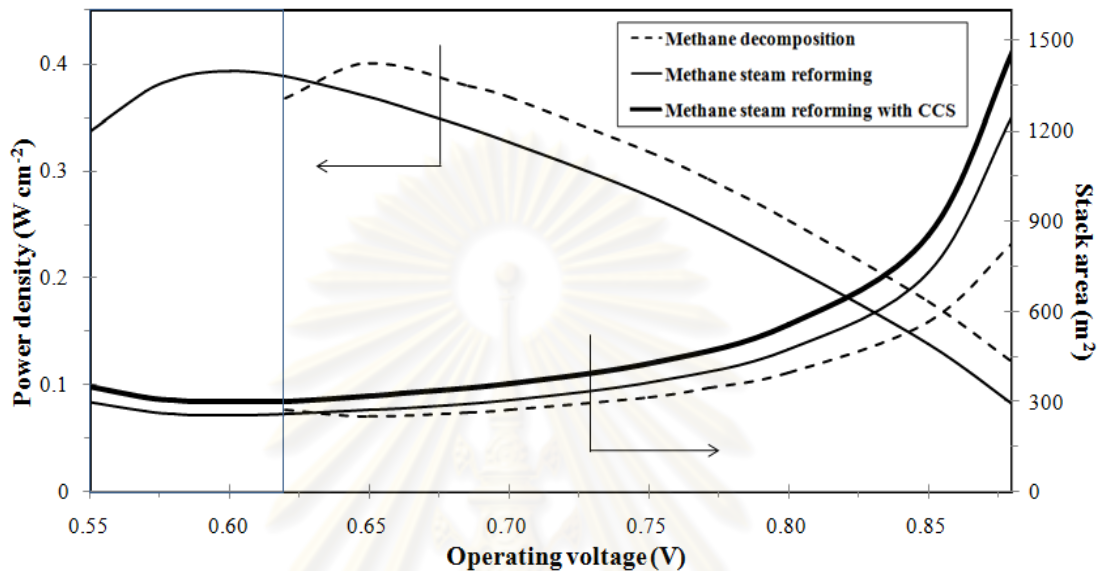


Figure 5.19 Power density and stack area for different SOFC systems at the energy self-sufficient operation ($Q_{\text{net}} = 0$).

These phenomena must be related with Figure 5.19 and the detail described in the previous section. This higher fuel utilization is consumed to generate the highest electrical power from the thermally self-sufficient operation, then, SOFC stack only needs the lower SOFC stack area. Concerning the optimal condition (where maximum power density is obtained) of each kinds of fuel processor, the MSR-SOFC (with CCS) and MD-SOFC system is at 0.60 V and 0.65 V, respectively. Not only MD gives the highest performance (power density and electrical efficiency) but it also has lower SOFC stack area compared to the MSR-SOFC and the MSR-SOFC-CCS. Moreover, MD also has lower thermal energy stack than the other system, this results in the lower cost of stack material. This must be confirmed that the proposed MD - SOFC has more advantages over conventional SOFC at the equivalent of net electricity.

Consideration in the investment cost for economic analysis is based on 1 MW of net electrical power generation. Five parameters are used to justify the economic benefits namely SOFC stack capital cost, additional of supplementary equipment, cost of raw material fuel, return profit from by-products and additional cost of CCS. Table 4.2 summarizes the costing model and parameters used in research's analysis. The economic profiles under thermally self-sufficient operation are summarized in Table 5.1. Firstly, MD-SOFC offers the less complexity than other systems, then, the less capacity of used equipment of MD-SOFC system is required. It can save the additional cost of supplement equipment over the conventional MSR-SOFC approximately \$120,000. With the optimal condition, the MD-SOFC system can reduce the SOFC stack size about 1.89% compared to the conventional MSR-SOFC, whereas the stack size in case of the MSR-SOFC-CCS is larger than that of the MSR-SOFC about 16.94% as it has to produce higher electrical power for the CCS facility. In addition, the MD-SOFC can improve the power density about 1.93% compared to the conventional MSR-SOFC. This is why the SOFC stack area of the MD-SOFC is smaller than that of the MSR-SOFC (approximately 4.8 m²), thus using the MD-SOFC can save the SOFC capital cost approximately \$20,000. Whereas MSR-SOFC-CCS has nearly the same performance and environmental friendly state of MD-SOFC, it requires the higher investment cost (including SOFC stack and CCS cost) than conventional SOFC approximately \$1,200,000.

Considering the reactants used and products obtained from different fuel processors, at the similar net electrical power production, the fuel feed cost of the MD-SOFC system is higher than that of the MSR-SOFC or the MSR-SOFC-CCS. This result is because the MD-SOFC requires higher number of methane to produce the same amount of H₂ for the SOFC. It is noted that although the fuel feed cost of the MSR-SOFC-CCS is more expensive than that of the MSR-SOFC system due to the need of more electrical power but it is still significantly lower than the case of MD-SOFC system. With a consideration only of the fuel feed cost, the MD-SOFC might not be a good alternative fuel processor supplying to the SOFC system. However, it is worthy to note that the MD system can remarkably return some precious benefit as the valuable by-product, solid carbon, can be obtained. Many types and forms of solid carbon can be generated depend upon the decomposition conditions such as graphite, carbon black, activated carbon, carbon nanotube, or carbon filaments , of which each

has different selling price (<http://www.timesnano.com/price.asp> and <http://www.helixmaterial.com/Ordering.html>). In this study, we chose to examine the return profit for the cheapest solid carbon, carbon black, along 5 years operation. The evaluation results in Table 5.1 show that the return profit is around 8.7 million dollars leads to the positive net cost saving ca. 6.6 million dollars. But in MSR-SOFC-CCS presents the negative net saving cost ca. 2 million dollars.

Last but not least with the eco-friendliness concerning the carbon captured from the ordinary reaction in fuel processor, MD-SOFC presents the positive effective cost of carbon capture around 840 \$ ton⁻¹, on the contrary way, CCS applied in conventional SOFC has the negative effective cost of carbon capture around 91\$ ton⁻¹. This indicates that not only MD-SOFC shows the high performance of electrical power generation, but also offers potential benefit regarding the environment conservation.



ศูนย์วิทยทรัพยากร
จุฬาลงกรณ์มหาวิทยาลัย

Table 5.1 The performance and economic analysis of interesting SOFC systems.

	MSR-SOFC		MD-SOFC
	Conventional unit	With CCS technology	
Net electricity produced (MW)	1.00	1.00	1.00
Feed rate (mol/s)	2.45	2.86	4.19
Operating voltage (volt)	0.6	0.6	0.65
% Fuel utilization	88.21	88.21	94.92
Power density (W/cm ²)	0.39	0.39	0.40
% Improvement of power density	-	-	1.93
SOFC active area (m ²)	254.58	297.72	249.77
% Improvement in SOFC area	-	-16.94	1.89
Electricity produced in SOFC (MW)	1.00	1.17	1.00
% Overall Electrical efficiency	45.89	45.89	26.84
% Stack cell efficiency	45.89	39.24	53.49
Capital cost of SOFC (\$)	1,055,018.92	1,233,765.39	1,035,074.30
Additional cost of supplementary equipment (\$)	711,143.39	831,629.07	592,985.83
Raw material fuel cost (\$)	3,123,270.53	3,652,431.61	5,340,367.76
Carbon by product selling cost(\$)	-	-	8,699,400.52
Additional cost of CCS (\$)	-	985,614.08	-
Saving capital cost of SOFC (\$)	-	-178,746.47	19,944.62
Saving additional cost of supplementary equipment (\$)	-	-120,485.68	118,157.56
Saving of raw material fuel (\$)	-	-529,161.08	-2,217,097.23
Return profit from carbon by product (\$)	-	-	8,699,400.52
Addition cost of CCS (\$)	-	-985,614.08	-
Net cost saving (\$)	-	-1,814,007.31	6,620,405.47
Effective cost of carbon capture (\$ ton⁻¹)		-91.34	838.88

CHAPTER VI

CONCLUSIONS AND RECOMMENDATIONS

6.1 Conclusions

Performance comparison between methane steam reforming (MSR) and decomposition (MD) for solid oxide fuel cell (SOFC) system with carbon capture is investigated in order to propose the alternative decomposition reaction to be the fuel processing reaction at the fuel processor. Under the conventional SOFC with the methane steam reforming (MSR), the high electrical efficiency can be achieved via integration with various possible complex and high cost of separation processes (membrane reactor, water-gas shift reactor and sorption enhanced MSR process) to obtain high hydrogen purity. For the nature of MD reaction, methane can be directly converted into separated phase of product compositions which are hydrogen and solid carbon. It may provide better performance than the conventional SOFC system. Therefore, this research investigates the proposed SOFC system integrated with MD. The results of the three parts presented in Chapter 5 can be concludes as follows;

Two fuel processors; MSR and MD are considered based on the assumption of thermodynamics equilibrium operated at the atmospheric pressure, various temperatures of 273-2000 K and varying steam to carbon ratio (S/C ratio) of MSR (more than minimum requirement). MSR can reach the complete conversion at lower temperature (1000 K) than MD, because the oxygenated reactant, such as steam, has an effect on the converting of methane to hydrogen. It also generates the higher amount of hydrogen fuel which can roughly approximate by the higher stoichiometric coefficient of hydrogen mole. However, methane in MD can be converted to the product without the appearance of side reactions unlike MSR such as carbon gasification, boudouard reaction, thus, it shows the higher purity of hydrogen more than MSR along the operating temperature range. Furthermore MD requires the total energy (for pre-heat and reaction) less than MSR. In order to compare the nature of reaction in fuel processor for direct use in SOFC, the appropriate condition is selected

with the basis of equivalent methane conversion. For MD, the operating temperature is 1523 K, but for MSR is 1073 K. S/C ratio of MSR is also chosen under the energy consideration and more than minimum S/C ratio requirement, thus S/C ratio is equivalent to 2.5.

Then, performances of two appropriate fuel processors, conventional methane steam reforming (MSR) and methane decomposition (MD), were investigated in the methane-fuelled SOFC system under thermally self-sufficient condition ($Q_{\text{net}} = 0$). At this condition, the system is operated with no external energy requirement. To operate with this condition, the tuning of fuel utilization and operating voltage in each SOFC system is by trial-and-error. As a result, at the same operating voltage MSR utilizes the lower fuel at the SOFC stack and performs the unburned fuel to supply thermally self-sufficient condition. This also supports that MSR is more endothermic reaction than MD. After that the fuel utilization and operating voltage are determined under the desired operation, the optimal condition of each SOFC system are selected for the performance and economic analysis. The results demonstrated that high performances and high electrical efficiency can be obtained when the system was operated at the self-sufficient condition. The MD-SOFC performs more advantages over the MSR-SOFC as high purity of H_2 feed is obtained, giving a lower polarization and thus higher in power density (0.4 W cm^{-2}) and cell stack efficiency (53.5%). As a performance result, lower cell stack area can be used in the case of MD-SOFC.

Moreover, the MD yields valuable by-products, solid carbon, rather than undesired-by-products such as CO_x as observed in the MSR. In addition, when CCS is applied to MSR-SOFC, of course the system become more complex with an increase in the capital cost and operating cost of surplus electricity for CCS unit. As a consequence, the MD is more environmental friendly and can gain the return profit from such by-product. Thus, effective cost of carbon capture of MD-SOFC presents the positive effective cost of carbon capture ($838.88 \$ \text{ ton}^{-1}$), whereas the MSR-SOFC-CCS show the negative effective cost. Economic analysis reveals that the MD-SOFC has the gratifying result with larger net saving cost (ca. 6.6 million dollars for 1 MW with 5 years of project life).

To sum up, applying the MD processor with SOFC system is proved to be an alternative fuel processor for electrical power generation. It is suggested that the economic success of this proposed SOFC system with MD should relies on the technology development on cogeneration of hydrogen and valuable carbon products.

6.2 Recommendations

6.2.1 Further economic analysis should be performed by including the overall cost of involved equipments and units in SOFC system such as the fuel processor cost.

6.2.2 To overcome the conventional overall electrical efficiency, the carbon solid from methane decomposition (MD) can be used as a fuel like the hydrogen for electrical power generation. It should be noted that this carbon has the highest volumetric energy density (Muradov *et al.*, 2010) among all electrochemically active fuels, battery and other type of hydrocarbon fuels. The carbon solid should be divided into generating power and selling. Therefore, the direct carbon fuel cell (DCFC) should be further investigated and installed parallel location of SOFC system in order to ensure that MD reaction offers both of the high overall electrical efficiency and economic benefit.

REFERENCES

- Abanades, J.C. The maximum capture efficiency of CO₂ using a carbonation/calcination cycle of CaO/CaCO₃. Chem. Eng. J. 90 (2002): 303-306.
- Abbas, H.F., and Wan Daud, W.M.A. Hydrogen production by methane decomposition: A review. Int. J. Hydrogen Energy (2009): 1-31.
- Abu-khader, Recent Progress in CO₂ Capture/Sequestration: A Review. Energy Sources Part A. 28 (2006):1261-1279.
- Abu-Zahra, M.R.M., Schneiders, L.H.J., Niederer, J.P.M., Feron, P.H.M., and Versteeg, G.F. CO₂ capture from power plants: Part I. A parametric study of the technical performance based on monoethanolamine. Int. J. of greenhouse gas control 1(1) (2005): 37-46.
- Achenbach, E., and Riensche, E. Methane/steam reforming kinetics for solid oxide fuel cells. J. Power Sources 52 (1994): 283-288.
- Ahmed, S., Aitani, A., Rahman, F., Al-Dawood, Ali., and Al-Muhaish, F. Decomposition of hydrocarbons to hydrogen and carbon. Appl. Catal. A: Gen 359 (2009): 1-24.
- Alexander Stern, S. Polymers for gas separations: the next decade. J. of Membrane Science 94(1) (1994): 1-65.
- Alie, C., Backham, L., Croiset, E., and Douglas, P.L. Simulation of CO₂ capture using MEA scrubbing: a flowsheet decomposition method. Energy Convers. Manage. 46 (3) (2005): 475.
- Amelio, M., Morrone, P., Gallucci, F., and Basile, A. Integrated gasification gas combined cycle plant with membrane reactors: Technological and economical analysis. Energy Convers. Manage. 48(10) (2007): 2680-2693.
- Anderson and Garcis, Support Metals in catalyst VOL5., London, Imperial College Press (2005)
- Andujar, J.M., and Segura, F., Fuel cells: History and updating. A walk along two centuries. Renewable and Sustainable Energy Reviews 13 (2009): 2309-2322.
- Arpornwichanop, A., Patcharavorachot, Y., and Assabumrungrat, S. Analysis of a proton-conducting SOFC with direct internal reforming. Chem Eng Sci. 65 (2010): 581- 589.

- Assabumrungrat S., et al. Thermodynamic analysis of carbon formation in solid oxide fuel cells with a direct internal reformer fueled by methanol. J. Power Sources 139 (2005): 55-60.
- Bai, Z., Chen, H., Li, B., and Li, W. Methane decomposition over Ni loaded activated carbon for hydrogen production and the formation of filamentous carbon. Int. J. of Hydrogen Energy. 32 (2007):32-37.
- Balasubramanian, B., Lopez Ortiz, A., Kaytakoglu, S., and Harrison, D.P. Hydrogen from methane in a single-step process. Chem. Eng. Sci. 54 (1999): 3543-3552.
- Baron, S., Brandon, N., Atkinson, A., Steele, B., and Rudkin, R. The impact of wood-derived gasification gases on Ni-CGO anodes in intermediate temperature solid oxide fuel cells. J. Power Sources 126 (2004): 58-66.
- Barelli, L., Bidini, G., Gallorini, F., and Servili, S. Hydrogen production through sorption-enhanced steam methane reforming and membrane technology: A review Energy 33 (2008): 554-570.
- Basile, A., Paturzo, L., and Gallucci, F. Co-current and counter-current modes for water gas shift membrane reactor. Catal. Today 82 (1-4) (2003): 275-281.
- Bellows, R.J. Technical Challenges for Hydrocarbon Fuel Reforming, DOE, Baltimore, MD (1999).
- Bhawn, S., Stromman, A.H., and Herwuch, E. Life cycle assessment of natural gas combined cycle power plant with post-combustion carbon capture, transport and storage. Int. J. of greenhouse gas control XXX (2010): XXX-XXX.
- Blom, R., et al. Carbon dioxide reforming of methane over lanthanum-modified catalysts in a fluidized-bed reactor. Catal. Today 21 (1994): 535-543.
- Bolland, O., and Undrum, H. Removal of CO₂ from gas turbine power plants: Evaluation of pre- and post-combustion methods. In Greenhouse Gas Control Technologies, Proceedings of the 4th International Conference on Greenhouse Gas Control Technologies, Interlaken, (1998): 125-130.
- Bonura, G., Di Blasi, O., Spadaro, L., Arena, F., and Frusteri, F. A basic assessment of the reactivity of Ni catalysts in the decomposition of methane for the production of CO_x-free hydrogen for fuel cells application. Catal Today 116 (2006): 298-303.
- Boudghene Stambouli, A.B., and Traversa, E. Solid oxide fuel cells (SOFCs): a review of an environmentally clean and efficient source of energy. Renewable and Sustainable Energy Rev. 6 (2002): 433-455.

- Bracht, M., et al. Water gas shift membrane reactor CO₂ Control in IGCC systems: techno-economic feasibility study. Paper presented at ICCDR-3 Boston 1996.
- Bradford, M.C.J., and Vannice, M.A. Catalytic reforming of methane with carbon dioxide over nickel catalysts. II: Reaction kinetics, *Appl. Catal. A:Gen.*, 142 (1996): 97-122.
- Bredesen, R., Jordal, K., and Bolland, O. High-temperature membranes in power generation with CO₂ capture. *Chem. Eng. Process* 43 (2004):1129-1158.
- Calin, C.C. Assessment of hydrogen and electricity co-production schemes based on gasification process with carbon capture and storage. *Int. J. of Hydrogen* 34 (2009): 6065- 6077.
- Chakma,A. An energy efficient mixed solvent for the separation of CO₂. *Energy Convers. Manage.* 36 (1995): 427–430.
- Chan, S.H., Khor, K.A., and Xia, Z.T. A complete polarization model of a solid oxide fuel cell and its sensitivity to the change of cell component thickness, *J. Power Sources*, 93 (2001): 130-140.
- Chapel, D.G., Mariz, C.L., and Ernest, J. Recovery of CO₂ from flue gases: commercial trends. in: Proceedings of the Canadian Society of Chemical Engineers Annual Meeting, Saskatoon, Saskatchewan (1999).
- Chinese Academic of Sciences. Carbon Nanotube price [Online], 2010, Available from <http://www.timesnano.com/price.asp> [2010, September]
- Choudhary, T.V., and Goodman, D.W. Catalysts for combustion of methane and lower alkanes-review. *Appl Catal A: Gen* 234(2002): 1-23.
- Clarke, S.H., Dick, A.L., Pointon, K., Smith, A., and Swann, A. Catalytic aspects of the steam reforming of hydrocarbons in internal reforming fuel cells. *Catal Today* 38 (1997): 411-423.
- Condorelli, P., Smelser, S.C., Mc Cleary, G.J., G.S., B., and Stuart, R.J. Engineering and Economic Evaluation of CO₂ Removal from Fossil-Fuel-Fired Power Plants Volume 2: Coal Gasification Combined-Cycle Power Plants. EPRI IE-7365 2 1991.
- Coutelieris,F.A., Douvartzides, S., and Tsiakaras, P. The importance of the fuel choice on the efficiency of a solid oxide fuel cell system. *J. Power Sources*123 (2003): 200-205.

- Dalle Nogare, D., Baggio, P., Tomasi, C., Mutri, L., and Canu, P. A thermodynamic analysis of natural gas reforming processes for fuel cell application. Chem. Eng. Sci 62 (2007) 5418-5424.
- Damen, K., Troost, M.V., Faaij, A., and Turkenburg, W. A comparison of electricity and hydrogen production systems with CO₂ capture and storage. Part A: Review and selection of promising conversion and capture technologies. Progress in Energy and Combustion Science. 32 (2006): 215-246.
- Damen, K., Troost, M.V., Faaij, A., and Turkenburg, W. A comparison of electricity and hydrogen production systems with CO₂ capture and storage. Part B: Chain analysis of promising CCS options. Progress in Energy and Combustion Science 32 (2007): 215-246.
- Dauenhauer, P.J., Salge, J.R., and Schmidt, L.D. Renewable hydrogen by autothermal steam reforming of volatile carbohydrates. J. Catal. 244 (2006): 23 8-247.
- Dias, J.A.C., and Assaf, J.M. The advantages of air addition on the methane steam reforming over Ni/ γ -Al₂O₃. J. Power Sources 137 (2004): 264-268.
- Dicks, A. L. Hydrogen generation from natural gas for the fuel cell systems of tomorrow. J. Power Sources 61(1996): 113-124.
- Dicks, A.L. Advances in catalysts for internal reforming in high temperature fuel cells. J. Power Sources 71 (1998): 111-122.
- Ding, Y., and Alpay, E. Adsorption-enhanced steam-methane reforming. Chem. Eng. Sci. 55 (2000): 3929-3940.
- Docter, A., and Lamm, A. Gasoline fuel cell systems. J. Power Sources 84 (1999): 194-200.
- Dokmaingam, P., Assabumrungrat, S., Soottitantawat, A., and Laosiripojanab, N. Modeling of tubular-designed solid oxide fuel cell with indirect internal reforming operation fed by different primary fuels. J. Power Sources 195 (2010): 69-78.
- Douvartzides, S.L., Coutelieres, F.A., Demin, K., and Tsiakaras, P.E. Fuel options for Solid Oxide Fuel Cells: A Thermodynamic Analysis. AIChE J. 49 (2003): 248-257.
- Eguchi, K., Kojo, H., Takeguchi, T., Kikuchi, R., and Sasaki K. Fuel flexibility in power generation by solid oxide fuel cells. Solid State Ionics 411(6) (2002): 152-153.

- Edwards, J.H., and Maitra, A.M. The chemistry of methane reforming with carbon dioxide and its current and potential applications. Fuel Proc. Tech. 42 (1995): 269-289.
- Edwards, P.P., Kuznetsov, V.L., David, W.I.F., and Brandon, N.P. Hydrogen and fuel cells: Towards a sustainable energy future. Energy Policy 36 (2008): 4356-4362.
- Ermakova, M.A., Ermakov, D.Yu., and Kuvshinov, G.G. Effective catalysts for direct cracking of methane to produce. Appl. Catal. A: Gen 201(2000): 61-70.
- Farhad, S., Hamdullahpur, F., and Yoo, Y. Performance evaluation of different configurations of biogas-fuelled SOFC micro-CHP systems for residential applications, Int. J. Hydrogen Energy, 35 (2010) :3758-3768.
- Ferguson, J.R., Fiard, J.M., and Herbin, R. Three-dimensional numerical simulation for various geometries of solid oxide fuel cells, J. Power Sources, 58 (1996): 109-122.
- Fernandes, F.A.N., and Soares Jr, A.B. Methane steam reforming modeling in a palladium membrane reactor. Fuel 85 (2006): 569-573.
- Figueroa, J.D., Fout, T., Plasynski, S., McIlvried, H., and Srivastava, R. Advances in CO₂ capture technology—The U.S. Department of Energy's Carbon Sequestration Program. Int. J. of greenhouse gas control 2 (2008): 9- 20.
- Fleig, J. Solid oxide fuel cell cathodes: polarization mechanisms and modeling of the electrochemical performance, Annu. Rev. Mater. Res., 33 (2003): 361-382.
- Fuel Cell Hand Book. 14th ed., West Virginia, EGandG Technical Services, Inc. (2004).
- Galucci, F., Paturzo, L., and Basile, A. A simulation study of the steam reforming of methane in a dense tubular membrane reactor. Int. J. Hydrogen Energy 29(6)(2004): 611-617.
- Gibbins, J., and Chalmers, H. Carbon capture and storage. Energy Policy. 36 (2008): 4317-4322.
- Granite, E.J., and O'Brien, T. Review of novel methods for carbon dioxide separation from flue and fuel gases. Fuel Proc. Tech. 86 (2005): 1423-1434.
- Grasa, G.S., Abanades, J.C., Alonso, M., and Gonzalez, B. Reactivity of highly cycled particles of CaO in a carbonation/calcination loop. Chem. Eng. J. 137 (2008): 561-567.

- Haile, S.M. Fuel cell materials and components. Acta Materialia 51 (2003) :5981-6000.
- Halabi, M.H., DeCroon, M.H.J.M., Van der Schaaf, J., Cobden, P.D., and Schouten, J.C. Low temperature catalytic methane steam reforming over ceria-zirconia supported rhodium, Appl. Catal. A (2010): *Gen.*, (In press).
- Hammou, A., and Guindet, J. “Chapter 12: Solid Oxide Fuel Cells”, in the CRC, Handbook of Solid State Electrochemistry, Gellings, P.J., Bouwmeester, H.J.M. (Eds.), CRC Press., Inc., New York 1997, p.407-443.
- Harasimowicz, M., Orluk, P., Zakrzewska-Trznadel, G., and Chmielewski, A.G. Application of polyimide membranes for biogas purification and enrichment. Journal of Hazardous Materials 144(3) (2007): 698-702.
- Hattenbach, R.P., Wilson, M., and Brown, K. Capture of carbon dioxide from coal combustion and its utilization for enhanced oil recovery. In: Eliasson B, Riemer P, Wokaun A, editors. Fourth International Conference on Greenhouse Gas Control Technologies, Interlaken. Switzerland, Amsterdam: Pergamon; 1999, p. 217–21.
- Helix Material Solution. Carbon Nanotube price [Online], 2010, Available from <http://www.helixmaterial.com/Ordering.html> [2010, September]
- Hernandez-Pacheco, E., Mann, M.D., Hutton, P.N., Singh, D., and Artin, K.E. A cell level model for a solid oxide fuel cell operated with syngas from a gasification process. Int. J. Hydrogen Energy 138 (2005):1221-1233.
- Herzog, H. The economics of CO₂ capture, Greenhouse gas control technologies, Oxford. Elsevier Science Ltd., (1999): 101-106.
- Holladay, J.D., Hu, D.L., King, and Wang, Y. An overview of hydrogen production technologies Review. Catal. Today 139 (2009):244-260. 139.
- Holmen, A. Direct conversion of methane to fuels and chemicals. Catal. Today 142 (2009): 2-8.
- Hoogers, G. Fuel Cell Technology Handbook. CRC Press, Boca Raton 2003.
- Hufton, J.R., Mayorga, S., and S., S. Sorption-enhanced reaction process for hydrogen production. AIChE J. 45 (1999): 248-256.
- Hussain, M.M., Li, X., and Dincer, I. Mathematical modeling of planar solid oxide fuel cells. J. Power Sources 161 (2006): 1012–1022.
- ICIS Company. Carbon price [Online], 2010, Available from <http://www.icispricing.com> [2010, September]

- International Energy Agency (IEA). Natural gas price [Online], 2010, Available from <http://www.iea.org> [2010, September]
- Jordanidisa, A.A., Kechagiopoulosb, P.N., Voutetakisa, S.S., Lemonidoub, A.A., and Vasalob, I.A. Autothermal sorption-enhanced steam reforming of bio-oil/biogas mixture and energy generation by fuel cells: Concept analysis and process simulation. Int. J. Hydrogen Energy 31 (2006): 1058-1065.
- IPCC Special Report on Carbon Dioxide Capture and Storage. Cambridge University Press, Cambridge, United Kingdom and New York, NY, USA 2005.
- Joensen, F., and Rostrup-Nielsen, J.R. Conversion of hydrocarbons and alcohols for fuel cells. J. Power Sources 105 (2002): 195-201.
- Karl, V.K., and Gunter, R.S. Environmental impact of fuel cell technology. Chem Rev. 95 (1995): 191-207.
- Khaleel, M.A., Lin, Z., Singh, P., Surdoval, W., and Collin, D., A finite element analysis modeling tool for solid oxide fuel cell development: coupled electrochemistry, thermal and flow analysis in MARC(R). J. Power Sources 130 (2004): 136-148.
- King, D.L., et al. Microreactor Technology and Process Intensification. ACS, Washington DC. (2005):119-128.
- Kirubakaran, A., Shailendra, J., and Nema, R.K. A review on fuel cell technologies and power electronic interface. Renewable and Sustainable Energy Reviews 13 (2009): 2430-2440.
- Knudsen, J.N., Vilhelmsen, P.J., Biede, O., and Jensen, J.N., CASTOR 1 t/h CO₂ absorption pilot plant at the Elsam Kraft A/S Esbjerg power plant—First year operation experience. In: Proceedings of the Greenhouse Gas Control Technologies, vol. 8, Trondheim, Norway 2006.
- Koornneef, J., Keulen, T.van, Faaij, A., and Turkenburg, W. Life cycle assessment of a pulverized coal power plant with post-combustion capture, transport and storage of CO₂. Int. J. of greenhouse gas control 2 (2008): 448- 467.
- Kurt, Z.H., Charles, F.H., Michael, J.A., and Daniel, P.S. The energy penalty of post-combustion CO₂ capture and storage and its implications for retrofitting the U.S. installed base. Energy Environ Sci 2 (2) (2009): 193-205.
- Kusakabe, K., Sotowa, K.I., Eda, T., and Iwamoto, Y. Methane steam reforming over Ce–ZrO₂-supported noble metal catalysts at low temperature. Fuel Processing Technology 86(3) (2004): 319-326.

- Laosiripojana, N., Sutthisripok, W., and Assabumrungrat, S. Synthesis gas production from dry reforming of methane over CeO₂ doped Ni/Al₂O₃: Influence of the doping ceria on the resistance toward carbon formation. Chem. Eng. J. 112 (2005): 13-22.
- Larminie and Dicks, Fuel Cell explained. England, Wiley, (2000).
- Lee, D.K., Baek, I.H., and Yoon, W.L. A simulation study for the hybrid reaction of methane steam reforming and in situ CO₂ removal in a moving bed reactor of a catalyst admixed with a CaO-based CO₂ acceptor for H₂ production. Int. J. Hydrogen Energy 31 (2006): 649-657.
- Li, W., Wang, H., Ren, Z., Wang, G., and Bai, J. Co-production of hydrogen and multi-wall carbon nanotubes from ethanol decomposition over Fe/Al₂O₃ catalysts. Appl. Catal. B: Environ 84(2008):433-439.
- Lopez Ortiz, A., and Harrison, D.P. Hydrogen Production Using Sorption-Enhanced Reaction. Ind. Eng. Chem. Res. 40(2001): 5102-5109.
- Lu, G.Q., et al. Inorganic membranes for hydrogen production and purification: A critical review and perspective. J. Colloid Interface Sci. 314(2) (2007): 589-603.
- Makris, T.D., Giorgi, L., Giorgi, R., Lisi, N., and Salernitano, E. CNT growth on alumina supported nickel catalyst by thermal CVD. Diamond and Related Materials 14(2005):815-819.
- Martin, W., and Ralph, J.B. What Are Batteries, Fuel Cells, and Supercapacitors? Chem Rev. 104 (2003): 4245-4269.
- Massman, W.J. A review of the molecular diffusivities of H₂O, CO₂, CH₄, CO, O₃, SO₂, NH₃, N₂O, NO, and NO₂ in air, O₂ and N₂ near STP. Atmos. Environ. 32(6) (1998): 1111-1127.
- McHugh, K. Hydrogen Production Methods. MPR Associates Inc. (2005).
- Merkel, T.C., Gupta, R.P., Turk, B.S., and Freeman, B.D. Mixed-gas permeation of syngas components in poly(dimethylsiloxane) and poly(1-trimethylsilyl-1-propyne) at elevated temperatures. Journal of Membrane Science 191(1-2) (2001): 85-94.
- Meyer, S. Application of the natural gas direct carbon fuel cell (NGDCFC) to a gas filling station for hydrogen and electricity supply. Energy Procedia 1 (2009): 1427-1434.
- Minh, N.Q., and Takahashi, T. Science and Technology of Ceramic Fuel Cells, Elsevier, New York, USA (1995).

- Muradov, N. Hydrogen via methane decomposition: an application for decarbonization of fossil fuels. Int. J. Hydrogen Energy 26 (2001): 1165-1175.
- Muradov, N., Choi, P., Smith, F., and Bokerman, G. Integration of direct carbon and hydrogen fuel cells for highly efficient power generation from hydrocarbon fuels. J. Power Sources 195 (2010): 1112-1121.
- Nakamura, N. US Patent, N^o.5914093, 1999.
- Naser, A.O., and Timothy, T.C. Life cycle GHG assessment of fossil fuel power plants with carbon capture and storage. Energy Policy 36 (2007): 367-380.
- Neef, H.J. International overview of hydrogen and fuel cell research. Energy 34 (2009):327-333.
- Ni, M., Leung, M.K.H., and Leung, D.Y.C. Parametric study of solid oxide fuel cell performance. Energy Convers. Manage. 48 (2007): 1525-1535.
- Nguyen, Q.M. Ceramic Fuel Cells. J. Am. Ceram. Soc. 76 (3) (1993):563–88.
- Oliveira, E.L.G., Grande, C.A., and Rodrigues, A. Methane steam reforming in large pore catalyst. Chem Eng Sci. 65 (5) (2010): 1539-1550.
- Osler, Hoskin, and Harcourt. Climate Change and Emissions [Online], 2009, Available from <http://www.osler.com/newsresources/Details.aspx?id=1324> [2010, September]
- Palazzi, F., Autissier, N., Marechal, F.M.A., and Favrat, D. A methodology for thermo-economic modeling and optimization of solid oxide fuel cell systems. App. Thermal Eng 27 (2007): 2703-2712.
- Palsson, J., Selimovic, A., and Sjunnesson, L. Combined solid oxide fuel cell and gas turbine systems for efficient power and heat generation. J. Power Sources 86 (2000): 442-448.
- Patcharavorachot, Y., Paengjuntuek W., Assabumrungrat, S., and Arpornwichanop, A. Performance evaluation of combined solid oxide fuel cells with different electrolytes. Int. J. Hydrogen Energy 35 (2010): 4301- 4310.
- Patel, K.S., and Sunol, A.K. Modeling and simulation of methane steam reforming in a thermally coupled membrane reactor. Int. J. Hydrogen Energy 32(13)(2007): 2344-2358.
- Petruzzi, L., Cocchi, S., and Fineschi, F. A global thermo-electrochemical model for SOFC systems design and engineering. J. Power Sources 118(1-2) (2003): 96-107.

- Piao, L., Li, Y., Chena, J., Changa, L., and Lin, J.Y.S. Methane decomposition to carbon nanotubes and hydrogen on an alumina supported nickel aerogel catalyst. Catal Today 74(2002): 145-155.
- Pipe line cost in CCS [Online], 2010, Available from <http://www.arc.ab.ca> [2010, September]
- Piroonlerkgul, P., Assabumrungrat, S., Laosiripojana, N., and Adesina, A.A. Selection of appropriate fuel processor for biogas-filled SOFC system. Chem. Eng .J. 140 (2008): 341-351.
- Piroonlerkgul, P., et al. Operation viability and performance of solid oxide fuel cell fuelled by different feeds. Chem. Eng .J. 155 (2009): 411-418.
- Piroonlerkgul, P., et al. Integration of solid oxide fuel cell and palladium membrane reactor: Technical and economic analysis. Int. J. Hydrogen Energy 34 (2009): 3894-3907.
- Piroonlerkgul, P., et al. Technical and economic study of integrated system of solid oxide fuel cell, palladium membrane reactor, and CO₂ sorption enhancement unit. Chem. Eng. Process 49 (2010): 1006-1016.
- Poirer, M.G., and Sapundzhiev, C. Catalytic Decomposition of natural gas hydrogen for fuel cell applications. Int. J. Hydrogen Energy 22(4) (1997): 429-433.
- Powell, C.E., and Qiao, G.G. Polymeric CO₂/N₂ gas separation membranes for the capture of carbon dioxide from power plant flue gases. J. Membrane Sci. 279 (2006): 1-49.
- Rabenstein, G., and Hacker, V. Hydrogen for fuel cells from ethanol by steam-reforming, partial-oxidation and combined auto-thermal reforming: A thermodynamic analysis. J. Power Sources 185 (2008): 1293–1304.
- Rao, A.B., Rubin, E.S., Keith, D.W., and Granger Morgan, M. Evaluation of potential cost reductions from improved amine-based CO₂ capture systems. Energy Policy 34 (2006): 3765–3772.
- Rawadieh, S., and Gomes, V.G. Steam reforming for hydrogen generation with in situ adsorptive separation. Int. J. Hydrogen Energy 34 (2009): 343-355.
- Rayment, C., and Sherwin, S. Introduction to Fuel Cell Technology. Department of Aerospace and Mechanical Engineering, University of Notre Dame, USA 2003.
- Renner, H.J., and Marschner, R. Catalytic reforming of natural gas and other hydrocarbon, Ullmann's Encyclopedia of Industrial Chemistry fifth edition, VCH Verlagsgesellschaft, Weinheim, Germany. A2 (1985):186-204.

- Romeo, L.M. Uso, S., Valero, A., and Escosa, J.M. Exergy analysis as a tool for the integration of very complex energy systems: The case of carbonation/calcination CO₂ systems in existing coal power plants. Int. J. of greenhouse gas control 4 (2010) : 647-654.
- Rostrup-Nielsen, J.R. Conversion of hydrocarbons and alcohols for fuel cells. Physical Chemistry Chemical Physics. 3(3) (2001): 283-288.
- Rostrup-Nielsen, J., and Horvath, I.T. Encyclopedia of Catalysis, Wiley Interscience, (2003).
- Roy, S., Cox, B.G., Adris, A.M., and Pruden, B.B. Economics and simulation of fluidized bed membrane reforming. Int. J. Hydrogen Energy 23(9) (1998):745.
- Sangtongkitcharoen, W., Assabumrungrat, S., Pavarajarn, V., Laosiripojana, N., and Praserttham, P. Comparison of carbon formation boundary in different modes of solid oxide fuel cells fueled by methane. J. Power Sources142 (2005): 75-80.
- Sangtongkitcharoen, W., Vivanpatarakij, S., Laosiripojana, N., Arpornwichanop, A., and Assabumrungrat, S. Performance analysis of methanol-fueled solid oxide fuel cell system incorporated with palladium membrane reactor. Chem. Eng. J. 138 (2008): 436-441.
- Serrano, D.P., et al. Hydrogen production by methane decomposition: Origin of the catalytic activity of carbon materials. Fuel 89 (2010): 1241-1248.
- Shekhawat, D., Luebke, D.R., and Pennline, H. A review of carbon dioxide selective membranes; U.S. Department of Energy Topical Report, DOE/NETL-2003/1200. 2003.
- Simbeck, D.R. CO₂ capture and storage: the essential bridge to the hydrogen economy. Energy 29 (2004): 1633-1641.
- Singh, B., Strømman, A.H., and Hertwich, E. Life cycle assessment of natural gas combined cycle power plant with post-combustion carbon capture, transport and storage. Int. J. of greenhouse gas control XXX (2010): XXX-XXX.
- Smelser, S.C., Stock, R.M., Mc Cleary, G.J., Booras, G.S., and R.J., S. Engineering and Economic Evaluation of CO Removal from Fossil-Fuel-Fired Power Plants. Volume 1: Pulverized Coal-Fired Power Plants. EPRI IE-7365 1 (1991).
- Song, C. Fuel processing for low-temperature and high-temperature fuel cells: Challenges, and opportunities for sustainable development in the 21st century. Catal Today. 77 (2002):17-49.

- Suelves, I., Lazaro, M.J., Moliner, R., Corbella, B.M., and Palacios, J.M. Hydrogen production by thermo catalytic decomposition of methane on Ni-based catalysts: influence of operating conditions on catalyst deactivation and carbon characteristics. Int. J. Hydrogen Energy 30(4) (2005): 1555-1567.
- Sun, L., et al. Methane catalytic decomposition integrated with on-line Pd membrane hydrogen separation for fuel cell application, Int. J. Hydrogen Energy 35 (2010): 2958-2963.
- Suwanwarangkul, R., et al. Experimental and modeling study of solid oxide fuel cell operating with syngas fuel. J. Power Sources 161 (2006): 308-322.
- Swaan, H.M., Kroll, V.C.H., Martin, G.A., and Mirodatos, C. Deactivation of supported nickel catalysts during the reforming of methane by carbon dioxide. Catal. Today 21 (1994): 571-578.
- Steinberg, M. Application of the natural gas direct carbon fuel cell (NGDCFC) to a gas filling station for hydrogen and electricity supply. Energy Procedia 1(2009): 1427-1434.
- Takenaka, S., Ogihara, H., Yamanaka, I., and Otsuka, K. Decomposition of methane over supported-Ni catalysts: effects of the supports on the catalytic lifetime. Appl. Catal. A: Gen 217 (2001): 101-110.
- Takenaka, S., Ishida, M., Serizawa, M., Tanabe, E., and Otsuka, K. Formation of Carbon Nanofibers and Carbon Nanotubes through Methane Decomposition over Supported Cobalt Catalysts. J. Phys. Chem. B 108(2004):11464-11472.
- Tao, G., Armstrong, T., and Virkar, A. Intermediate temperature solid oxide fuel cell (IT-SOFC) research and development activities at MSRI. In: Nineteenth annual ACERC&ICES conference. Utah 2005.
- Temkin, M.I. Industrial Heterogeneous Catalytic Reactions. Adv. Catal. 28 (1979): 175-292.
- Teramoto, M., et al. Separation and enrichment of carbon dioxide by capillary membrane module with permeation of carrier solution. Separation and Purification Technology 30(3)(2003) :215-227.
- Timmermann, H., Sawady, W., Reimart, R., and Ivers-Tiffée, E. Kinetics of (reversible) internal reforming of methane in solid oxide fuel cells under stationary and APU condition J. Power Sources 195 (2010): 214-222.
- Torniainen, P.M., Chu, X., and Schmidt, L.D. Comparison of monolith-supported metals for the direct oxidation of methane to syngas. J. Catal. 146 (1994): 1-10.

- Turpeinen, E., Raudaskoski, R., Pongracz, E., and Keiski, R.L. Thermodynamic analysis of conversion of alternative hydrocarbon-based feedstocks to hydrogen. Int J. of hydrogen energy 33 (2008): 6635-6643.
- Wang, G., Wang, H., Tang, Z., Li, W., and Bai, J. Simultaneous production of hydrogen and multi-walled carbon nanotubes by ethanol decomposition over Ni/Al₂O₃ catalysts. Appl. Catal B: Environ 88 (2009), 142-151.
- Wikipedia-the free encyclopedia. Fossil fuel [Online], 2010, Available from http://en.wikipedia.org/wiki/Fossil_fuel [2010, March]
- Villacampa, J.I., Royo, C., Romeo, E., Montoya, J.A., Del Angel, P., and Monzón, A. Catalytic decomposition of methane over Ni-Al₂O₃ coprecipitated catalysts Reaction and regeneration studies. Appl. Catal. A: Gen 252 (2003): 363-383.
- Vivanpatarakij, S., Assabumrungrat, S., and Laosiripojanab, N. Improvement of solid oxide fuel cell performance by using non-uniform potential operation. J. Power Sources 167 (2007):139-144.
- Vivanpatarakij, S., Laosiripojana, N., Arpornwichanop, A., and Assabumrungrat, S. Performance improvement of solid oxide fuel cell system using palladium membrane reactor with different operation modes. Chem. Eng. J. 146(1) (2009): 112-119.
- Yakabe, H., Hishinuma, M., Uratani, M., Matsuzaki, Y., and Yasuda, I. Evaluation and modeling of performance of anode-supported solid oxide fuel cell. J. Power Sources 86(1-2) (2000): 423-431.
- Yamamoto, O. Solid Oxide Fuel Cells: Fundamental Aspect and Prospects. Electrochim. Acta 45 (2000): 2423-2435.
- Yanbing, L., Baosheng, J., and Rui, X. Carbon dioxide reforming of methane with a free energy minimization approach. Korean J. Chem. Eng. 24 (2007): 688-692.
- Yusuke, A., et al. Efficient production of H₂ and carbon nanotube from CH₄ over single wall carbon nanohorn. Chem Phy Letters 482 (2009): 269-273.
- Zhao, F., and Virkar, A.V. Dependence of polarization in anode-supported solid oxide fuel cells on various cell parameters. J. Power Sources 141 (2005): 79-95.
- Zhang, W., Croiset, E., Douglas, P.L., and Fowler, M.W. Simulation of a tubular solid oxide fuel cell stack using AspenPlusTM unit operation models, Energy Conversion and Management, 46 (2005): 181-196.



APPENDICES

ศูนย์วิทยทรัพยากร
จุฬาลงกรณ์มหาวิทยาลัย

APPENDIX A

DETERMINING HEAT CAPACITY AND THE ENTHALPY CHANGE OF RELATED COMPOSITION

A.1 Heat capacity correlation is a series expansion in temperature (Kelvin).

$$C_p = A + BT + CT^2 + DT^3 + ET^4, \quad [\text{J mol}^{-1} \text{K}^{-1}] \quad (\text{A1})$$

Where

- C_p = heat capacity of ideal state, $\text{J mol}^{-1} \text{K}^{-1}$
 A, B, C, D and E = regression coefficients for chemical compound
 T = temperature, K

Table A1 Heat capacities of selected component (C_p)

Components	$C_p [\text{J mol}^{-1} \text{K}^{-1}] = A + BT + CT^2 + DT^3 + ET^4$; T - Kelvin				
	A	B	C	D	E
Methane	34.942	-3.9957×10^{-2}	1.9184×10^{-4}	-1.5303×10^{-7}	3.9321×10^{-11}
Carbon (s)	-0.832	3.4846×10^{-2}	-1.3233×10^{-5}	0	0
Carbon monoxide	29.556	-6.5807×10^{-3}	2.0130×10^{-5}	-1.2227×10^{-8}	2.2617×10^{-12}
Carbon dioxide	27.437	4.2315×10^{-2}	-1.9555×10^{-5}	3.9968×10^{-9}	-2.9872×10^{-13}
Water	33.933	-8.4186×10^{-3}	2.9906×10^{-5}	-1.7825×10^{-8}	3.6934×10^{-12}
Hydrogen	25.399	2.0178×10^{-2}	-3.8549×10^{-5}	3.188×10^{-8}	-8.7585×10^{-12}
Nitrogen	29.342	-3.5395×10^{-3}	1.0076×10^{-5}	-4.3116×10^{-9}	2.5935×10^{-13}
Oxygen	29.526	-8.8999×10^{-3}	3.8083×10^{-5}	-3.2629×10^{-8}	8.8607×10^{-12}

A.2 The change in enthalpy, $\Delta H(T)$ at constant pressure is

$$H_f(T) = H_f^0 + \int_{298}^T C_p dT \quad (\text{A2})$$

$$\Delta H(T) = \int_{298}^T C_p dT \quad (\text{A3})$$

APPENDIX B

DETERMINING GIBBS ENERGY OF FORMATION AND EQUILIBRIUM CONSTANT OF RELATED COMPOSITION

B.1 Gibbs energy of formation is important to analysis of chemical reaction. Values for individual compounds (reactants and products) are required to determine the change in Gibbs energy for the reaction.

$$\Delta G_{\text{reaction}} = \Sigma(n\Delta G_f)_{\text{products}} - \Sigma(n\Delta G_f)_{\text{reactants}} \quad (\text{B1})$$

The change in Gibbs energy for a reaction may be use in a preliminary work to determine if a reaction is thermodynamically favorable at a given temperature. For thermodynamic equilibrium, the following rough criterion is useful for quick screenings of chemical reactions:

$$\begin{aligned} \Delta G_{\text{reaction}} < 0 \text{ kJ mol}^{-1} & \quad \text{reaction favorable} \\ 0 < \Delta G_{\text{reaction}} < 50 \text{ kJ mol}^{-1} & \quad \text{reaction possibly favorable} \\ \Delta G_{\text{reaction}} > 50 \text{ kJ mol}^{-1} & \quad \text{reaction not favorable} \end{aligned}$$

The correlation of Gibbs energy of formation is a series expansion in temperature (Kelvin).

$$\Delta G_f = A + BT + CT^2, \quad [\text{kJ mol}^{-1}] \quad (\text{B2})$$

Where

$$\begin{aligned} \Delta G_f & = \text{gibbs energy of formation of ideal state,} \quad \text{kJ mol}^{-1} \\ A, B \text{ and } C & = \text{regression coefficients for chemical compound} \\ T & = \text{temperature, K} \end{aligned}$$

Table B1 Gibbs energy of formation of selected component (ΔG_f)

Components	ΔG_f [kJ mol ⁻¹] = $A + BT + CT^2$; T - Kelvin		
	<i>A</i>	<i>B</i>	<i>C</i>
Methane	-75.262	7.5925×10^{-2}	1.87×10^{-5}
Carbon (S)	0	0	0
Carbon monoxide	-109.885	-9.2218×10^{-2}	1.4547×10^{-6}
Carbon dioxide	-393.36	-3.8212×10^{-3}	1.3322×10^{-6}
Water	33.933	-8.4186×10^{-3}	2.9906×10^{-5}
Hydrogen	0	0	0
Nitrogen	0	0	0
Oxygen	0	0	0

B.2 Determining the equilibrium constant (*K*) The change is significantly because of the associated chemical equilibrium for the reaction.

$$\Delta G_{\text{reaction}} = RT \ln K \quad (\text{B3})$$

ศูนย์วิทยทรัพยากร
จุฬาลงกรณ์มหาวิทยาลัย

APPENDIX C

LIST OF PUBLICATIONS

INTERNATIONAL CONFERENCE

Triphob, N., Charinpanitkul, T., Soottitantawat, A., Arpornwichanop, A., Praserttham, P., and Assabumrungrat, S. Selection of appropriate hydrogen processor for efficient electrical power generation and carbon capture and storage in methane-fuelled solid oxide fuel cell system. RSCE 2010 by Thammasat University, Queen Sirikit National Convention Center, Bangkok, Thailand, November 22-23, 2010 (Oral presentation).

NATIONAL CONFERENCE

Triphob, N., Kiatkittipong, W., Charinpanitkul, T., Soottitantawat, A., Arpornwichanop, A., Praserttham, P., and Assabumrungrat, S. Comparison of different system of electrical power generation and CO₂ capture for methane fuelled SOFC systems. Recent progress in Catalysis and Catalytic Reaction Engineering by Thailand Research Fund (TRF), Chulalongkorn University, Bangkok, Thailand, November 26, 2010 (Oral presentation).

ศูนย์วิทยทรัพยากร
จุฬาลงกรณ์มหาวิทยาลัย

VITAE

Miss Narisra Triphob was born in February 21, 1987 in Chachoengsao, Thailand. She finished high school from Saint Louis College, Chachoengsao in academic year of 2004 and received her Bachelor's Degree with the first class honors in Chemical Engineering, from the Department of Chemical Engineering, Thammasat University in academic year of 2008. Afterward, she continued studying Master degree of Chemical Engineering, Chulalongkorn University since academic year of 2009.



ศูนย์วิทยทรัพยากร
จุฬาลงกรณ์มหาวิทยาลัย